Aggregator-Assisted Residential Participation in Demand Response Program

Mehedi Hasan

Thesis submitted to the faculty of the Virginia Polytechnic Institute and State University in partial fulfillment of the requirements for the degree

Master of Science
in
Electrical Engineering

Saifur Rahman
Manisa Pipattanasomporn
Lamine Mili

May 09, 2012
Arlington, Virginia

Keywords: Incentive-Based Demand Response, Aggregator Company, Controllable Loads, Water Preheating, House Pre-cooling, Demand Scheduling.

Aggregator-Assisted Residential Participation in Demand Response Program

Mehedi Hasan

ABSTRACT

The demand for electricity of a particular location can vary significantly based on season, ambient temperature, time of the day etc. High demand can result in very high wholesale price of electricity. The reason for this is very short operating duration of peaking power plants which require large capital investments to establish. Those power plants remain idle for most of the time of a year except for some peak demand periods during hot summer days. This process is inherently inefficient but it is necessary to meet the uninterrupted power supply criterion. With the advantage of new technologies, demand response can be a preferable alternative, where peak reduction can be obtained during the short durations of peak demand by controlling loads. Some controllable loads are with thermal inertia and some loads are deferrable for a short duration without making any significant impact on users' lifestyle and comfort. Demand response can help to attain supply - demand balance without completely depending on expensive peaking power plants.

In this research work, an incentive-based model is considered to determine the potential of peak demand reduction due to the participation of residential customers in a demand response program. Electric water heating and air-conditioning are two largest residential loads. In this work, hot water preheating and air-conditioning pre-cooling techniques are investigated with the help of developed mathematical models to find out demand response potentials of those loads. The developed water heater model is validated by comparing results of two test-case simulations with the expected outcomes. Additional energy loss possibility associated with water preheating is also investigated using the developed energy loss model. The preheating temperature set-point

is mathematically determined to obtain maximum demand reduction by keeping thermal loss to a minimal level. Case studies are performed for 15 summer days to investigate the demand response potential of water preheating. Similarly, demand response potential associated with pre-cooling operation of air-conditioning is also investigated with the help of the developed mathematical model. The required temperature set-point modification is determined mathematically and validated with the help of known outdoor temperature profiles. Case studies are performed for 15 summer days to demonstrate effectiveness of this procedure. On the other hand, total load and demand response potential of a single house is usually too small to participate in an incentive-based demand response program. Thus, the scope of combining several houses together under a single platform is also investigated in this work. Monte Carlo procedure-based simulations are performed to get an insight about the best and the worst case demand response outcomes of a cluster of houses. In case of electrical water heater control, aggregate demand response potential of 25 houses is determined. Similarly, in case of air-conditioning control (pre-cooling), approximate values of maximum, minimum and mean demand reduction amounts are determined for a cluster of 25 houses. Expected increase in indoor temperature of a house is calculated. Afterwards, the air-conditioning demand scheduling algorithm is developed to keep aggregate air-conditioning power demand to a minimal level during a demand response event. Simulation results are provided to demonstrate the effectiveness of the proposed algorithm.

ACKNOWLEDGEMENT

I would like to offer my sincere gratitude to my advisor Dr. Saifur Rahman for his guidance and valuable time. I have joined ARI as a young and inexperienced student. He has provided me adequate time to learn and adapt. He has exposed me to unlimited potential of self-growth. He has provided me all the facilities a student can dream of. I should have utilized this opportunity more effectively. Thank you sir, thanks for having me here.

My special thanks to my thesis committee co-chair Dr. Manisa Pipattanasomporn for her valuable advice and guidance. She has been always ready to help. Thanks ma'am, for your time and friendly attitude.

I would like to thank Dr. Lamine Mili for his kind consent to be a member of my thesis committee. I have really enjoyed his classes about power system, robust estimation etc. Thanks sir, for sharing your knowledge and experience with us.

I want to thank all my colleagues at ARI. I have really felt at home here. Specially, Dr. Murat has been so supportive. I should also mention Srivat and Ibrahima of NVC. I really enjoyed that day; you guys were teaching me power electronics. Thanks.

My eldest brother Md. Moshiur Rahman has been incredible. He has contributed in all the major phases of my life. I got admitted in BUET, he advised me before the admission test. I got funding from American universities, he funded my application fees. During the last phase of my thesis writing, I got strength from his objective opinions and advice. I dedicate my thesis to my brother.

TABLE OF CONTENTS

LIST OF FIGURES

LIST OF TABLES

PARAMETER NOTATIONS

C_{air}	Thermal capacitance of indoor air of a house
$C_{thermal}$	Combined thermal capacitance of a house
cop	Coefficient of performance
D	Density of water
E_{ac}	Air-conditioning energy demand during demand response event
E_{dr}	Target amount of demand response energy reduction
f	Hot water flow rate
$H_{air.cond}$	Heat removal rate of air-conditioner
$H_{element}$	Heat release rate of indoor elements of a house
H_{gain}	Net heat gain rate of a house
H_{out2in}	Heat absorption rate of a house from outside
n_{ac}	Number of air-conditioners in "on"-state during a particular time block
$n_{ac.max}$	Maximum allowable n_{ac} value during demand response event
n_{on}	Number of time blocks one air-conditioner remains 'on' during demand response
N_{on}	Summation of n_{on}-values of all the air-conditioners under consideration
$P_{coil,L}$, $P_{coil,U}$	Lower and upper coil powers
P_{hw}	Thermal energy flow rate for hot water draw
$P_{loss,L}$, $P_{loss,U}$	Heat loss rates in lower and upper level
P_{rated}	Power rating of water heater
$P_{transfer}$	Power flow from lower to upper level of water heater
$P_{ventilation}$	HVAC power demand for ventilation/ air circulation
$R_{thermal}$	Combined thermal resistance of a house
S	Specific heat of water
SW_L	Switch state of lower coil (state '1' or '0')
SW_U	Switch state of upper coil (state '1' or '0')
T_{avg}	Average outdoor temperature during demand response event
T_{dr}	Readjusted temperature set-point for water preheating
$Time_{dr}$	Demand response event duration
T_{hot}	Hot water temperature of upper layer
T_{in}	Indoor temperature of house
T_{inlet}	Temperature of inlet water
T_{mixed}	Temperatures of lower mixed water
T_{out}	Outdoor temperature of a house
T_{set}	Regular Temperature set-point of water heater/ air-conditioner
V	Volume of water heater tank
V_L, V_U	Water volumes of lower and upper layer of electric water heater
η_{wh}	Efficiency of coils of water heater
δ	Temperature dead-band for water heating
Δ_{ac}	Pre-cooling temperature reduction of air-conditioner

CHAPTER 1

Introduction

Federal Energy Regulatory Commission (FERC) of the United States provides following definition of demand response [1]:

"Changes in electric usage by demand-side resources from their normal consumption patterns in response to changes in the price of electricity over time, or to incentive payments designed to induce lower electricity use at times of high wholesale market prices or when system reliability is jeopardized."

Simply put, demand response is an activity of reducing electricity demand compared to the usual demand level in response to an event of high energy cost and/ or stressed condition of power system. Implementation of demand response program is a very complex task involving various levels of decision making regarding demand response amount determination, demand response target group, demand response duration, demand response price/ incentive structure etc. Thus, adequate research and proper planning is required to ensure that demand response target will be achieved cost effectively and with minimal side effect. Stochastic nature of electricity demand, consumer preferences, weather conditions etc. provide tough challenges towards demand response model development and analysis. Small residential loads are highly dependent on residents' preferences and life styles. Aggregation of several residential loads can provide significant demand response scope. Peak demand can be reduced by controlling residential non-critical loads such as water heater, Heating Ventilation and Air-Conditioning (HVAC) system, electric vehicle charging, dishwasher, clothes-dryer etc. Potential benefits of residential demand response have spurred research and study interest on this topic and also have attracted many entrepreneurial investments leading to aggregator companies with residential loads as their target demand response sector.

1.1 Problem Statement

Demand response models are usually variants of either price signal based or incentive-based demand response programs [2]. Price signal based residential demand response is discussed at length in [3]. Authors of [3] categorized price signal based demand response into three modes: active, interactive and trans-active market based. Trans-active market based demand response promises automatic and interactive residential demand response participation [3]. Active market based demand response is discussed in [4]. Mathematical model for price signal based demand response is developed in [5]. Authors of [5] considered price and demand as state variables. Probabilities of various state transitions are considered to analyze the impact of probable future energy price and demand on the current decision regarding energy demand state change. However, that work has not considered any realistic appliance model. Dynamic pricing based demand response is proposed in [6]. Authors of [6] considered smart-grid architecture with control units in both utility and customer sides. Power line communication (X-10, A-10) based home energy management system is also proposed in [6]. Price signal based demand response and control strategies are also discussed in [7] and [8]. However, price signal based demand response model fails to guarantee the demand response goal achievement and also lacks in structural solidarity. Grid Friendly Appliances (GFA) can participate in demand response by responding to frequency fluctuations. However, large geographical distances between generators and GFA loads can cause system instability [9]. Therefore in this work, residential demand response participation potential will be analyzed under the consideration of incentive-based demand response model. In this model, loads of several houses can be combined together under an aggregator company to register in a demand response program. Aggregator bears the responsibility to ensure proper demand response participation of those houses. Benefit of residential demand response is demonstrated by simulations in [10]. Aggregation of large number of houses is proposed in [11]. However, that paper does not provide any methodology for aggregate load control. Aggregator Company has to ensure the contracted amount of demand reduction during a demand response event. Therefore, proper methodology for the evaluation of demand response potential and proper action strategies for load control are required to obtain target demand response with minimal possible intervention to client residents' lifestyle. Challenges associated with residential demand response are mainly following: small load size

per house, highly stochastic nature of residential load, individual monitoring and control overhead, lack of proper smart grid infrastructure, concern regarding comfort violation etc. Despite these challenges, there is enormous demand response potential for residential loads if several houses can be aggregated together. Two key issues must be satisfied to popularize residential demand response participation. First is to satisfy residents' comfort for the entire demand response event duration and the second is to keep the residents free from the concern of incentive penalty in case of any demand response threshold violation. Therefore, this research work highly focuses on those two aspects.

1.2 Objective

The goal of this thesis is to analyze demand response potential of residential loads, in particular, electric water heater and air-conditioner. To achieve this objective, the following tasks are performed:

1. The simulation model that can represent electric water heater operation is developed in Matlab, with the help of the mathematical description provided in the literature. The water preheating methodology is developed for demand response participation of residential water heaters. A set of equations are derived to determine preheating temperature set-point for demand response participation of electric water heaters.
2. Case studies are performed for 15 summer days to verify effectiveness of the proposed water preheating methodology. Preheating start times are varied to observe the effect of thermal loss associated with water preheating on the overall electric water heater power load profile.
3. The simulation model of air-conditioning load is developed in Matlab, with the help of thermal to electrical analogy available in the literature. The house pre-cooling methodology is developed to allow analysis of demand response participation of residential air-conditioners. A set of equations are derived to determine any necessary changes in indoor temperature set-point for demand response participation of residential air-conditioning loads.
4. Case studies are performed for 15 summer days to observe effectiveness of the proposed house pre-cooling method. The effect of rebound load on the air-conditioning load profile associated with air-conditioner control is also determined from case study results.
5. The aggregated demand response potential of water heaters of 25 houses is determined with the help of Monte Carlo simulation. Similarly, the aggregated demand response potential of air-conditioning loads of 25 houses is also determined by Monte Carlo method. Simulation samples associated with high and low demand response amounts are tracked to get insight into the best and the worst case scenarios.
6. A demand scheduling algorithm is developed for air-conditioners of several houses to keep the aggregated air-conditioning demand low for the entire duration of a demand

response event. Simulation results are provided to demonstrate the effectiveness of the proposed algorithm.

1.3 Assumptions

1. Demand response event duration is 4 hours. This is based on the Distribution Load Relief program of ConEdison [25].

2. Upper limit of hot water temperature set-point is considered 140 °F.

3. Maximum allowable change in indoor temperature set-point of any house is considered ± 3 °F.

Results obtained in this thesis are dependent on these assumptions. However, the methodologies and models used in this thesis are also valid for short or longer duration of a demand response event. If the upper limit of hot water temperature is increased then demand response potential can increase in expense of increased thermal loss. On the other hand, indoor temperature set-point variation is considered maximum ± 3 °F to satisfy a required thermal comfort of household residents.

1.4 Contribution

Modeling and mathematical descriptions provided in this thesis are expected to serve as the first stepping stone that will allow researchers in the academia and electric utilities to comprehensively analyze demand response potential of residential customers. Research findings as presented in this thesis can also provide aggregator companies an added insight into expected benefits and constrains of residential load control, in particular, of electric water heater and air-conditioning loads. The preheating/ pre-cooling and demand scheduling methodologies introduced in this thesis are also expected to contribute to future electric power system planning and operation with demand response as a design criterion.

CHAPTER 2

Literature Review

A Closer look on Load Management (Kupzog *et al*.) [13]:

Controllability of electricity generation is gradually decreasing with the rising share of renewable energies [13]. Therefore, demand side management of electrical loads is gaining higher importance. This paper discussed a methodology of demand side management of thermal processes such as air-conditioning, refrigeration, cold storage, boiler etc.

Generalized standard model for thermal loads is proposed by the authors of this paper. Electrical heating and cooling systems convert electric energy to thermal energy. Thermal processes have certain amount of inertia (the capability of hold temperature for certain duration with slow gain or decay) which can be considered as energy storage capability. These capabilities can be utilized for demand side load shifting purposes. Standard model for thermal processes is developed by taking thermal to electrical analogy. Equivalent circuit model is developed by taking temperature (T), heat flow rate (P), thermal capacitance (C), thermal resistance (R) as analogues to electrical parameters such as, voltage (V), current (I), capacitance (C), resistance (R) respectively. Afterwards, the authors proposed two methods for load shifting:

1. Set point variation.
2. Immediate recharge.

In the first case, temperature set points are varied according to the requirement for demand response. On the other hand, second method is applicable if the thermostats are not accessible. In that case, appliances will be completely switched off for certain duration and afterwards will be turned on for thermal energy recharge. Duration for energy decay during turn-off period is much higher than the required energy recharge duration. Thus, it can be a potentially effective way of demand response.

Frequency Waves, Grid Friendly Appliances and Geographical Limits in Smart Grid (Li *et al*.) [10]:

Grid Friendly Appliances (GFA) have controllers to monitor the supply frequency. If the frequency drops below 59.95 Hz then the appliances get turned off automatically and remain off until the frequency recovers to 60 Hz. However, frequency variation does not reach all the appliances at the same time, rather frequency signal travels at a rate of about 500 miles per second. Therefore, the delay resulting from the relatively slow speed of frequency signal must have to be accounted in case of analysis of the impact of GFA.

In this paper, the dynamic behavior of power system is described by using synchronous machine model. Two cases are considered and corresponding system stabilities are mathematically analyzed. Case-1 considers one generating unit and two loads. One load is near to the generator and another is geographically in a distant location. On the other hand, Case-2 considers two generating units with high geographical distance and two loads near to the generating units. System stability is analyzed in both cases and the effect of propagation delay is discussed. It is shown that, in both scenarios GFA can cause system failure or at least can exacerbate the disturbances of power system if there are large distances among various load units.

An Evaluation of the Water Heater Load Potential for Providing Regulation Service (Kondoh *et al*.) [14]:

Authors of this paper provided a comprehensive Electric Water Heater (EWH) model based on the considerations of various thermodynamic heat flow rates in terms of equivalent kW demands. Afterwards; authors investigated the possibility of providing regulation service (demand response) by aggregating large numbers of electrical water heater loads. Switching based thermostat control methods are discussed to obtain load regulation goal. Two types of regulation signals are considered. In first case, constant load reduction target is considered. In second case, variable bidirectional regulation signal is considered to obtain necessity based variable load reduction targets by controlling electric water heaters. It is found that 33,000 EWHs (each 4.5

kW) are required to provide regulation service for 24 hours, while the number is much smaller (20,000) when regulation requirement is only between 6:00 to 24:00.

Modeling of Demand Side Shifting Potentials for Smart Power Grids (Pollhammer *et al*.) [15]:

Demand response potential is modeled by the authors of this paper by considering the concept of energy packets. 15 minutes interval is considered as time unit for energy packets. Each packet has two indices indicating its capability to shift towards left or right (pre-operation and post-operation respectively). Total demand profile is composed of energy packets corresponding to various appliances/ loads (as bricks to build a wall). Various amounts of flexibility values are considered to demonstrate the concept without accounting for real appliance model. It is argued that various energy packets can be rearranged to the left (pre-operation) or to the right (post-operation) of the peak load period to obtain demand response target. Hypothetical energy storage analogy is considered to describe pre or post-operation of appliances. For example, pre-operation is logical equivalent of storing energy in a battery for future use, while post-operation is equivalent to depleting energy from a battery which will require refilling in the near future. However, there will be loss associated with both cases and that is also considered in the discussion of this concept level paper. Scopes of improvement on this work are following:

- Fixed block size is considered in this paper by just conceptual consideration. In practice, energy packet size will depend on the load.
- Flexibility indices are considered as arbitrary numbers without considering any load model. Load model should be incorporated and the likelihoods of load operation at various times, especially near the demand response point are to be considered.
- This paper did not discuss anything regarding the relationship among flexibility indices and customer comfort level. It is necessary to bridge flexibility index of energy packet and associate effect on customer comfort.
- This paper introduced the concept of rebound effect but did not discuss that in details. This model can be utilized to analyze rebound loads in various scenarios.

Next Generation of HVAC System (Ito *et al*.) [16]:

Conventional Air Handling Unit (AHU) of Heating Ventilation and Air Conditioning (HVAC) system has only one coil. In this case, chiller water temperature is around 7 °C. However, efficiency and Coefficient of Performance (COP) of AHU is lower in case lower operating temperature. Therefore, this paper proposed AHU with two coils with two operating temperatures. One coil is used to cool down and dehumidify fresh air intake from outside. This coil uses chiller water of 7 °C temperature, resulting in chiller COP equal to 2.7. Another coil is used for the circulation of inside air and for the removal of sensible heat from that air. This coil operates with chiller water of 15 °C temperature, resulting in higher value (i.e. 12) of COP. Electrical power consumption in compression stage depends on the temperature difference of evaporation and condensation stages. Condensation temperature depends on the chiller water temperature. Thus, higher temperature of water increases energy efficiency of HVAC system.

Analysis of Residential Demand Response and Double-Auction Markets (Fuller *et al*.) [17]:

Double auction market means a two way market where both energy suppliers and end-users or consumers can simultaneously bid for energy quantity and energy price into a single market. Depending on the supply and demand bidding, price of electricity is determined and cleared market price is sent back to both supplier and end-customers. In case of 'transactive' market strategy, a central auction unit receives all the bids and sends back cleared market price to the distributed controllers associated with each load. 5 minutes market clearing interval is considered in this paper. Depending on the whole sale energy price of various time intervals, end-user controllers change temperature set points of air conditioning, electric water heater etc. For example, if the price of electricity is more than the average electricity price at a certain time interval then controller will increase air conditioning temperature set point to reduce energy consumption. On the other hand, distributed controllers also participate in energy auction by bidding energy price depending on the necessity of energy. For example, if the air temperature of a house is higher than the temperature set-point of air conditioner then the controller will bid relatively high price for electricity. This paper provides examples to demonstrate the analytical details required for this kind of price bidding based demand response model. However, it has not

discussed anything regarding the practical considerations of communication requirements and the potential system complexities associated with this kind of bidding based demand response realization.

Simulated Demand Response of a Residential Energy Management System (Roe *et al*.) [11]:

Household appliances such as HVAC, electric water heater, cloth dryer, electric vehicle etc. can be controlled with the help of Residential Energy Management System (REMS). Demand Response (DR) duration is considered from 4 pm to 7 pm. Simulation result is presented for four scenarios such as: 1.

- Scenario 1: Without any control
- Scenario 2: With one programmable thermostat but without REMS.
- Scenario 3: House with REMS but without any energy storage facility.
- Scenario 4: House with programmable thermostats, REMS and battery storage.

For each scenario, four performance metrics are evaluated, such as: daily energy usage, daily energy cost, average DR power and the DR energy. It is shown that DR power and energy are significantly lower in case of the third and fourth scenarios. This paper used randomization of the start and end times of appliances to model random behavior of residents. However, it does not provide any comprehensive algorithm for load control which can be used by the REMS.

Capacity Assessment of Residential Demand Response Mechanisms (Pagliuca *et al*.) [12]:

Conventional power system has been designed with the concept of supply side control to maintain supply-demand balance. However, with the increasing share of renewable energies, necessity of demand response is growing. In this paper, residential demand response capacity is determined by using Monte Carlo simulation. Fixed load profiles are considered and start times of those loads are randomized to generate aggregate residential load profiles. Load reduction possibility is discussed based on the aggregate load profile. This paper also discussed the

possibility of aggregating large number of houses to obtain a demand response target. However, it does not provide any methodology for aggregate load management.

Simulating Demand Response and Energy Storage in Energy Distribution Systems (Ahcin *et al*.) [18]:

Authors of this paper incorporated demand response into the matrix based energy modeling framework developed previously at ETH (Swiss Federal Institute of Technology), Zurich. In that framework, inputs and outputs of an energy generation network is linked by coupling matrix to provide a mathematical model for energy flow analysis. Moreover, in presence of storage capability, storage energy flow and resulting power system energy flows are linked via a storage coupling matrix. This model is further extended in this paper to include demand response as a logical equivalent of storage facility. Afterwards, the utilization of such model for the computation of energy cost and greenhouse gas emissions is also demonstrated with multiple example scenarios.

Dynamic Load Modeling of an HVAC Chiller for Demand Response Applications (Berardino *et al*.) [2]:

Authors of this paper argued that component based load modeling better suits for demand response analysis. Unlike traditional complex power based lump load model, component based modeling focuses on the operating principles and practical constrains of the components. Therefore, component based modeling provides increased resolution of electrical load models which is essential for demand side management analysis. In this work, a dynamic model of HVAC load is developed based on tests performed on an actual HVAC unit. Mathematical model is developed and various parameters of that model are estimated based on the collected behavioral test data of the HVAC unit.

Analysis of Distribution Level Residential Demand Response (Schneider *et al.*) [4]:

Demand response technique is moving towards interactive communication based approach. Traditional direct load control strategy is giving way to more sophisticated active, interactive or transactive market based supply demand models. In this paper, active market based demand response is considered where there is no energy bidding from the buyers' side. Price signal is used to obtain demand response, where active controllers adjust various internal parameters (such as: temperature set-points) based on the received price signals. Three scenarios are considered to analyze price signal based demand response, such as: no price signal, one hour's price signal and 15 minutes' price signal. Peak reduction is obtained in both cases of price signals. However, smaller time unit provides better demand response outcome in expense of added communication overhead.

Residential Demand Response Using Reinforcement Learning (O'Neill *et al.*) [5]:

An algorithm and mathematical model is provided in this paper for the home energy management in response to the variable energy price. Consumer Automated Energy Management System (CAES) has the capability to learn the electricity consumption behavior of residents and automatically makes decision regarding the time of operation and speed of operation (rate of energy consumption) of various appliances. Electricity prices are modeled as price-states and the information regarding transition of states are fed into CAES. Similarly, residential energy demand is also modeled with various demand states. Probabilities of transition from one state to other states are considered to analyze the impact of probable future energy price and demand on the current decision regarding energy demand state change. In this paper, optimal energy demand decisions are mathematically derived based on the assumed flexible pricing and demand model. However, it did not take realistic models of the appliances into account. For example, it cannot answer the question regarding what is the degree of flexibility to change the speed of HVAC and what can be the impact of such action on customers' comfort. It can be possible to incorporate realistic appliance models, real life operating constrains and customer comfort issues with the developed algorithm. Thus it may be possible to incorporate practical constrains with the developed algorithm for decision making regarding electrical energy usage.

Next Generation of Energy Residential Gateways for Demand Response and Dynamic Pricing (Cuevas *et al*.) [6]:

Authors of this paper proposed smart-grid architecture with Utility Smart Grid Manager (USGM) in the utility side and Energy Residential Gateway in the residential customer side. Home Area Network (HAN) is proposed where ERG can interact with various home devices via Power Line Carrier communication protocols such as X-10 or A-10. Maximum 256 devices can be connected to the HAN. ERG can monitor energy consumption of various devices and also can send data periodically to USGM. It is also capable of providing demand response services such as peak clipping and valley filling. Algorithm is developed for ERG to control home appliances based on real time pricing signals received from USGM. Implementation of ERG is done on an ARM-926 (Advanced RISC Machine) processor based platform with touchscreen capability. Firmware of ERG comprises of following functional modules:

- Control Module: For communication between ERG and HAN devices.
- Graphical User Interface (GUI) Module: A user friendly and intuitive interface for users' interaction with the ERG.
- Energy Management and Demand Response Module: It provides energy consumption monitoring, price monitoring, demand scheduling to obtain peak clipping and valley filling etc.

The energy residential gateway is installed in a test lab and various HAN devices area configured with that ERG. It is found that ERG can provide very fast (30 second) demand response with respect to dynamic energy price, thus it is capable of providing peak clipping service in case of any demand response event.

Automated residential Demand Response: Algorithmic Implications of Price Models (Li *et al*.) [7]:

Authors of this paper discussed an algorithm of automatic demand response and energy scheduling to obtain flat aggregate demand curve. It argued that utility company has the lowest overall cost if energy usage is flat overtime. Rebound effect after a demand response event is

also demonstrated. The algorithm is based on optimization problem, where optimality is proven by using Karush Kuhn Tucker (KKT) conditions. However, load models and operating constrains of the practical appliances such as HVAC, water heater, cloth dryer etc. are not considered in this mathematical algorithm formation. The impacts of optimal load scheduling on customers' comfort and suitability of such scheduling in real life have not been discussed in this paper.

A Residential Consumer-Centered Load Control Strategy in Real-Time electricity Pricing Environment (Tiptipakorn *et al*.) [9]:

A customer centered load control algorithm is proposed in this paper with the assumption of real time electricity pricing. Electric water heater and air-conditioning units are controlled based on real time electricity price. Outlet hot water temperature set-point is changed in response to the electricity price variation. Hot water temperature set point is the lowest if electricity price is the highest. However, this paper fails to take into account the relative hot water flow rate depending on the temperature. If outlet temperature is set low then flow rate will increase, because users will mix more hot water to obtain their desired temperature. Moreover, hot water consumption profile is not considered in this paper, making the analysis incomplete.

The Potential and Limits of Residential Demand Response Control Strategies (Chassin *et al*.) [19]:

Residential loads can be divided into two categories: thermostatic (such as air conditioning, water heating etc.) and non-thermostatic (such as lighting, computer etc.). Thermostatic loads exhibit sequential on/off behavior and there may also be several stages of operation, leading to several levels of power demands. Therefore, control strategies of these thermal loads are constrained by the duty cycle, power levels of these loads and also by the associated thermal storage capacities. This paper defines state vector, state transition matrix and load control vector to analyze the effectiveness of various load control strategies. Analysis is provided regarding load control scopes ensuring no perceivable impact on the customers' comfort.

CHAPTER 3

Demand Response Model

3.1 Demand Response Motivation

To realize the necessity of demand response, it is necessary to visualize variations of load profiles depending on seasons, temperature, weather conditions etc. Therefore, comparison between load profiles of one winter weekday and one summer weekday is shown in Fig. 3.1. Load profiles are generated by using data from New York Independent System Operator's (NYISO) daily reports [20].

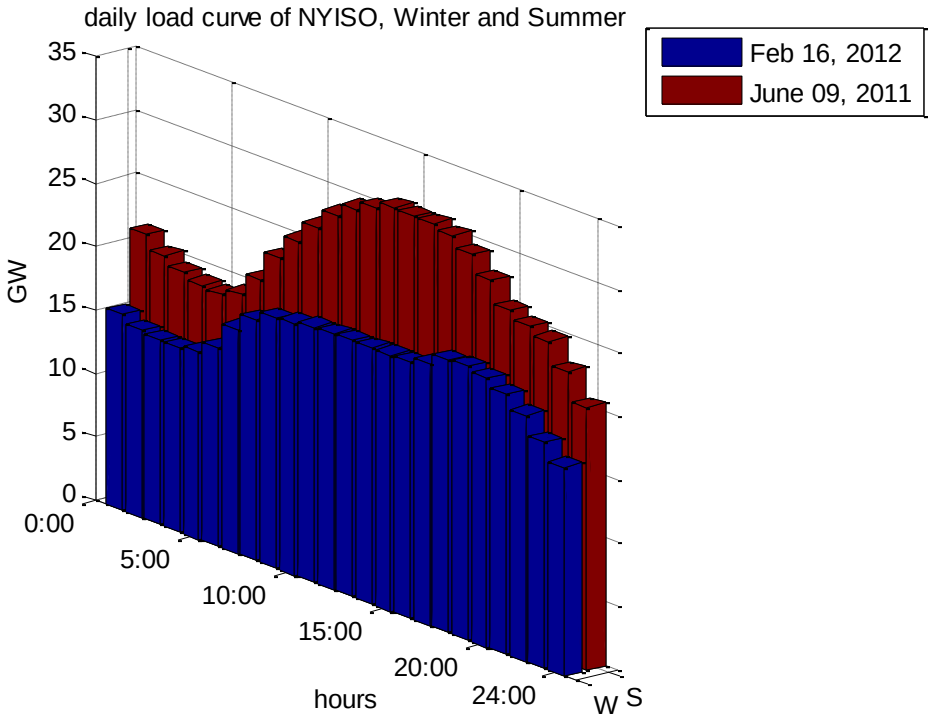

Fig. 3.1: Comparison between summer and winter load profiles of NYISO (both Thursday).

It is easily observable from Fig. 3.1 that summer load is significantly higher than winter load. Electricity demand depends significantly on temperature. Temperature profile of June 09, 2011 for Central Park, NYC is generated by using data from [21]. Temperature profile is shown in Fig. 3.2. Typically, electricity demand becomes high in very hot summer weekdays. However, excessively high electricity demand happens for only few days and few hours in a year. Nevertheless, power system has to be sized based on the highest possible demand, to ensure uninterrupted power supply. Therefore, capital investment for supplying the excessively high demand does not generate any revenue during most of the time of a year. Consequently, cost of energy associated with peak load becomes excessively high. In case of typical flat energy rate, utilities have to pay lot more wholesale electricity price than the retail energy price paid by customers during peak load period. On the other hand, to compensate for this excessively high cost of peak time energy, per-unit retail price of electricity is set relatively higher. Thus, ultimately customers need to pay all year round for this inefficient process. Demand side load management can thus be beneficial to both utilities and end customers by making power generation and supply process more efficient. Demand response can reduce the requirement of expensive and inefficient peaking power plants.

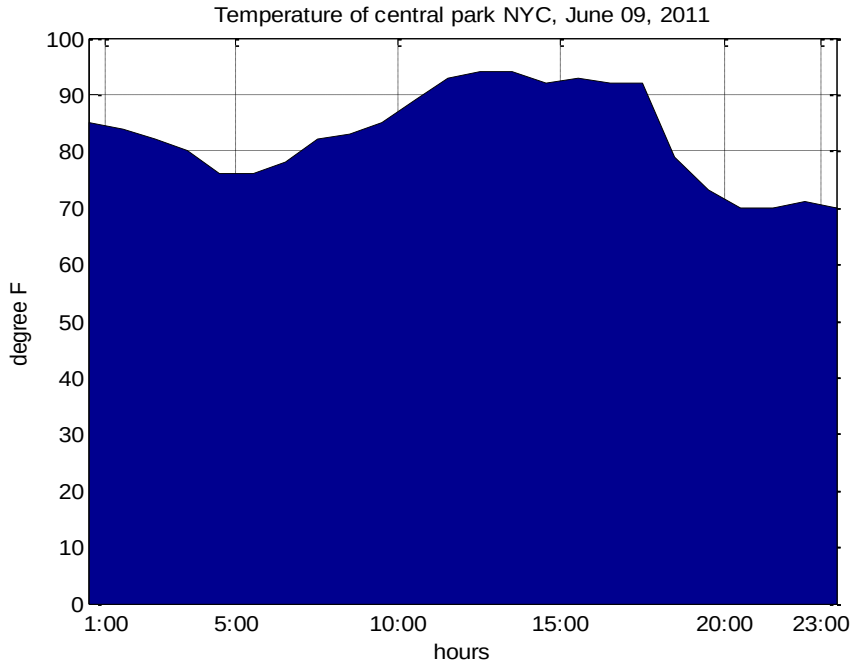

Fig. 3.2: Temperature profile of June 09, 2011, Central Park, NYC.

Depending on demand, price of wholesale electricity can vary significantly. For example, electricity price data of June 09, 2011 for various zones of NYISO is collected from [20]. Variation of wholesale electricity price is shown in Fig. 3.3.

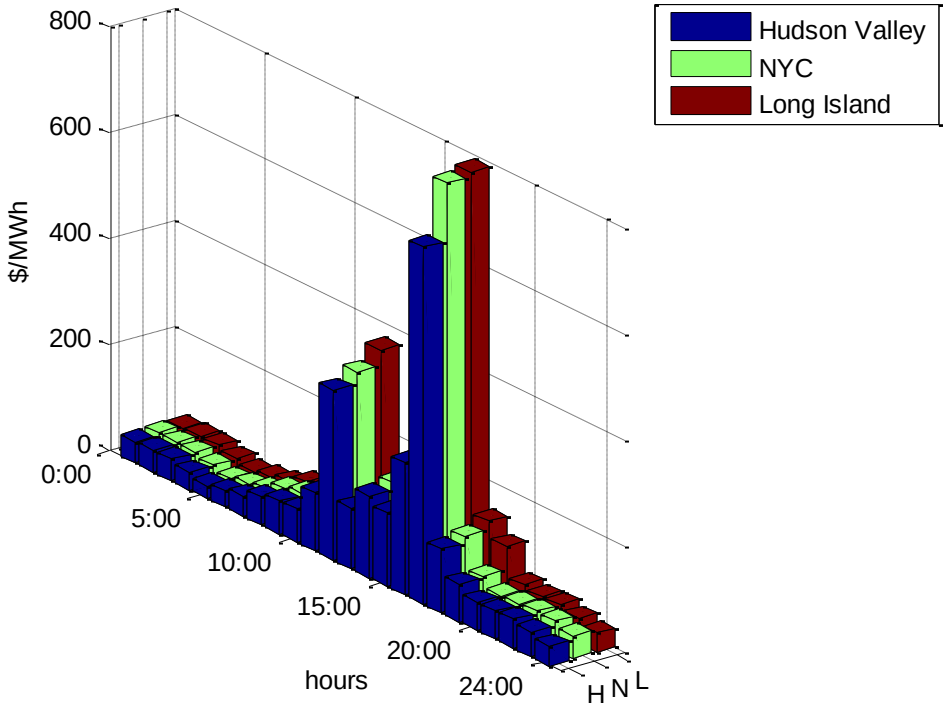

Fig. 3.3: Wholesale electricity price for various zones of NYISO. June 09, 2011.

It is observable from Fig. 3.3 that electricity price is extremely high during few hours such as: 12 pm, 4 pm, 5 pm etc. This kind of huge price imbalance works as a motivation towards demand response. During such peak hours, it is profitable to reduce electricity demand by providing incentive to customers to decrease their electricity demand below typical level. On the other hand, excessive demand of electricity occurs for very short periods in a year. This is easily observable from the load duration curve of California, shown in Fig. 3.4. Therefore, some non-critical loads can be reduced for those short periods to obtain supply-demand balance.

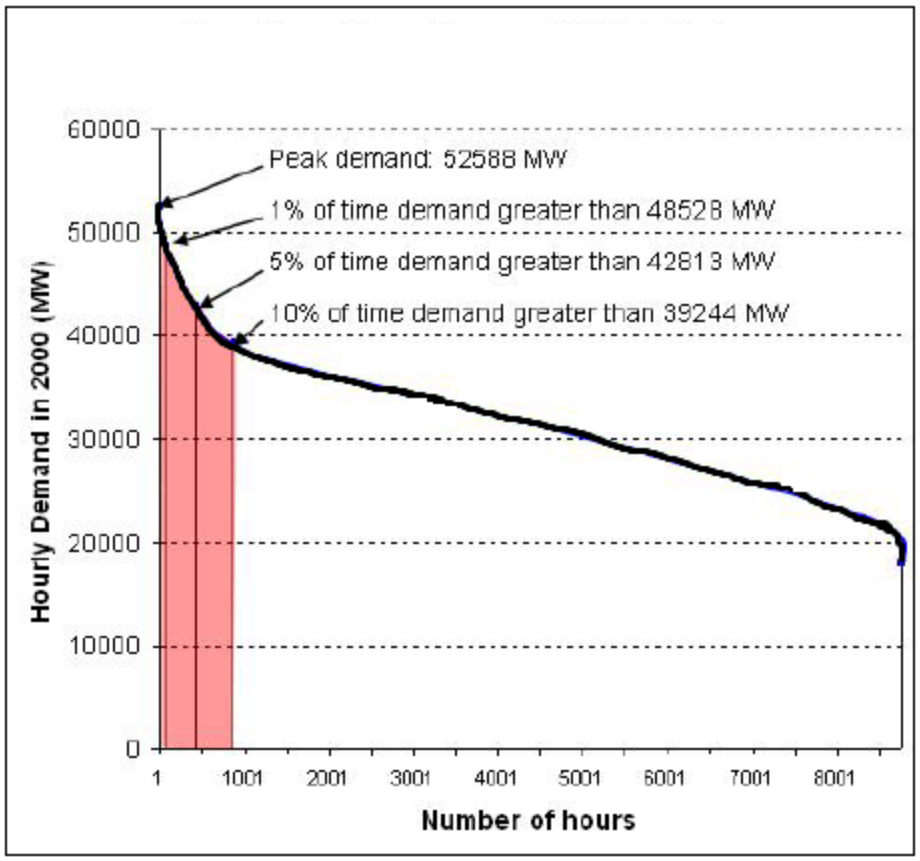

Fig. 3.4: Load duration curve of California (reproduced from fig. 3 of [22]).

3.2 Demand Response Model

Demand response models are mainly based on retail energy pricing and/ or incentive structure.

3.2.1 Price-Based Demand Response

Time of Use (TOU): Usually there are three levels of prices. Portland General Electric provided their TOU pricing model for summer weekdays as shown in Table 3.1.

Table 3.1: Time of Use (TOU) pricing by PGE for summer weekdays [23].

		Durations	Prices	
1	On Peak	3 pm-8 pm	13.266	cents/ kWh
2	Mid Peak	(6 am to 3 pm) and (8 pm to 10 pm)	7.5	cents/ kWh
3	Off Peak	10 pm to 6 am	4.422	cents/ kWh

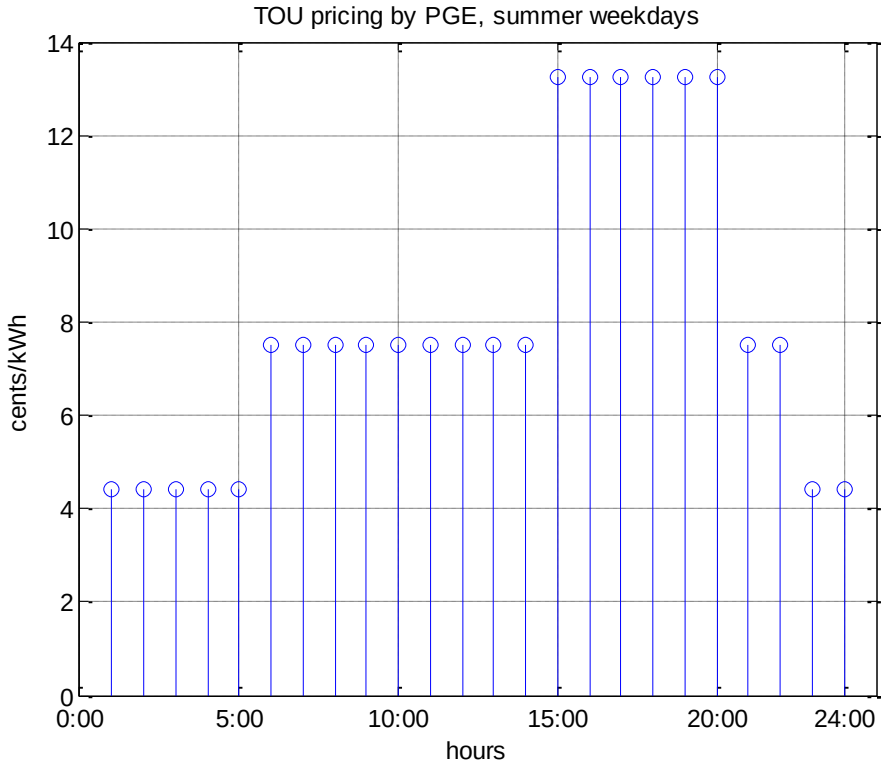

Fig. 3.5: TOU pricing by PGE, summer weekdays.

Critical Peak Pricing: In this type, very high electricity price is set for certain critical peak hours of demand response event days [24]. Number of events is often limited to 15 days per year. Electricity price can be 3 to 10 times higher during critical peak period.

3.2.2 Incentive-Based Demand Response

In this case, there are contracts between electricity consumers and the demand response service provider. According to the contract, consumers need to reduce certain amount of load during pre-declared dates and hours. This kind of demand response model is followed by some companies such as Consolidated Edison, Inc. (ConEdison) [25]. There can be two broad forms of incentive-based demand response.

1. Voluntary: In this case, customer has the choice to voluntarily participate in demand reduction during a demand response event. Participants receive monetary incentive, based on their level of participation.
2. Mandatory: This is a contract based demand response. Participant electricity consumers must reduce contracted amount of load during pre-declared demand response events of summer time.

Following the Distribution Load Relief Program (DRLP) of ConEdison [25], let's consider a Demand Response (DR) model with following criteria:

- Conditions for registration in a demand response program: Participant should have at least 100 kW of total load. Participant should be willing to reduce at least 50 kW of load during demand response hours.
- Aggregators: Several residential customers can be grouped together to meet registration criteria of a demand response program. A middle layer company can work as an aggregator and can be responsible to ensure combined load reduction of the grouped houses. Load reduction capability of an aggregator must be at least 50 kW with respect to the usual level of power demand.
- Events: There can be five demand response events per month, each with duration of 4 hours. DR events will be declared at least 23 hours ahead based on day-ahead load forecasts.
- Incentives: There are monthly contracted capacity based incentives and also demand reduction amount (energy) based incentives. For example, if an aggregator company is contracted to reduce 100 kW of load during demand response event, then monthly fixed

payment = 100 kW * Capacity rate per kW (e.g. $5 per kW per month). There is also participation based energy payment.

- Penalty Factor: If an aggregator fails to meet the mandatory contracted load reduction target then there will be penalty in the incentive, determined by the Penalty Factor Index. In case of failure to meet the contracted amount of demand reduction, Penalty Factor will be less than 1.

Contract and incentive based demand response programs usually require relatively large load reduction capability to be eligible for participation. According to the considered demand response model, there should be at least 50 kW load reduction willingness to participate in the demand response program. Load reduction capability of a single house is much smaller than 50 kW. Therefore, it is essential to combine several houses under a single platform facilitated by an Aggregator Company. Baseline power demand is measured by demand response service provider using smart meter. Demand response amount is assessed with respect to the pre-measured baseline load level. Violation of the contracted demand response amount causes penalty in financial incentive. Therefore Aggregator Company must satisfy following inequality during a demand response event:

$$\text{DR Event Time Demand (kW)} \leq [\text{Baseline Load (kW)} - \text{Contracted DR Amount (kW)}].$$

CHAPTER 4

Electric Water Heater Model

PARAMETER NOTATIONS

A	Area of water heater tank
D	Density of water
ef	Energy factor of water heater
f	Hot water flow rate
$P_{coil,L}$	Power from lower coil
$P_{coil,U}$	Power from upper coil
P_{hw}	Thermal energy flow rate for hot water draw
$P_{loss,L}$	Thermal heat loss rate in lower level of water heater tank
$P_{loss,U}$	Thermal heat loss rate in upper level of water heater tank
P_{rated}	Power rating of water heater
$P_{transfer}$	Power flow from lower to upper level of water heater
R	Thermal insulation of water heater tank
S	Specific heat of water
SW_L	Switch state of lower coil (state '1' for on and state '0' for off)
SW_U	Switch state of upper coil (state '1' for on and state '0' for off)
T_{dr}	Readjusted temperature set-point for water preheating
T_{hot}	Hot water temperature of upper layer
T_{inlet}	Temperature of inlet water
T_{mixed}	Temperatures of lower mixed water
T_{out}	Outdoor temperature of a house
T_{set}	Regular Temperature set-point of water heater
V	Volume of water heater tank
V_L	Water volumes of lower level of electric water heater
V_U	Water volumes of upper level of electric water heater
η_{wh}	Efficiency of coils of water heater
δ	Temperature dead-band for water heating

4.1 Basic Description of Electric Water Heater

Electric water heating accounts for the second highest residential electricity demand [8]. Therefore, it is very important to understand its operating principle and residential usage pattern of hot water. A mathematical model of electric water heater will be developed in this chapter. Typical residential hot water consumption pattern will also be discussed. Equivalent circuit of an electric water heater is provided below:

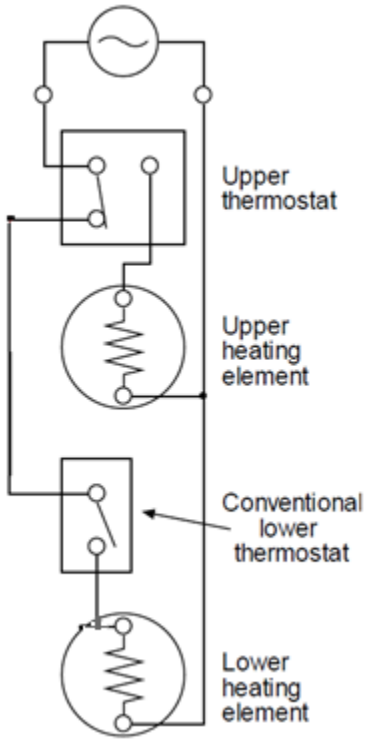

Fig. 4.1: Equivalent circuit of an electrical water heater (reproduced from fig. 6 of [14]).

Let's consider a water heater with total storage capacity of V gallons. There are two heating coils in an electric water heater. Lower coil works as a primary heating element whereas upper coil works as a surface level heater. Upper coil turns on if excessive water draw results in significant temperature drop of hot water. Two coils do not work together. If upper coil turns on then lower coil automatically switches off. For modeling purpose, two levels of water can be considered [14].

Lower level: It contains mixture of heated water and cooler inlet water. Usually this layer undergoes heating (from lower coil) and transfers heat to upper layer primarily by convection flow of hot water.

Upper level: It contains hot water ready for supply. This is relatively thin layer of surface level hot water. Hot water is supplied from this layer and consequently heated water from lower layer flows into this layer. Upper heating coil is present in this layer to provide surface level heating in case of excessive temperature drop of hot water.

4.2 Mathematical Description of Various Energy Flow Rates

Hot water temperature of an electric water heater is determined by various energy flows inside and outside of the tank. Thermodynamic balance between these energy flow rates provides steady temperature of hot water ($T_{set} \pm \delta$). If temperature drops below ($T_{set} - \delta$), then heating coil turns on to increase thermal energy of water. On the other hand, if hot water temperature rises to ($T_{set} + \delta$) then heating coil turns off automatically. Descriptions of various energy flow rates are provided below:

Inlet cold water's energy: Water enters into the water heater tank with temperature T_{in}. Afterwards, water absorbs energy from the heating coil and its temperature rises to T_{out}. Thus, inlet water's thermal energy is increased to the level of outlet water's thermal energy. Inlet water's energy is considered as reference energy level, because if we want to keep water at temperature T_{in} then there is no requirement of energy supply from the heating coil.

Coil power: Upper and lower coils convert electrical energy to heat and transfer that heat to water. These two coils never operate together. Thermal power output of lower coil:

$$P_{coil,L} = \eta_{wh} * SW_L * P_{rated}$$

Thermal power output of upper coil:

$$P_{coil,U} = \eta_{wh} * SW_U * P_{rated}$$

Energy transfer from lower to upper layer: In case of water draw from the upper layer, cold water enters into the lower layer and hot water is transferred to upper layer to fill up the volumetric gap resulted from water draw. Energy transfer rate from lower to upper layer:

$$P_{transfer} = S * D * f * (T_{mixed} - T_{inlet})$$

Energy of supplied hot water: If hot water is drawn out from the tank then it carries out certain amount of energy. Inlet water is considered to be at reference energy level. Thus, E_{hw} indicates the amount of thermal energy required to raise temperature of water from T_{in} to T_{out}. Similarly, P_{hw} indicates the rate of thermal energy flow associated with a certain rate of outlet water flow. All the units are converted to kW for both cases of thermal and electrical energy flow rates. Thermal energy flow rate associated with hot water supply:

$$P_{hw} = S * D * f * (T_{hot} - T_{inlet})$$

Switching conditions:

$$If: T_{mixed} > (T_{set} + \delta)\ ;\ then:\ SW_L = 0;$$

$$If: T_{mixed} < (T_{set} - \delta)\ and\ SW_U = 0;\quad then: SW_L = 1;$$

$$If: T_{hot} < (T_{set} - \delta);\quad then: SW_U = 1\ and\ SW_L = 0;$$

$$If: T_{hot} > (T_{set} + \delta);\quad then: SW_U = 0\ ;$$

Power balance equation of upper level [14]:

$$S * D * V_U * \frac{dT_{hot}}{dt} = P_{coil,U} + P_{transfer} - P_{hw} - P_{loss,U} \quad \ldots\ldots\ldots\ldots\ldots\ldots\ldots \quad (4.1)$$

Power balance equation of lower level [14]:

$$S * D * V_L * \frac{dT_{mixed}}{dt} = P_{coil,L} - P_{transfer} - P_{loss,L} \quad \ldots\ldots\ldots\ldots\ldots\ldots . (4.2)$$

4.3 Energy Loss Model of Water Heater

Insulation heat loss is usually modeled as, H = A* (T_{hot} - T_{env}) / R. If the unit of surface area A is square feet and insulation's heat resistance R is in (ft^2hr°F/Btu) then we get H in Btu / hr unit. This value of H can be converted to kW by dividing by 3412 [26]. On the other hand, inner and outer areas of a cylindrical tank are different. Thus, neither inner nor outer area is appropriate for being used in the heat loss equation [27]. So, average of inner and outer heights and average of inner and outer radii are used to calculate effective surface area. Let us consider a cylinder shaped water heater tank with following parameters:

Inner radius of tank	:	10	inches
Outer radius of tank	:	14	inches
Inner height	:	63	inches
Outer height	:	66	inches
Avg. height (h)	:	64.5	inches
Avg. radius (r)	:	12	inches
Insulation value (R)	:	16	ft^2hr°F/btu

According to the electric water heater model, lower layer volume is V_L gallons and upper layer volume is V_U gallons. Heights of those two layers are proportional to respective volumes.

$$h_u = h * \frac{V_U}{V};\ h_l = h * \frac{V_L}{V}$$

$$A_L = \pi * r^2 + 2 * \pi * r * h_l$$

$$A_U = \pi * r^2 + 2\,\pi * r * h_u$$

Heat loss rate

$$= \left[\frac{A_L(T_{mixed} - T_{env})}{R} + \frac{A_U(T_{hot} - T_{env})}{R}\right] * \frac{1}{3412}$$

Besides insulation heat loss, there are other losses such as: loss around the pressure relief valve; loss from the supply pipe connected to water heater etc. Thus, actual water heater loss can be twice as much of the calculated insulation loss. To accommodate those losses, an empirical weight of (1.5/energy factor) is included in the equation [26]. Energy factor is the water heaters overall energy efficiency, listed by manufacturer.

Heat loss rate, $P_{loss} = P_{loss,L} + P_{loss,U}$

$$P_{loss,L} = \left(\frac{1.5}{ef}\right) * \left[\frac{A_L(T_{mixed} - T_{env})}{R}\right] * \frac{1}{3412}$$

$$P_{loss,U} = \left(\frac{1.5}{ef}\right) * \left[\frac{A_U(T_{hot} - T_{env})}{R}\right] * \frac{1}{3412}$$

$$P_{loss} = \left(\frac{1.5}{ef}\right) * \left[\frac{A_L(T_{mixed} - T_{env})}{R} + \frac{A_U(T_{hot} - T_{env})}{R}\right] * \frac{1}{3412}$$

Water flow adjustment:

Hot water consumption rate depends on the water temperature. Users have their preferred temperature of mixed water coming out of the fixture. If hot water temperature is low then users increase hot water flow to obtain proper mix for desired temperature. Therefore, water flow data available for a reference hot water temperature (e.g. 140 °F) should be adjusted according to the actual hot water temperature. Hot water flow adjustment can be done by using following equation:

$$f_T = f_{ref} * \frac{(T_{ref} - T_{inlet})}{(T_{actual} - T_{inlet})}$$

Underwriters Laboratory (UL) requires all new water heaters have a factory default temperature set-point at 125 °F or below [28]. After purchase, customers can reset the temperature setting to any other temperature according to their wish.

4.4 Determination of Power Demand and Temperature Profile

Electric water heater power demand depends on the temperature profile of hot water. If temperature of water falls below threshold level then heating coil turns on to reheat water. Water temperature profile can be obtained by using equation (4.1) and (4.2). By putting values of $P_{transfer}, P_{hw}, P_{loss,U}$ etc. in equation (4.1) we get,

$$or, S * D * V_U * \frac{dT_{hot}}{dt} = \eta_{wh} * SW_U * P_{rated} + S * D * f * (T_{mixed} - T_{inlet}) - S * D * f * (T_{hot} - T_{inlet}) - \left(\frac{1.5}{ef}\right) * \left[\frac{A_U(T_{hot} - T_{env})}{R}\right] * \frac{1}{3412}$$

$$or, \int dT_{hot} = \frac{1}{S * D * V_U} \int [\eta_{wh} * SW_U * P_{rated} + S * D * f * (T_{mixed} - T_{inlet}) - S * D * f * (T_{hot} - T_{inlet}) - \frac{1.5}{ef} * \{\frac{A_U(T_{hot} - T_{env})}{R * 3412}\}] dt. \ldots\ldots (4.3)$$

Similarly, by putting values of $P_{transfer}, P_{coil,L}, P_{loss,L}$ etc. in equation (4.2) we get,

$$S * D * V_L * \frac{dT_{mixed}}{dt} = \eta_{wh} * SW_L * P_{rated} - S * D * f * (T_{mixed} - T_{inlet}) - \left(\frac{1.5}{ef}\right) * \left[\frac{A_L(T_{mixed} - T_{env})}{R}\right] * \frac{1}{3412}$$

$$or, \int dT_{mixed} = \frac{1}{S * D * V_L} \int [\eta_{wh} * SW_L * P_{rated} - S * D * f * (T_{mixed} - T_{inlet}) - \frac{1.5}{ef} * \{\frac{A_L(T_{mixed} - T_{env})}{R}\} * \frac{1}{3412}] dt \ldots\ldots\ldots\ldots\ldots\ldots\ldots\ldots\ldots\ldots (4.4)$$

Here, it is noticeable that values such as $P_{transfer}, P_{hw}, P_{loss,U}, P_{loss,L}$ are dependent on either T_{hot} or T_{mixed}. Similarly, $P_{coil,U}, P_{coil,L}$ are also dependent on T_{hot} and T_{mixed}

respectively, because of switching dependencies. Equations (4.1) and (4.2) are differential equations which can be solved by numerical method. For this purpose, it is considered that temperature change (ΔT) during time duration Δt will be linear if the value of Δt is small (e.g. 1 minute). In that case, we can obtain following iterative forms of equation (4.1) and (4.2) respectively:

$$S * D * V_U * (\Delta T_{hot})_{k+1} = \left(\left[P_{coil,U} + P_{transfer} - P_{hw} - P_{loss,U}\right]\right)_k * \Delta t \quad \ldots\ldots\ldots \quad (4.5)$$

$$S * D * V_L * (\Delta T_{mixed})_{k+1} = \left(\left[P_{coil,L} - P_{transfer} - P_{loss,L}\right]\right)_k * \Delta t \quad \ldots\ldots\ldots\ldots\ldots . \quad (4.6)$$

$$(T_{mixed})_{k+1} = (T_{mixed})_k + (\Delta T_{mixed})_{k+1}$$

$$(T_{hot})_{k+1} = (T_{hot})_k + (\Delta T_{hot})_{k+1}$$

$$\left(P_{transfer}\right)_{k+1} = S * D * f * ((T_{mixed})_{k+1} - T_{inlet});$$

$$(P_{hw})_{k+1} = S * D * f * ((T_{hot})_{k+1} - T_{inlet}); \ etc.$$

Simulations are performed in Matlab. Iterations are performed for every minute. Temperature variation during one minute is almost linear. Smaller time units also produce similar results. However, simulation time increases significantly if the interval time step is reduced.

4.5 Model Validation

4.5.1 Comparison with Published Result

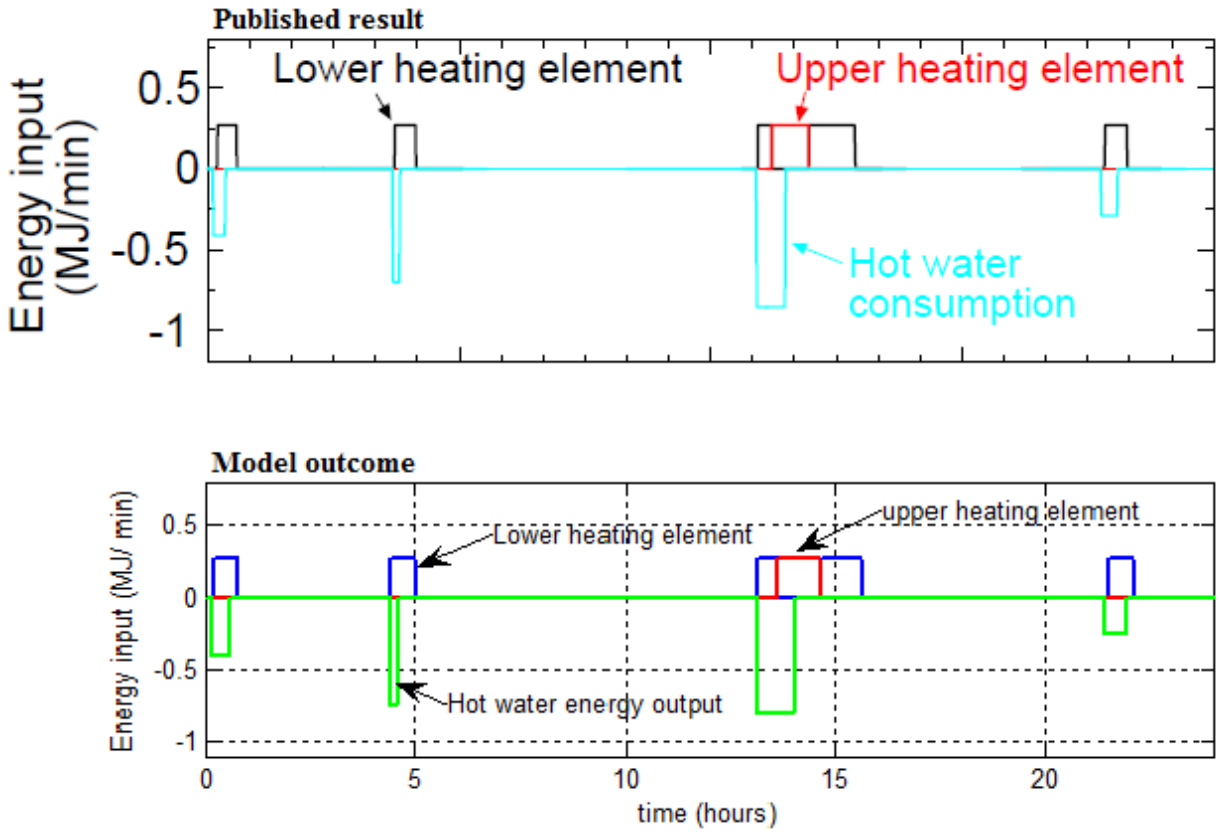

Fig. 4.2: Comparison of water heater model outcome with published result in [14].

Profile of hot water consumption and associated energy demand profile electric water heater is provided in [14]. Profile from literature is shown in the upper part of Fig. 4.2. Similar inputs are provided to the developed Matlab model of electrical water heater. Energy demand profile obtained from the model is provided in the lower part of Fig. 4.2. Model output matches with the published demand profile.

For test simulation, two constant hot water flow rates are considered. Afterwards simulation is performed to observe if the behavior of the water heater model is in accordance with theoretically expected outcome.

Parameters used for simulation are given below:

Tank vol.	:	85	gal
Lower vol.	:	65	gal
Upper vol.	:	20	gal
T_{set}	:	125	°F
δ	:	5	°F
T_{in}	:	60	°F
T_{env}	:	70	°F
η_{wh}	:	0.95	

4.5.2 Test-Case 1: Hot water's constant flow rate of 0.5 gallon per minute

Expected outcome:

In this case, 0.5 gallons of hot water flow out in every 60 seconds. Temperature of water is risen from 60 °F (inlet) to 125 °F (outlet). Therefore,

$$Energy\ output\ =\ 0.5\ *\ 3.7854\ *\ 1\ *\ 4200\ *\ 65\ *\ 5/9\ *\ 1/1000\ =\ 287\ kJ$$

Possible amount of energy input from heating coils is,

$$Energy\ input\ =\ \eta_{wh}\ *\ P_{rated}\ *\ 60\ =\ 0.95\ *\ 4.5\ *\ 60\ =\ 256\ kJ$$

$$Energy\ input\ <\ Energy\ output$$

Similarly, it can also be shown that energy input is lower than energy output in case of any outlet hot water temperature between 120 °F to 130 °F. Therefore, it is expected that this water heater will run under stressed condition in case of 0.5 gpm constant water draw. Upper heating coil is expected to turn-on. Reserved water will keep losing energy over time. Thus, the turn-on

frequency of upper coil is also expected to increase. Over all temperature should also decrease over time.

Simulation results are obtained for a 4.5 kW electric water heater and 0.5 gallon per minute (gpm) constant hot water draw. Results are shown below:

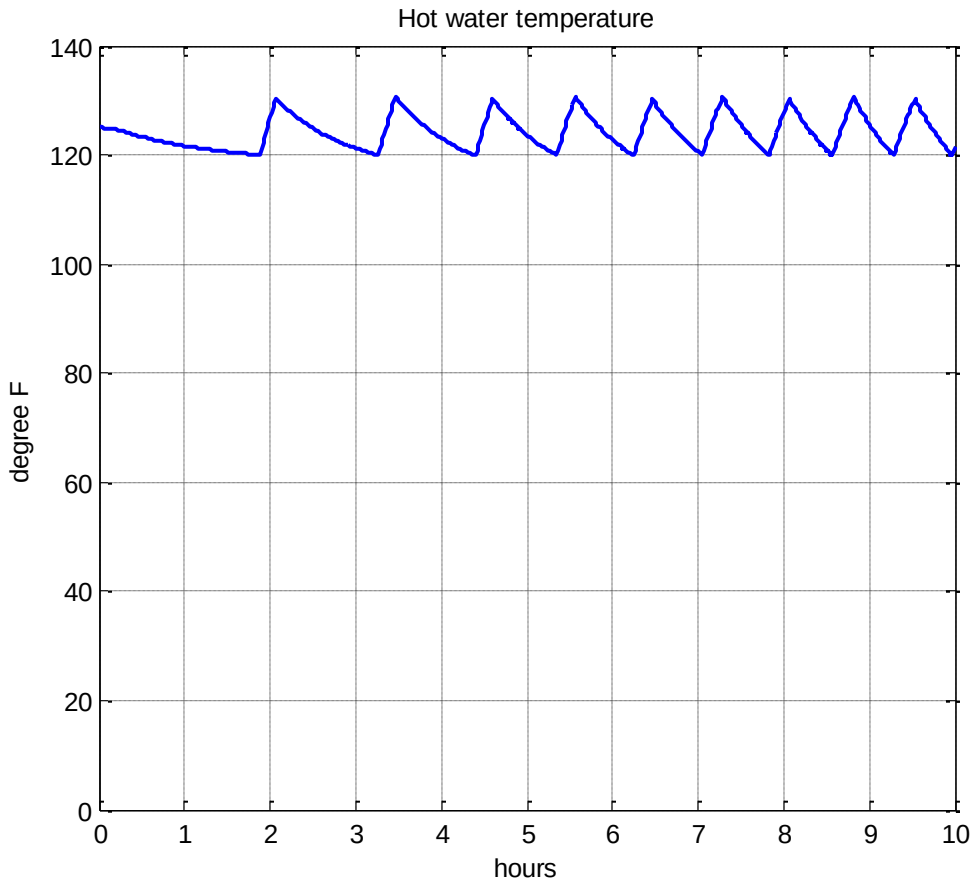

Fig. 4.3: Outlet hot water temperature profile, in case of continuous water draw rate of 0.5 gpm.

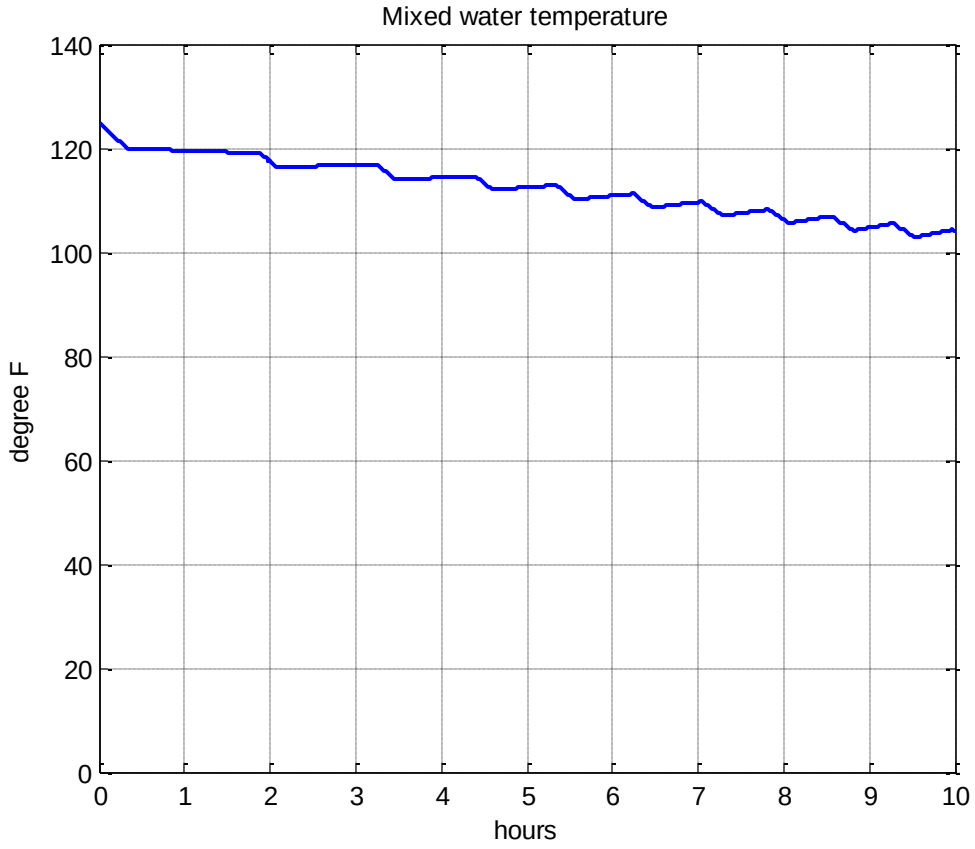

Fig. 4.4: Lower level mixed water temperature profile, in case of continuous water draw rate of 0.5 gpm. (Overall water temperature decreases, as expected in case of stressed condition).

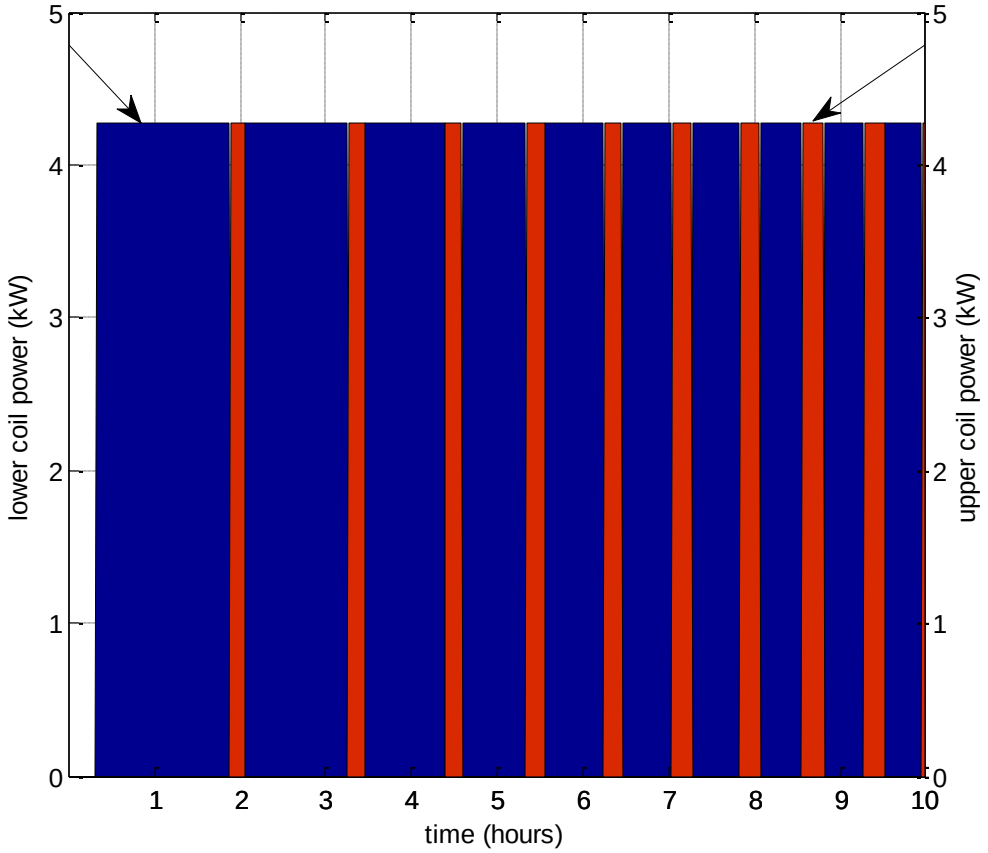

Fig. 4.5: Power profiles of lower (blue) and upper (red) heating coils, in case of continuous water draw rate of 0.5 gpm. Turn-on frequency of upper heating coil increases, as expected.

Comparison of simulation results with expected outcomes:

- It can be seen from Fig. 4.4, that overall temperature of reserved water in the tank decreases with time. This is an expected result.
- It can be observed from Fig. 4.5 that turn-on frequency of upper heating coil increases with time. This is because the energy supplied from lower heating coil cannot fully replenish the energy released with hot water. Therefore, overall energy of the hot water reserve drops over time. Upper heating coil only turns on during stressed condition. Therefore, this observation is also in accordance with expected outcome.

4.5.3 Test-Case 2: Hot water's constant flow rate of 0.3 gallon per minute

Expected outcome:

In this case, 0.3 gallons of hot water flow out in every 60 seconds. Temperature of water is risen from 60 °F (inlet) to 125 °F (outlet). Therefore,

$$Energy\ output\ =\ 0.3\ *\ 3.7854\ *\ 1\ *\ 4200\ *\ 65\ *\ 5/9\ *\ 1/1000\ =\ 172\ kJ$$

Possible amount of energy input from heating coils is,

$$Energy\ input\ =\ \eta_{wh}\ *\ P_{rated}\ *\ 60\ =\ 0.95\ *\ 4.5\ *\ 60\ =\ 256\ kJ$$

$$Energy\ input\ >\ Energy\ output$$

Similarly, it can also be shown that energy input is higher than energy output even in case of any hot water temperature between 120 °F to 130 °F. Therefore, it is expected that this water heater will run under regular operating condition in case of 0.3 gpm constant water draw. Upper heating coil is expected to remain off. Lower heating coil will only turn-on periodically.

Simulation results are obtained for a 4.5 kW electric water heater and 0.3 gallon per minute (gpm) constant hot water draw. Results are shown below:

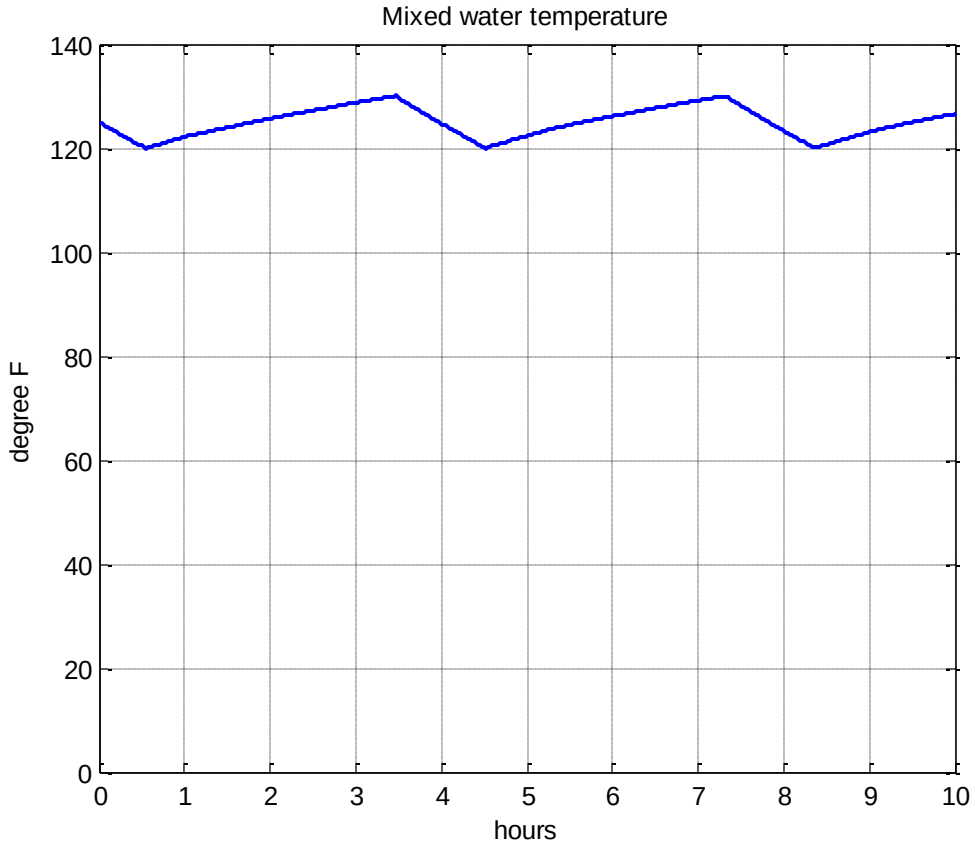

Fig. 4.6: Lower level mixed water temperature profile, in case of continuous water draw rate of 0.3 gpm. (Overall water temperature varies between 120 °F to 130 °F, as expected for regular operation).

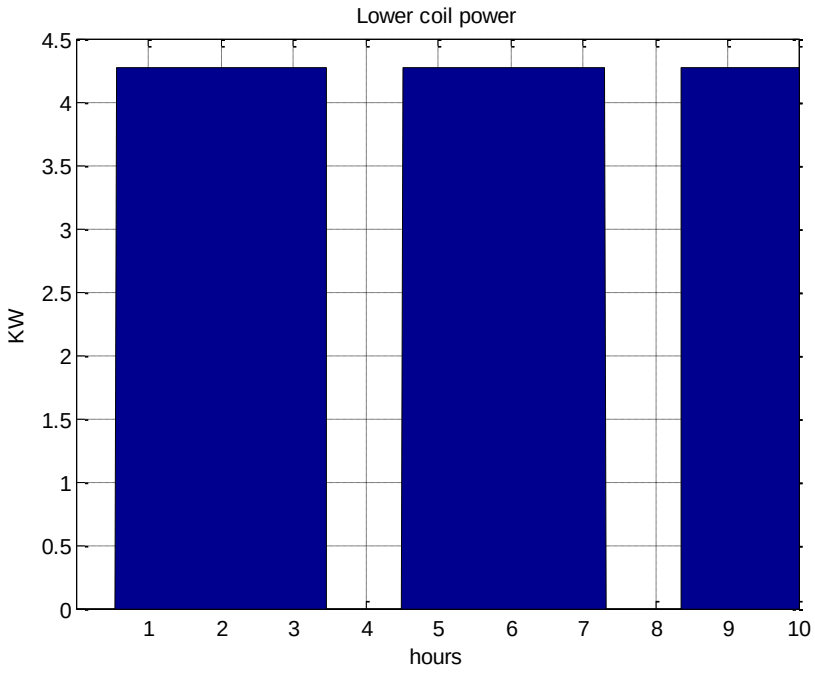

Fig. 4.7: Lower heating coil power profile, in case of continuous water draw rate of 0.3 gpm. (Lower heating coil only turns on periodically, as expected).

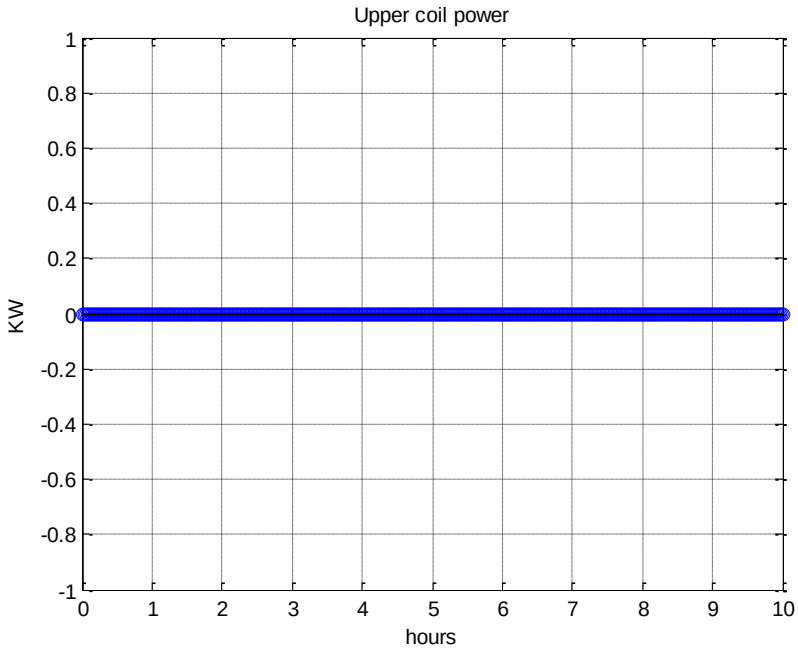

.

Fig. 4.8: Upper heating coil power profile, in case of continuous water draw rate of 0.3 gpm. (Upper heating coil remains turned off, as expected)

Comparison of simulation results with expected outcomes:

- It can be seen from Fig. 4.6 that overall temperature of tank water varies between 120 °F to 130 °F. This is an expected result for regular operation of water heater.
- It can be observed from Fig. 4.7 that lower coil of the water heater only turns on periodically. This is because the energy supplied from lower heating coil can fully replenish the energy released with hot water. Therefore, upper heating coil remains off for the entire duration (Fig. 4.8).

Therefore, all the simulation results of both test cases are valid with respect to the theoretically expected outcomes.

CHAPTER 5

Air-Conditioning Load Model

PARAMETER NOTATIONS

A_{floor}	Total floor space of a house
A_{wall}	Area of walls of a house
A_{window}	Area of windows of a house
C_{air}	Thermal capacitance of indoor air of a house
$C_{thermal}$	Combined thermal capacitance of a house
$C_{thermal.mass}$	Thermal mass heat capacitance of a house
cop	Coefficient of performance
E_{ac}	Air-conditioning energy demand during demand response event
$G_{leakage}$	Leakage thermal conductivity of house
$H_{air.cond}$	Heat removal rate of air-conditioner
$H_{element}$	Heat release rate of indoor elements of a house
H_{gain}	Net heat gain rate of a house
H_{out2in}	Heat absorption rate of a house from outside
$P_{ventilation}$	HVAC power demand for ventilation/ air circulation
$R_{ceiling}$	Insulation level of ceiling
$R_{thermal}$	Combined thermal resistance of a house
R_{wall}	Insulation level of wall
R_{window}	Insulation level of window
T_{avg}	Average outdoor temperature during demand response event
$Time_{dr}$	Demand response event duration
T_{in}	Indoor temperature of house
T_{out}	Outdoor temperature of a house
Δ_{ac}	Pre-cooling temperature reduction of air-conditioner

5.1 Thermal Equivalent Circuit of a Simple House

Let us consider a simple house with boundary surface areas: A_{wall}, $A_{ceiling}$ and A_{window} (in ft^2). Similarly, insulation values are R_{wall}, $R_{ceiling}$ and R_{window} (in ft^2hr°F/btu). So, equivalent heat conductivity for this house can be expressed by the following equation:

$$\mathrm{G} = \left(\frac{A_{wall}}{R_{wall}} + \frac{A_{ceiling}}{R_{ceiling}} + \frac{A_{window}}{R_{window}}\right) + G_{leakage}$$

Unit of G can be readjusted from Btu/(hr-°F) to kW/°F by dividing by 3412. Leakage conductivity ($G_{leakage}$) is the heat gain of a house during summer through window opening, sun shine, door opening etc. Thermally sealed houses have lower leakage gain. Combined thermal resistance (in °F/ kW unit) of the house can be expressed as,

$$\mathrm{R_{thermal}} = \frac{1}{\mathrm{G}} = \frac{3412}{\left[\left(\frac{A_{wall}}{R_{wall}} + \frac{A_{ceiling}}{R_{ceiling}} + \frac{A_{window}}{R_{window}}\right) + G_{leakage}\right]}$$

$R_{thermal}$ is the equivalent thermal resistance of a house. Conduction, convection and radiation heat resistances work in parallel [32]. Therefore, their combined effect can be modeled by an equivalent resistance $R_{thermal}$. Thermal equivalent circuit with analogy to electrical circuit is discussed in [13]. Analogy table is provided below:

Table 5.1: Thermal to electrical analogies of various parameters [13].

Thermal		Electrical	
Heat flow rate	H = Q/ t	Current	I
Temperature	T	Voltage	V
Thermal Resistance	$R_{thermal}$	Resistance	R
Heat Capacity	$C_{thermal}$	Capacitance	C

Following the similar concept of [13], summer time thermal equivalent circuit of this simple house is shown in Fig. 5.1. Outdoor environment works as a heat source. Heat flow rate inside a house is proportional to outdoor and indoor temperature difference. It is inversely proportional to

the thermal resistance of house. Thermal capacity of the house is modeled by $C_{thermal}$. Rate of indoor temperature change ($\frac{dT_{in}}{dt}$) is inversely proportional to thermal capacitance of the house.

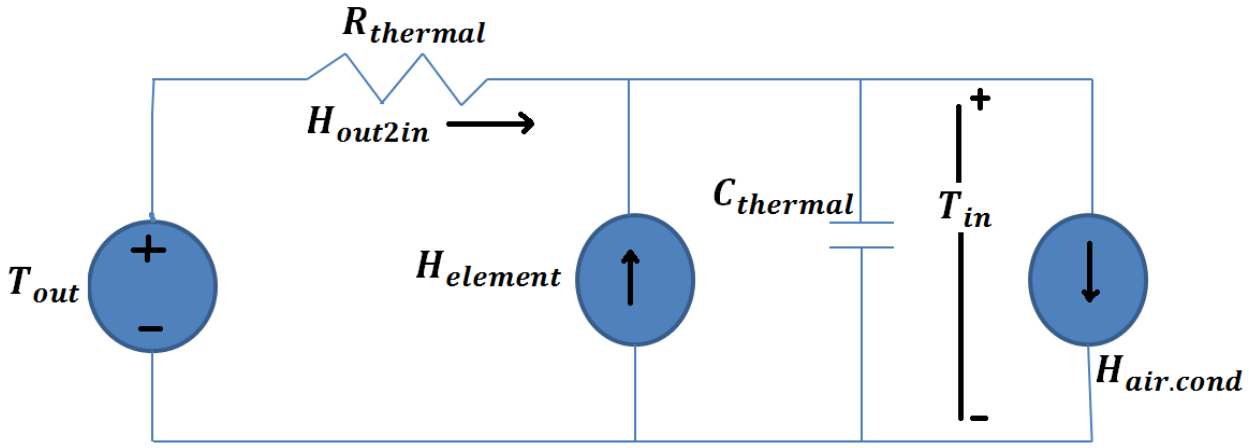

Fig. 5.1: Thermal equivalent circuit of a simple house.

In the equivalent circuit, heat flow rate from outside to inside of the house depends on outdoor and indoor temperature difference and thermal resistance of the house. Household elements such as human, appliances, light bulbs etc. also produce heat that contributes to temperature rise. This component of heat is modeled by heat flow rate $H_{elements}$. Total heat release rate of human skin is 91.7 J/s-m^2 [34]. Usual heat release rate of human body is considered in the range of 116 J/s.

Heat capacity of a house is presented by $C_{thermal.}$ It is a measure of required heat energy for 1 unit increase of temperature of the house. Heat capacity of the house depends on the specific heat capacity of air, volume of indoor air and also volume and specific heat capacity of other heat absorbing materials in the house. Heat capacity of air mass of the house can be computed by the following equation:

$$C_{air} = S_{air} * D_{air} * AirVolume; \qquad unit: kWh/°F$$

[Specific heat (S), density (D)]

Heat gain rate of the house:

$$H_{out2in} = \frac{T_{out} - T_{in}}{R_{thermal}}$$

Heat gain rate of thermal capacitance or net heat gain rate of the house can be found by using similar concept of Kirchhoff's current law.

$$H_{gain} = H_{out2in} + H_{elements} - H_{air.cond}$$

$H_{air.cond}$ is the rate of heat removal by the air conditioner. H_{out2in} depends on outside and inside temperature difference. $H_{elements}$ also depends on inside temperature. However, since inside temperature of an air-conditioned house is supposed to be nearly constant, thus $H_{elements}$ is considered constant for a particular house. With the analogy to electrical capacitance, voltage and current, following relationship can be written:

$$H_{gain} = C_{thermal} * \frac{dT_{in}}{dt} \dots\dots\dots\dots\dots\dots\dots (5.1)$$

In thermal equilibrium condition, inside temperature of the house is constant. Thus, $\frac{dT_{in}}{dt} = 0$. This results in net heat gain rate of the house $H_{gain} = 0$. Thus, heat removal rate of air-conditioner during thermal equilibrium [$H_{air.cond}$] can be found by the following equation:

$$[H_{air.cond}] = H_{out2in} + H_{elements}$$

Coefficient of performance of air-conditioner is directly related to SEER (Seasonal Energy Efficiency Ratio) value. $P_{ventilation}$ is the required power for air circulation and latent heat removal by air-conditioner.

SEER Rating: This rating of air-conditioner is the ratio of cooling output in Btu (British thermal unit) during a typical cooling-season and total electric energy input in watt-hours during the same period. Higher SEER rating of an air-conditioning unit indicates better energy efficiency. Minimum acceptable value of SEER is 13 in the USA [36]. However, cutting edge appliances are available with ratings as high as SEER 24.5 [37].

5.2 Thermal Capacitance of a House

Thermal capacitance of indoor air is calculated by using the values provided in Table 5.2.

Table 5.2: Parameters for the calculation of thermal capacitance of indoor air.

Parameters	Values
S_{air}	1005 $JKg^{-1}k^{-1}$
D_{air}	1.205 Kg m^{-3}
Floor space	2500 ft^2
Average room height	10 ft
Cubic feet to cubic meter conversion	0.0283168
ΔK or ΔC to ΔF conversion (Celsius to Fahrenheit)	9/5
Joule to kWh conversion	$(1000*3600)^{-1}$

However, total thermal mass of a house is much larger than the value of C_{air}. Various important parameters for the calculation of thermal mass of a house are: heat absorption capabilities of various structural materials, surface areas of those materials, effective heat absorption depth etc. Houses with high thermal mass are less sensitive to the outside temperature fluctuation. Therefore, thermal mass is an important criterion for comfortable building design. Volumetric thermal mass values of various building materials are available in [38]. Values are shown in Table 5.3.

Table 5.3: Volumetric thermal mass values of various common materials [38].

	Density (Kg/m^3)	Specific Heat (KJ/Kg.K)	Volumetric Thermal Mass ($KJ/m^3.K$)
Water	1000	4.186	4186
Concrete	2240	0.92	2060
Brick	1700	0.92	1360
Stone (Sandstone)	2000	0.9	1800
Rammed Earth	2000	0.837	1673
Wood	480	1.883	904
Compressed Earth Blocks	2080	0.837	1740

Various dimensions and associated R-values for a house of floor space 2500 ft^2 are provided in Table 5.4.

Table 5.4: Dimensions and insulation/ R-values of a house.

Area	Area (ft^2)	R value (ft^2 °F h/Btu) [8]
Floor	2500	
Ceiling	2500	R-30
Wall	2000	R-16
Window	250	R-3

Effective heat absorption depth is 3 inch (0.25 ft) [38]. Leakage heat gain is related to the level of insulation of the house.

5.3 Load Calculation and Sizing of Air-Conditioner

Basic load calculation of a house is a process of looking at the house as a whole and calculating thermal load without considering room to room temperature variations. This is also called block load calculation. Several considerations for block load calculation are listed below [39]:

- Foundation type
- Roof type and color
- Insulation values (R values) of walls, floors, and ceilings
- Window and door types, locations, and quantities
- Desired inside temperature and expected ranges of outside temperature
- Area and size/ volume of the house

However, block load calculation only provides rough insight about the thermal load of a house. It does not account for the room to room temperature variations. Therefore, 'Air Conditioning Contractors of America (ACCA)' provides standard and methodology to calculate residential heat gain and loss more accurately. Proprietary computer programs are available, which take into account every details of the construction and perform load calculation considering temperature

balance of all the rooms and areas of the house. There are varied opinions available in internet regarding rule of thumb for the sizing of air-conditioning (1 ton per 400 to 700 square feet, depending on insulation). However, load calculation is essential for accurate HVAC sizing for a house. Let us consider a 2500 square feet house. Two air-conditioning units for this house can be of capacity 21,500 Btu/hr supporting 1400 square feet and 18,000 Btu/hr supporting 1100 square feet [40], (1 Ton = 12000 Btu/hr).

Table 5.5: Examples of 3-stage air-conditioning units with various ratings [40].

Model	Ton	Square feet	Power rating	SEER rating
Frigidaire FRS22PYS2	1.8	1400	1.79 kW (0.5 kW – 2.65 kW)	18
Frigidaire FRS18PYS2	1.5	1100	1.5 kW (0.38 kW – 2.65 kW)	18

1 Ton = 12000 Btu/hr. Therefore, ratings of the air-conditioning units approximately follow the upper bound of per ton coverage rule of thumb. FRS22PYS2 air conditioners have variable speed compressor which adapts speed according to the difference between room temperature and temperature set-point. There are usually three speeds of operation, e.g. 1200, 1050 and 900 rpm. Similarly, fan speed is also variable, providing air volume output of maximum/ medium/ minimum cfm (cubic feet per minute), e.g. 470, 411, 353 cfm. However, more advanced HVAC units, such as Frigidaire iQ Drive can provide seamlessly variable speed of compressor with the help of inverter-driver based technology. Let us consider an iQ drive HVAC system with following configurations:

Table 5.6: Example of iQ Drive air-conditioning unit.

Model	Ton	Coverage area	Power rating	SEER rating
iQ Drive HVAC	3	2500 ft^2	Rated 3.5 kW (.5 kW – 5 kW)	22

Inverter drive technology allows variable speed of the compressor at any required level depending on the difference between temperature set-point and actual temperature of the house. Comparison between 3-stage unit and iQ drive technology is provided in Table 5.7 ([37], [40]).

Table 5.7: Comparison between traditional 3-stage air-conditioner and iQ Drive air-conditioner.

	3-stage air-conditioner	iQ Drive
Compressor speed (rpm)	1200/ 1050/ 900 (e.g.)	any
Air circulation (cfm)	470/ 411/ 353 (e.g.)	any
SEER rating (typical)	13 to 18	22 to 24

Variable power and energy demands of air-conditioning are discussed in [41]. Dependency on outside temperature and different temperature set-points are also discussed in [41].

5.4 Indoor Temperature Profile Determination

Indoor temperature of a house depends on heat flow rate from outside to inside, air-conditioning heat removal rate, thermal capacitance of the house etc. In the previous section, we have already found equation (5.1) as following,

$$H_{gain} = C_{thermal} * \frac{dT_{in}}{dt}$$

Therefore, indoor temperature of an air-conditioned house can be determined by following equation,

$$\int dT_{in} = \frac{1}{C_{thermal}} * \int H_{gain} dt$$

$$or, \int dT_{in} = \frac{1}{C_{thermal}} * \int (H_{element} + H_{out2in} - H_{air.cond})\, dt$$

$$or, \int dT_{in} = \frac{1}{C_{thermal}} * \int (H_{element} + \frac{(T_{out} - T_{in})}{R_{thermal}} - H_{air.cond})\, dt \quad \ldots\ldots\ldots\ldots (5.2)$$

(5.1) is a differential equation. Therefore, indoor temperature change can be calculated by numerical method. For small time steps Δt, temperature rise of the house can be calculated by following iterative equation:

$$[\Delta T_{in}]_{k+1} = \frac{H_{element} + \frac{(T_{out} - T_{in})_k}{R_{thermal}} - (H_{air.cond})_k}{C_{thermal}} * \Delta t \ldots\ldots\ldots\ldots\ldots\ldots\ldots (5.3)$$

Therefore, indoor temperature profile can be calculated by using equation (5.3). Iteration is done for every 1 minute time interval. Air-conditioning demand profiles are investigated in Chapter 6 to find out demand response participation potential.

Simulations are performed in Matlab. Similar to the electric water heater case, the time step for air-conditioning simulation is chosen at one minute intervals. This is because temperature variation during one minute is almost linear. Smaller time units also produce similar result. However, simulation time increases significantly if simulation intervals are reduced.

5.5 Model Validation

5.5.1 Comparison with Published Result

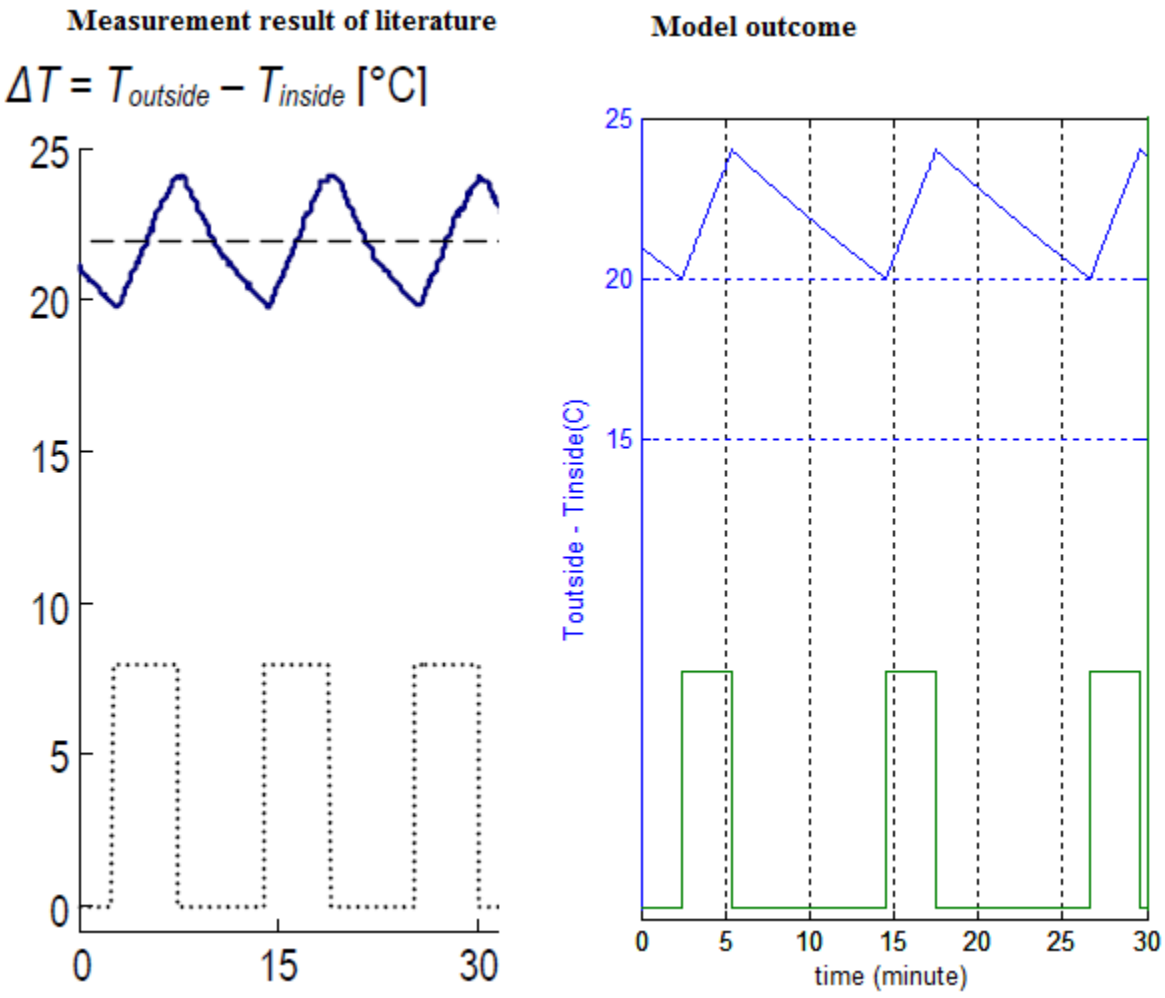

Fig. 5.2: Comparison of model outcome and the measurement data published in [13].

Temperature and power demand measurement results are provided in [13]. Similar input is provided to the model to observe demand and temperature profiles. Model outcome is similar to the measurement based plot provided in [13].

5.5.2 Test-Case 1: Constant Outdoor Temperature of 90 °F

Let's consider temperature set-point of a house is 72 °F. Heat gain rate from outside is = 18 *3412/1.71 = 36127 btu/hr. Internal heat gain is considered 1700 btu/hr. Therefore, combined heat gain rate = 37827 btu/hr. Air-conditioning is configured to remove heat at a rate of 36000 btu/hr. So, net heat gain is 1827 btu/ hr. Therefore, indoor temperature should rise slowly from the set-point level. Simulation result is provided in Fig. 5.3.

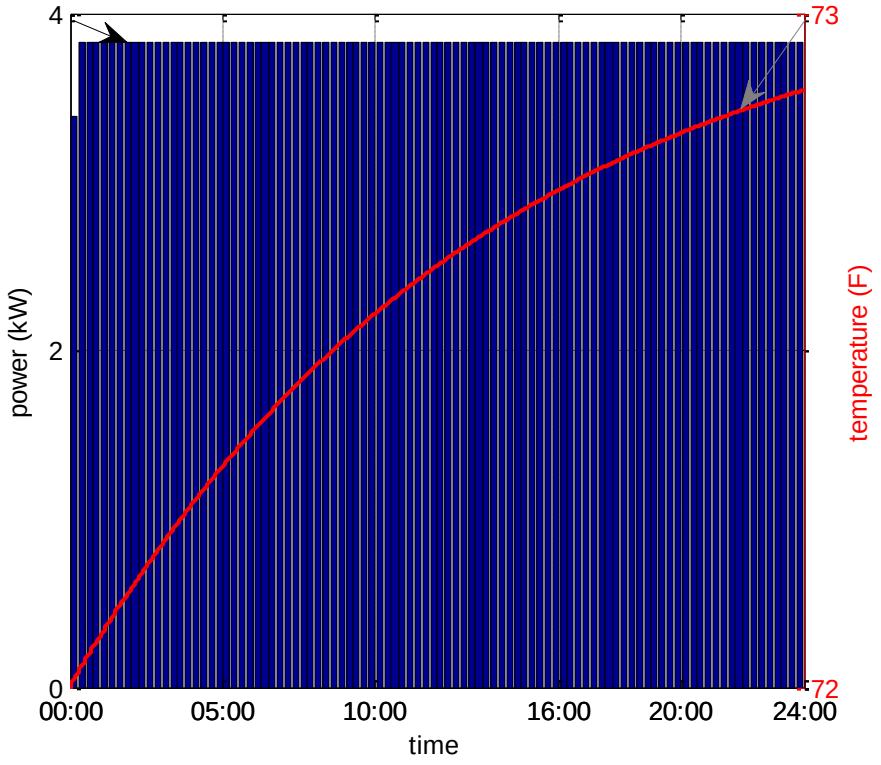

Fig. 5.3: Indoor temperature profile for test-case 1 (constant outdoor temperature of 90 °F). Indoor temperature rises very slowly, as expected.

5.5.3 Test-Case 2: Constant Outdoor Temperature of 89 °F

If outdoor temperature is constant at 89 °F then combined heat gain is, (89-72) * 3412/ 1.71 + 1700 = 35620 btu/ hr. Therefore, heat gain rate is lower than the heat removal capacity of the considered air-conditioner. It is expected that indoor temperature will remain at the temperature set-point level. Simulation result is provided in Fig. 5.4.

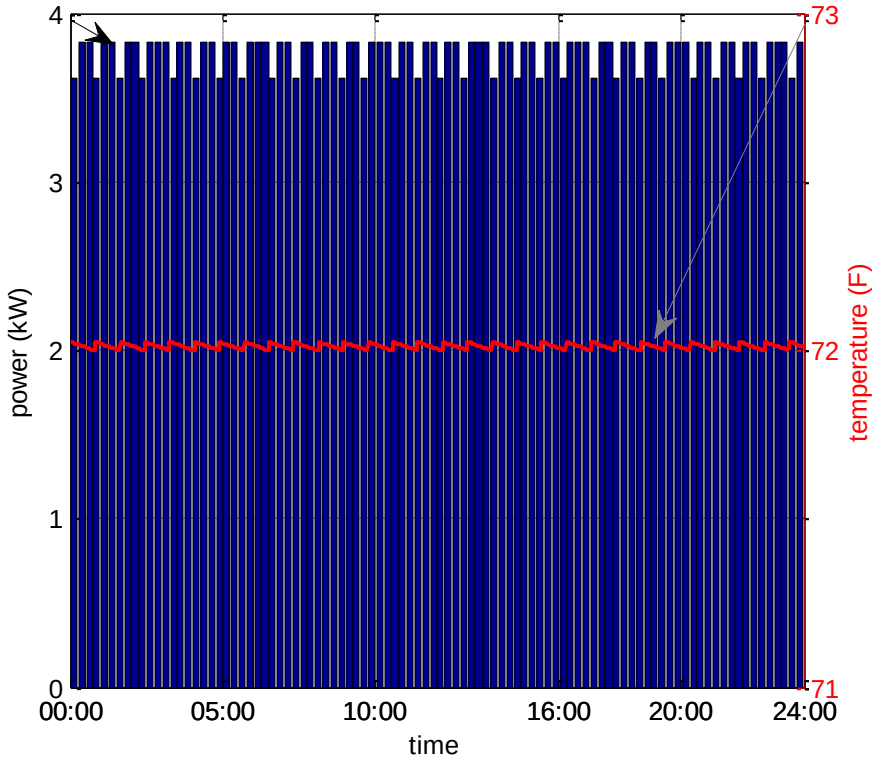

Fig. 5.4: Indoor temperature profile for test-case 2 (constant outdoor temperature of 89 °F). Indoor temperature remains tied to T_{set}, as expected.

It can be seen from Fig. 5.4 that indoor temperature remains at the set-point level. Moreover, compressor speed of air-conditioner decreases periodically for short durations. For that reason, average power consumption reduces slightly periodically. Results obtained in Fig. 5.3 and Fig. 5.4 are both valid in comparison to the expected outcomes.

CHAPTER 6

Demand Response Participation of Residential Loads

Some residential loads are suitable for demand response participation such as electric water heater, HVAC, clothes-dryer, dishwasher, electric vehicle charging etc. First two loads refer to thermal loads. Three other loads are deferrable for short duration without significantly impacting users' comfort and lifestyle. Various aspects of demand response participation potential of air-conditioning and water heating loads will be discussed in this chapter.

6.1 Demand Response Participation of Electric Water Heater

PARAMETER NOTATIONS

A	Area of water heater tank
D	Density of water
E_{loss}	Thermal energy loss of hot water during demand response event
$E_{supplied}$	Energy of supplied hot water during demand response event
E_{wh}	Energy demand by the water heater during demand response event
ef	Energy factor of water heater
f	Hot water flow rate
$P_{coil,L}$	Power from lower coil
$P_{coil,U}$	Power from upper coil
P_{rated}	Power rating of water heater
R	Thermal insulation of water heater tank
S	Specific heat of water
SW_L	Switch state of lower coil (state '1' for on and state '0' for off)
SW_U	Switch state of upper coil (state '1' for on and state '0' for off)
T	Steady state temperature of hot water
T_{dr}	Readjusted temperature set-point for water preheating
T_{hot}	Hot water temperature of upper layer
T_{inlet}	Temperature of inlet water
T_{mixed}	Temperatures of lower mixed water

T_{out}	Outdoor temperature of a house
T_{set}	Regular Temperature set-point of water heater
V	Volume of water heater tank
V_L	Water volumes of lower level of electric water heater
V_U	Water volumes of upper level of electric water heater
η_{wh}	Efficiency of coils of water heater
δ	Temperature dead-band for water heating

For demand response participation of electric water heating load, first it is required to determine the potential amount of energy demand by the electric water heater during a demand response event. Afterwards, it is required to determine appropriate control strategy to obtain load reduction to meet demand response target. Water can be preheated during off peak hours to obtain hot water reserve to avoid peak time operation. Demand response event is declared at least 23 hours earlier in time. Thus, preheating can be done during the hours of low demand. Two important considerations for preheating are following:

1. Amount of preheating: Temperature set-point of hot water should be raised to an upper level to obtain adequate thermal reserve for demand response day.
2. Time of preheating: High temperature of hot water results in high rate of thermal energy loss. Therefore, heating time of hot water should not be long before the time of use. On the other hand, demand response event is usually called on a day of peak demand. Thus, excessive water heating near the demand response event can cause unwanted secondary peak. To avoid this kind of side-effect, pre-heating start time is kept in the morning off-peak hours of demand response day.

6.1.1 Preheating Temperature Set-point Calculation

From the electric water heater model of Chapter 4, following two equations are found,

$$S * D * V_U * \frac{dT_{hot}}{dt} = \eta_{wh} * SW_U * P_{rated} + S * D * f * (T_{mixed} - T_{inlet}) - S * D * f * (T_{hot} - T_{inlet}) - \left(\frac{1.5}{ef}\right) * \left[\frac{A_U(T_{hot} - T_{env})}{R}\right] * \frac{1}{3412} \quad \ldots\ldots\ldots (6.1)$$

$$S * D * V_L * \frac{dT_{mixed}}{dt} = \eta_{wh} * SW_L * P_{rated} - S * D * f * (T_{mixed} - T_{inlet}) - \left(\frac{1.5}{ef}\right) * \left[\frac{A_L(T_{mixed} - T_{env})}{R}\right] * \frac{1}{3412} \ldots\ldots\ldots\ldots\ldots\ldots\ldots\ldots\ldots\ldots\ldots\ldots\ldots\ldots (6.2)$$

In case of steady state operation of water heater as thermal energy storage, T_{mixed} and T_{hot} become same. Therefore, in steady state $T_{mixed} = T_{hot} = T$. Total thermal loss of water heater is represented by P_{loss}. Total volume of the tank $V = V_L + V_U$. Combined switching state $SW = SW_U + SW_L$. Therefore, equation (6.1) and (6.2) can be combined as following:

$$S * D * V * \frac{dT}{dt} = \eta_{wh} * SW * P_{rated} - S * D * f * (T - T_{inlet}) - P_{loss} \ldots\ldots\ldots\ldots (6.2)$$

$$or, S * D * V * \int dT = \int [\eta_{wh} * SW * P_{rated} - S * D * f * (T - T_{inlet}) - P_{loss}]\, dt$$

$$or, S * D * V * \int dT = \eta_{wh} * \int SW * P_{rated} dt - \int S * D * f * (T - T_{inlet}) dt - \int P_{loss}\, dt \ldots. (6.3)$$

Energy demand by water heater, $E_{wh} = \int SW * P_{rated} dt$

Thermal energy of supplied hot water, $E_{supplied} = \int S * D * f * (T - T_{inlet}) dt$

Thermal energy loss, $E_{loss} = \int P_{loss}\, dt$

So, equation (6.3) becomes,

$$or, S * D * V * \int dT = \eta_{wh} * E_{wh} - E_{supplied} - E_{loss}$$

For regular operation:

$\int dT \approx 0$; Hot water temperature should remain around T_{set}

So, $\eta_{wh} * E_{wh} \approx (E_{supplied} + E_{loss})$

For demand response participation:

$E_{wh} = 0$

$(E_{supplied} + E_{loss}) = \eta_{wh} * \ demand\ response\ target\ energy\ reduction = \ \eta_{wh} * E_{dr}$

Therefore,

$$S * D * V * \int_{DR} dT = -\eta_{wh} * E_{dr} \ldots\ldots\ldots\ldots\ldots (6.4)$$

Minus (-) sign indicates temperature drop. New temperature set-point (T_{dr}) is required to provide additional thermal storage on the day of demand response. For a preheating temperature set-point T_{dr}, hot water can have any temperature between (T_{dr} + δ) and (T_{dr} – δ) just before demand response event, to keep the coils turned off. We need to ensure that water temperature will not reach as low as regular (T_{set} – δ) during DR event. Therefore, for the duration of demand response event-

$$\int_{DR} dT = -\big((T_{dr} \pm \delta) - (T_{set} - \delta)\big)$$

From (6.4),

$$\big((T_{dr} \pm \delta) - (T_{set} - \delta)\big) = \frac{\eta_{wh} * E_{dr}}{S * D * V}$$

Therefore,

$$T_{dr} = T_{set} + \frac{\eta_{wh} * E_{dr}}{S * D * V} - x\,; \qquad x = [0\ to\ 2\delta]; \ldots\ldots\ldots (6.5)$$

Required value of 'x' can vary from 0 to 2δ depending on initial condition of hot water just before demand response event. Temperature set-point manipulation for water preheating is shown in Fig. 6.1. Temperature set-point is raised to T_{dr} before demand response event. Adequate time has to be provided to raise water temperature from T_{set} to T_{dr}. Moreover, it is preferable to preheat water during off-peak hours. Just in the beginning of demand response event, temperature set-point is reduced down to the original level T_{set}.

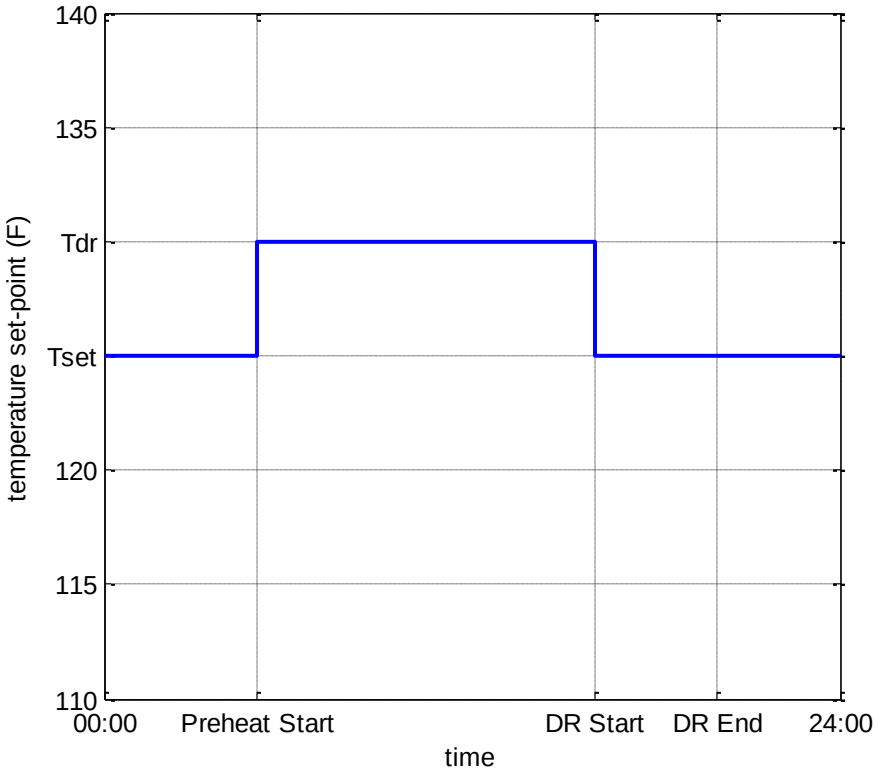

Fig. 6.1: Temperature set-point manipulation for water preheating.

6.1.2 Case Studies and Validation of Water Preheating Method

To verify the effectiveness of water pre-heating, let's consider some known hot water consumption profiles taken from IEA website [31]. Simulation is performed for electric water heater's regular operation with temperature set-point at 125 °F. Tank volume and all other parameters are kept same as of Chapter 4. Afterwards, a demand response event is considered between 4 pm to 8 pm. Demand response temperature set point (T_{dr}) is calculated for those scenarios to observe if that temperature set-point manipulation can effectively avoid water heater operation during the demand response event. Simulation results are provided for various days of June.

June 01, 02:

There is no power demand between 4 pm to 8 pm. Therefore, temperature set-point manipulation is not required in these two days.

June 03:

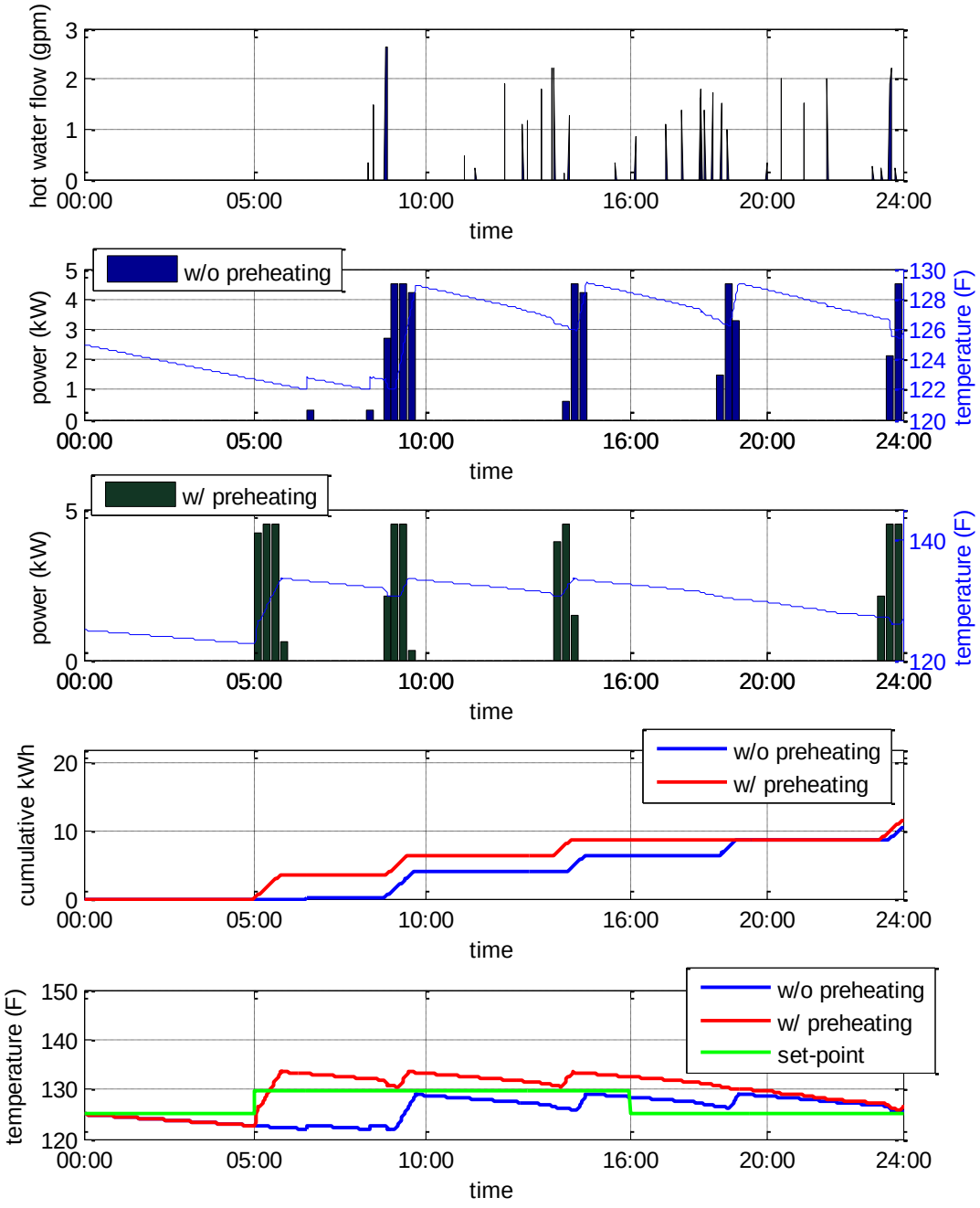

Fig. 6.2: Comparison between profiles with and without preheating for power demand, cumulative energy demand and hot water temperature. June 03. DR event is hours 16-20.

Temperature set-point manipulation is required to avoid water heating power demand during demand response event hours (4 pm to 8 pm). Hot water consumption profile of June 03 is shown in first subplot of Fig. 6.2. Demand profile without water preheating is shown in second subplot of Fig. 6.2. There is 2.32 kWh of energy demand during the demand response event hours (16-20) of June 03. To shift this demand away, temperature set-point is increased from 125 °F to 129.6 °F (calculated value). It can be observed from the third subplot of Fig. 6.2 that power demand is completely shifted away from the demand response event duration (4 pm to 8 pm) in case of preheating operation. Comparison of cumulative energy demands without and with preheating is shown in fourth subplot Fig. 6.2. Total energy demand is slightly higher in case of water preheating operation. Energy demand slightly increases because thermal energy loss increases with hot water temperature. Comparison of hot water temperature profiles is shown in fifth subplot of Fig. 6.2. It can be seen from the third subplot of Fig. 6.2 that modified temperature set-point successfully reduce energy demand during demand response event hours from 2.32 kWh to 0 kWh. In case of June 03, additional energy requirement for different preheating start times are shown in Table 6.1.

Table 6.1: Additional energy demand for various preheating start times (date: June 03)

Start time (am)	Additional energy (kWh)
5	1.01
8	0.975
10	0.6

Therefore, if the preheating start time is delayed then energy loss reduces. In the case studies, preheating start times are kept in the off-peak hours.

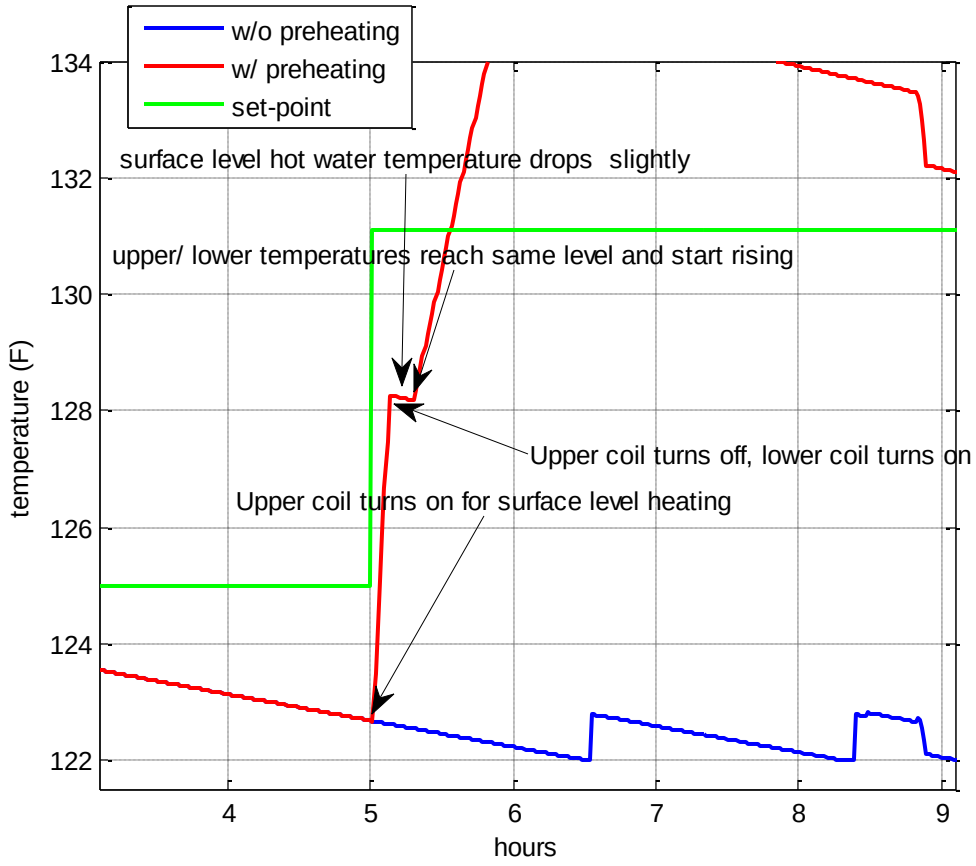

Fig. 6.3: Explanation of changes of hot water temperature profile during preheating (June 03).

It can be seen from Fig. 6.3 that temperature set-point is raised to T_{dr} at 5 am in the morning. In that case, upper thermostat of water heater turns on upper heating coil to increase temperature of surface level hot water. In case of abrupt change in temperature set-point, upper heating coil turns off when temperature reaches the level ($T_{dr} - \delta$). Afterwards, lower heating coil turns on to heat entire volume of water in the tank. Initially surface level hot water's temperature reduces slightly by mixing with lower level water. Lower coil heats up entire volume of water to the temperature level of surface level hot water. Afterwards, water temperature rises to the level ($T_{dr} + \delta$) and lower coil turns off.

June 04, 05, 06:

Temperature set-point modification is not required. Energy demand during DR event is zero.

June 07:

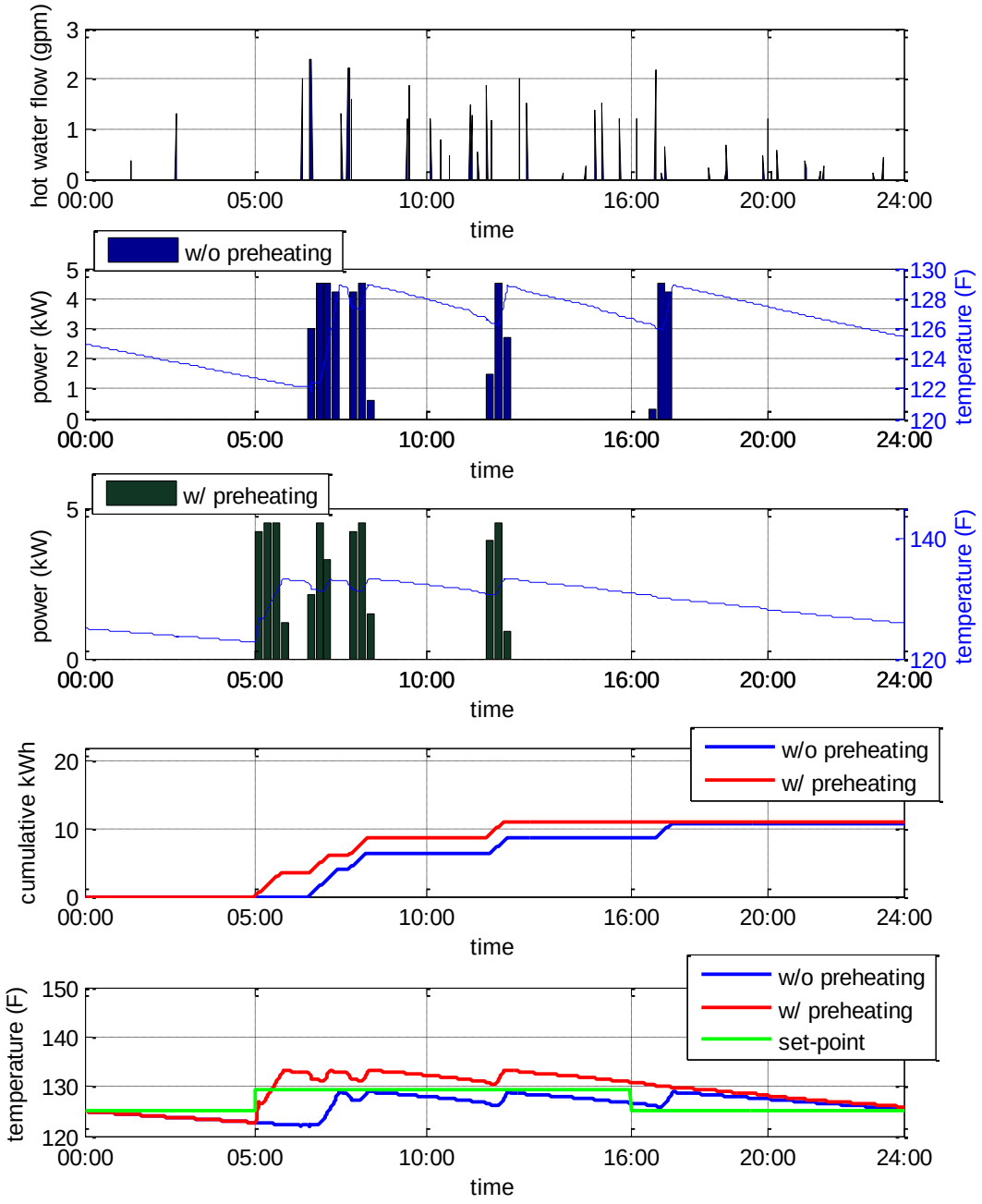

Fig. 6.4: Comparison between profiles with and without preheating for power demand, cumulative energy demand and hot water temperature. June 07. DR event is hours 16-20.

Temperature set-point manipulation is required to avoid water heating power demand during demand response event hours (4 pm to 8 pm). Hot water consumption profile of June 07 is shown in first subplot of Fig. 6.4. Demand profile without water preheating is shown in second subplot of Fig. 6.4. There is 2.25 kWh of energy demand during the demand response event hours (16-20) of June 07. To shift this demand away, temperature set-point is increased from 125 °F to 129 °F (calculated value). It can be observed from the third subplot of Fig. 6.4 that power demand is completely shifted away from the demand response event duration (4 pm to 8 pm) in case of preheating operation. Comparison of cumulative energy demands without and with preheating is shown in fourth subplot Fig. 6.4. Total energy demand is slightly higher in case of water preheating operation. Energy demand slightly increases because thermal energy loss increases with hot water temperature. Comparison of hot water temperature profiles is shown in fifth subplot of Fig. 6.4. It can be seen from the third subplot of Fig. 6.4 that modified temperature set-point successfully reduce energy demand during demand response event hours from 2.25 kWh to 0 kWh.

June08:

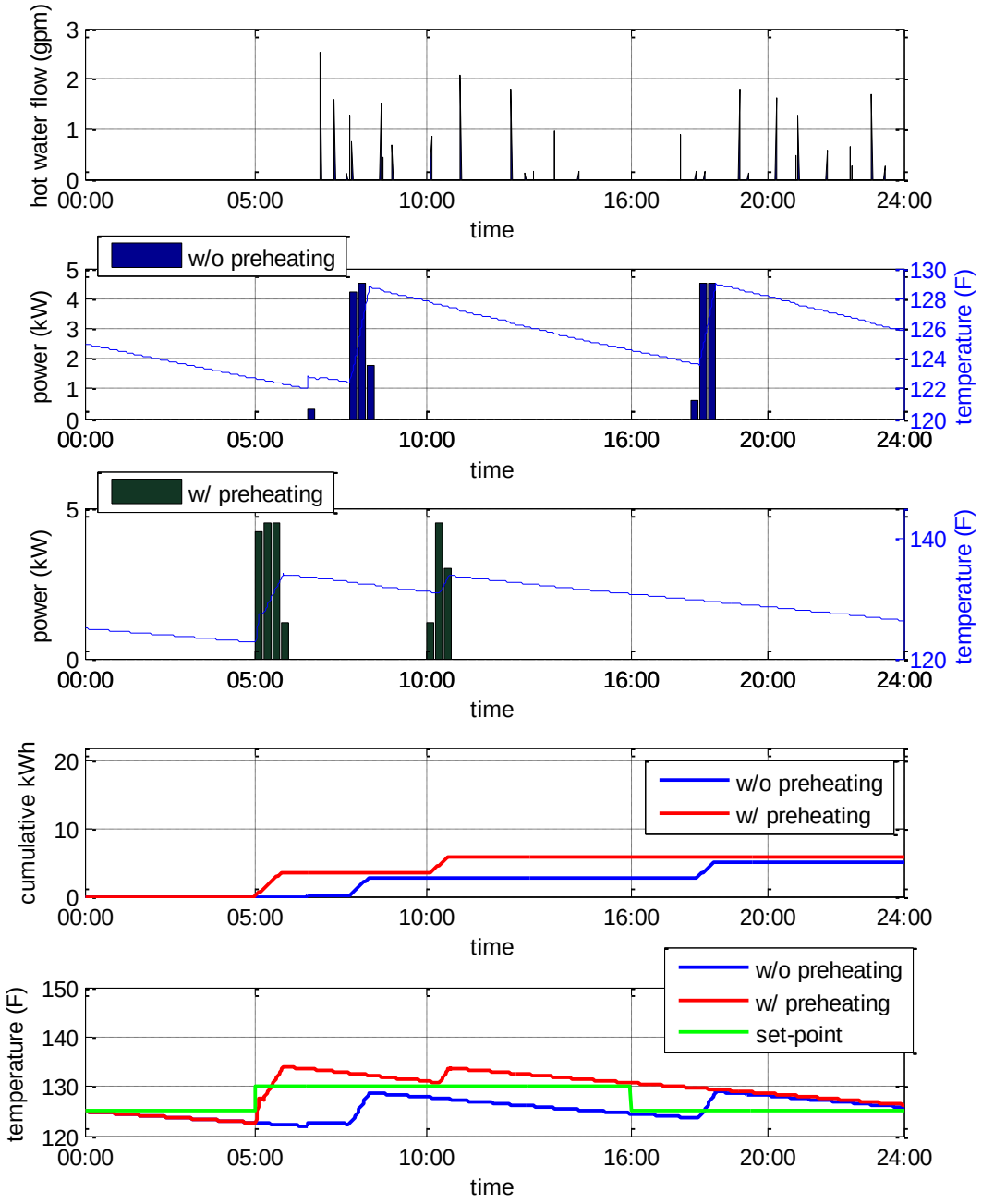

Fig. 6.5: Comparison between profiles with and without preheating for power demand, cumulative energy demand and hot water temperature. June 08. DR event is hours 16-20.

Hot water consumption profile of June 08 is shown in first subplot of Fig. 6.5. Demand profile without water preheating is shown in second subplot of Fig. 6.5. There is 2.4 kWh of energy demand during the demand response event hours (16-20) of June 08. To shift this demand away, temperature set-point is increased from 125 °F to 130 °F (calculated value). It can be observed from the third subplot of Fig. 6.5 that power demand is completely shifted away from the demand response event duration (4 pm to 8 pm) in case of preheating operation. Comparison of cumulative energy demands without and with preheating is shown in fourth subplot Fig. 6.5. Total energy demand is slightly higher in case of water preheating operation. Energy demand slightly increases because thermal energy loss increases with hot water temperature. Comparison of hot water temperature profiles is shown in fifth subplot of Fig. 6.5 It can be seen from the third subplot of Fig. 6.5 that modified temperature set-point successfully reduce energy demand during demand response event hours from 2.4 kWh to 0 kWh.

June 09:

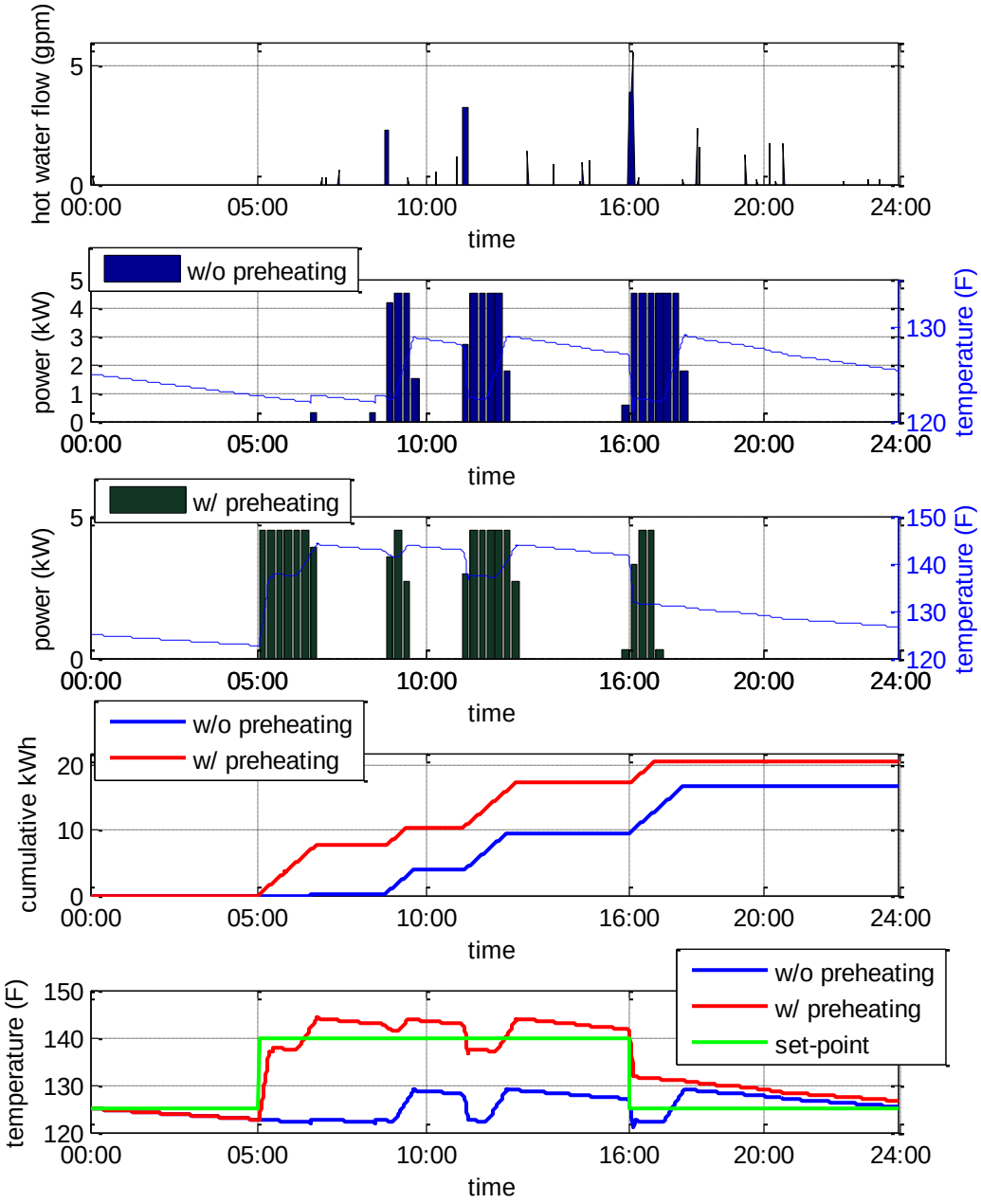

Fig. 6.6: Comparison between profiles with and without preheating for power demand, cumulative energy demand and hot water temperature. June 09. DR event is hours 16-20. Preheat start time 5 am.

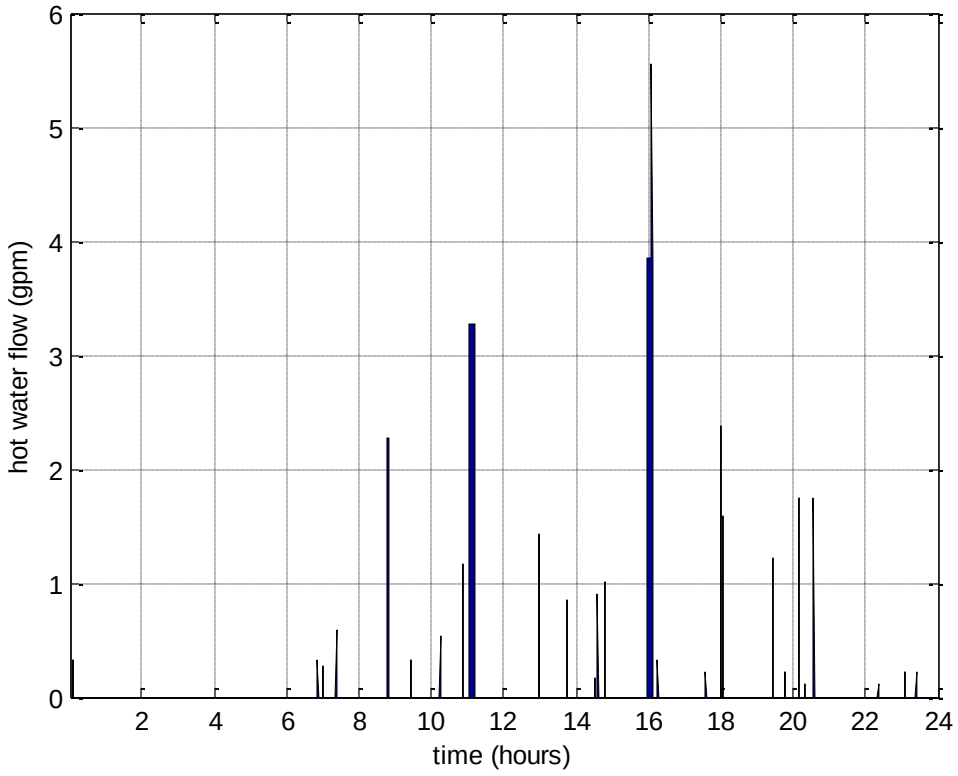

Fig. 6.7: Hot water consumption profile of June 09 (gpm: gallon per minute).

In June 09, hot water consumption between 16th to 20th hours is excessively high. Therefore, associated power demand is also very high. Demand profile without water preheating is shown in second subplot of Fig. 6.6. There is 7.2 kWh of energy demand during the demand response event hours (16-20) of June 09. Required temperature set-point is 154 °F for 100% demand reduction. If maximum allowable temperature set-point of water heater is 140 °F, then demand can only be reduced partially. It can be observed from the third subplot of Fig. 6.6 that power demand is partially shifted away from the demand response event duration (4 pm to 8 pm) in case of preheating operation. Comparison of cumulative energy demands without and with preheating is shown in fourth subplot Fig. 6.6. Cumulative energy demand of June 09 is 3.9 kWh more in case of preheating. This is because of 15 °F rise of temperature. This high temperature caused high rate of thermal energy loss. It can be seen from the fourth subplot of Fig. 6.6 that there is still certain amount of electricity demand by the water heater in hour 16-17. This is because of the excessively high hot water consumption in the 16th hour (can be seen in Fig. 6.7). Very high rate of water flow causes water temperature to drop severely. So, heating coil runs for

a long duration to bring back water temperature to the set-point level. It can be seen from the fifth subplot of Fig. 6.6 that hot water temperature rises slightly above 140 °F. This is because of the temperature deadband (δ). Heating coil stops when water temperature reaches the level T_{set} + δ. Moreover, water temperature of lower part of water heater tank is slightly lower than the surface level hot water. Because, inlet water enters in the lower part. Therefore, outlet hot water temperature can rise slightly above T_{set} + δ. 57% demand reduction has been possible by using 140 °F temperature set-point. Demand response event time energy demand has been reduced from 7.2 kWh to 3.15 kWh, with the help of preheating.

Change of preheating start time:

Cumulative energy demand of June 09 is 3.9 kWh more in case of preheating start time at 5 am. This is because of 15 °F rise of temperature. Increased temperature for long duration resulted high thermal energy loss. However, this thermal loss can be minimized by bringing preheating time closer to demand response event. To verify this, preheat start time is modified to 12 pm and 3 pm. Case study results are shown below:

June 09 (Preheating start time 12 pm):

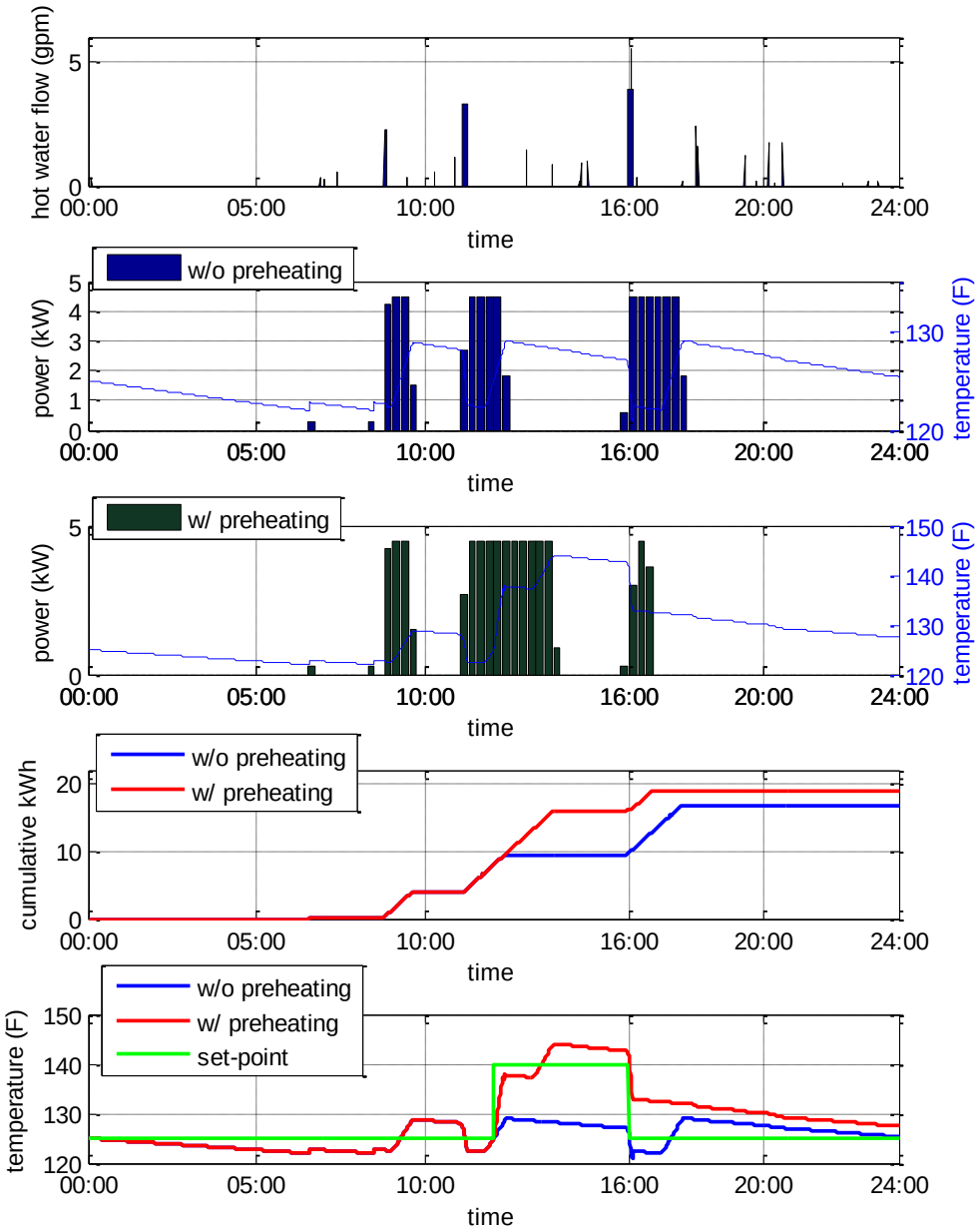

Fig. 6.8: Comparison between profiles with and without preheating for power demand, cumulative energy demand and hot water temperature. June 09. DR event is hours 16-20. Preheat start time 12 pm.

June 09 (Preheating start time 3 pm):

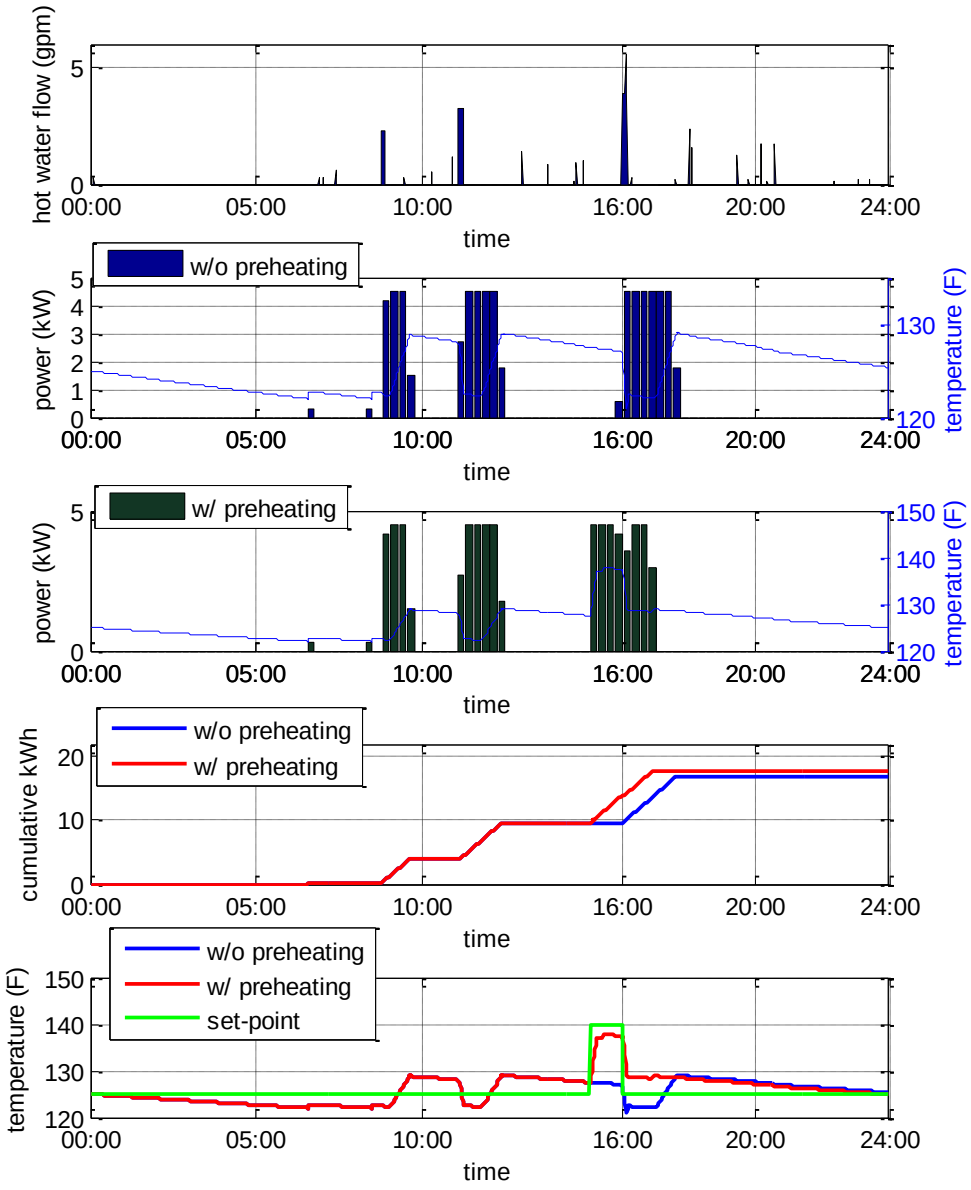

Fig. 6.9: Comparison between profiles with and without preheating for power demand, cumulative energy demand and hot water temperature. June 09. DR event is hours 16-20. Preheat start time 3 pm.

It is observable from fourth subplots of Fig. 6.6, Fig. 6.8, and Fig. 6.9 that cumulative energy demand reduces if preheating start time comes closer to demand response event. Comparison of cumulative energy demands for various pre-heating start times is shown in Fig. 6.10.

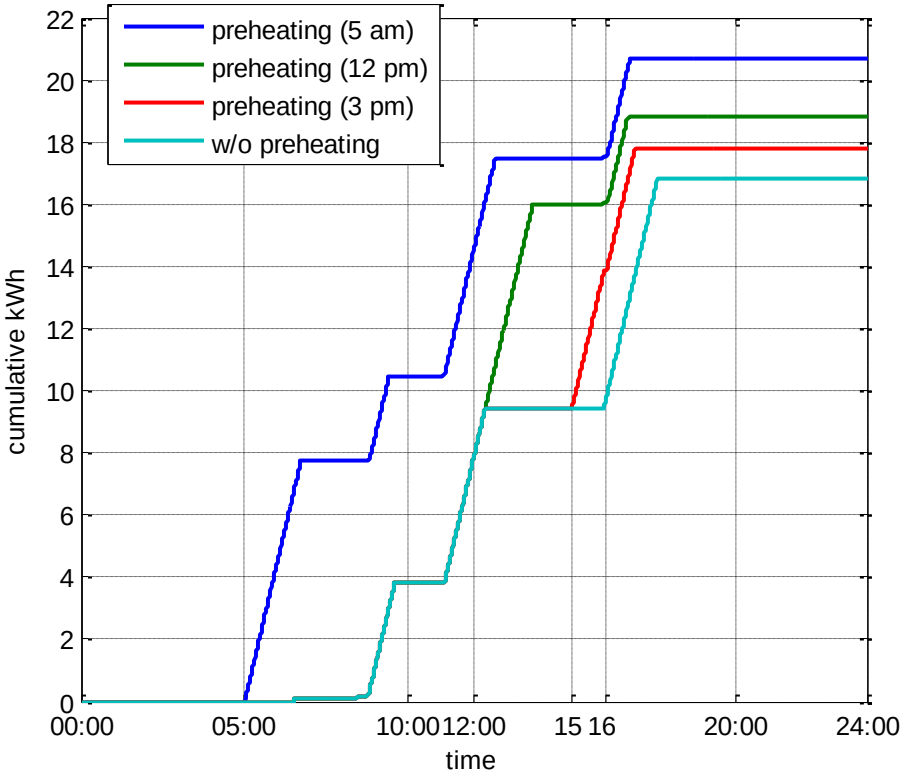

Fig. 6.10: Comparison of cumulative energy demand profiles for various start times of hot water preheating. June 09. DR event is hours 16-20.

It is observable from Fig. 6.10 that total energy demand of 24 hours decreases if preheating start time is closer to demand response event. It is because water temperature remains in the raised level for shorter duration if preheating is delayed. However, this can result in high water heating demand in the hours prior to demand response event. Thus, it can result in a secondary peak. Trade-off should be made between thermal efficiency and demand profile preference.

June 10:

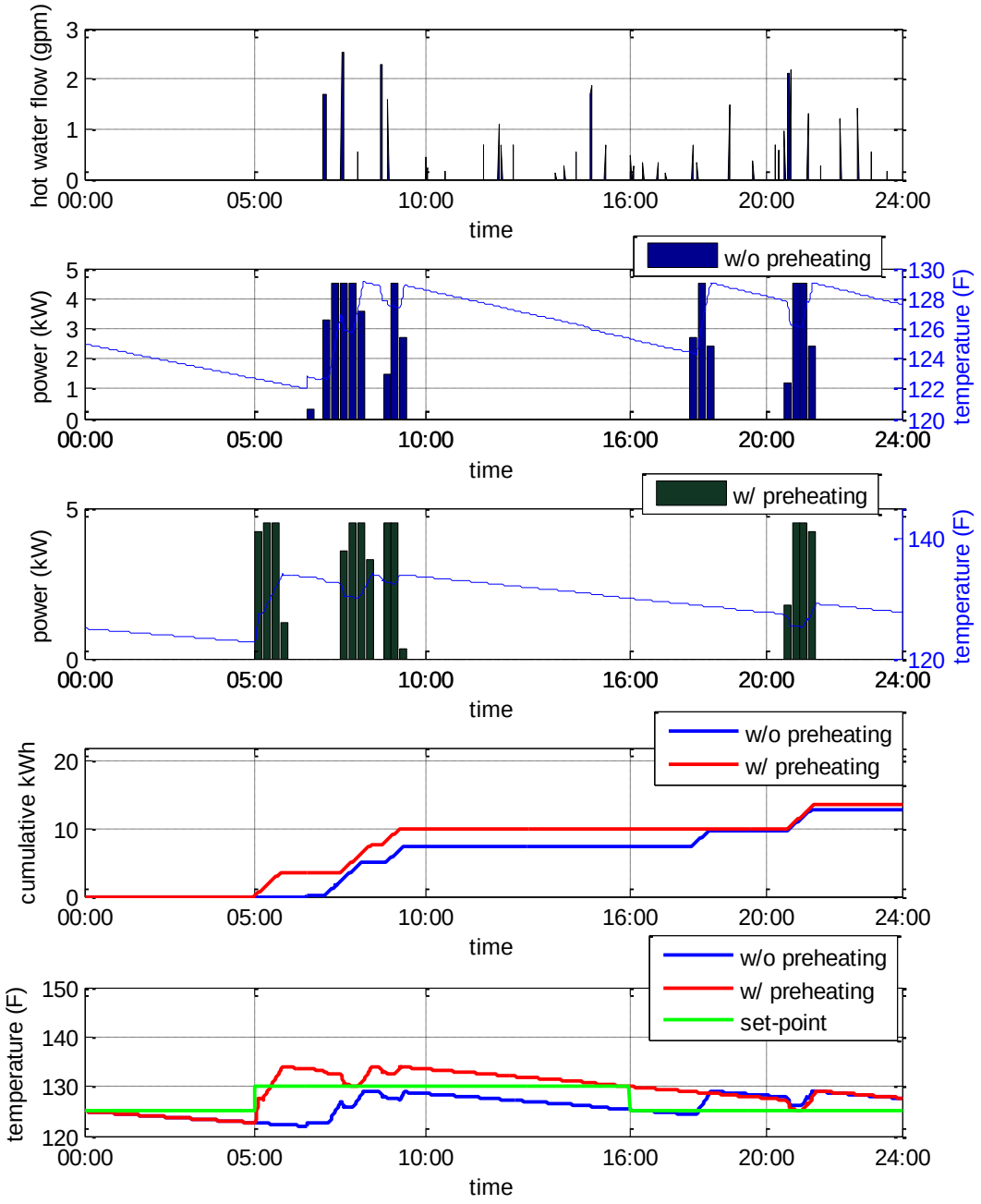

Fig. 6.11: Comparison between profiles with and without preheating for power demand, cumulative energy demand and hot water temperature. June 10. DR event is hours 16-20.

Hot water consumption profile of June 10 is shown in first subplot of Fig. 6.11. Demand profile without water preheating is shown in second subplot of Fig. 6.11. There is 2.4 kWh of energy demand during the demand response event hours (16-20) of June 10. To shift this demand away, temperature set-point is increased from 125 °F to 130 °F (calculated value). It can be observed from the third subplot of Fig. 6.11 that power demand is completely shifted away from the demand response event duration (4 pm to 8 pm) in case of preheating operation. Comparison of cumulative energy demands without and with preheating is shown in fourth subplot Fig. 6.11. Total energy demand is slightly higher in case of water preheating operation. Energy demand slightly increases because thermal energy loss increases with hot water temperature. Comparison of hot water temperature profiles is shown in fifth subplot of Fig. 6.11 It can be seen from the third subplot of Fig. 6.11 that modified temperature set-point successfully reduce energy demand during demand response event hours from 2.4 kWh to 0 kWh.

June 11, 12, 13, 14:

Temperature set-point modification is not required. Energy demand during DR event is zero.

June 15:

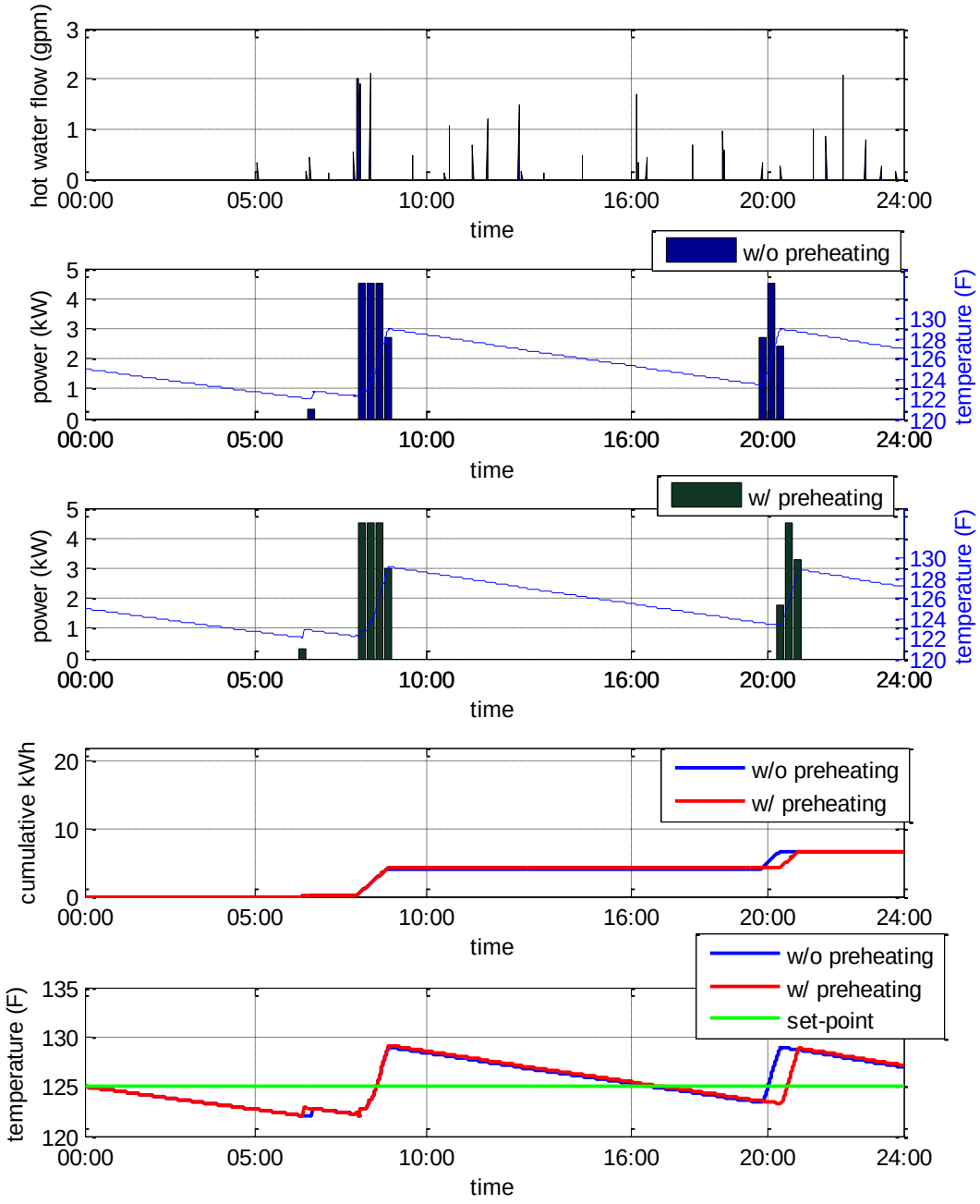

Fig. 6.12: Comparison between profiles with and without preheating for power demand, cumulative energy demand and hot water temperature. June 15. DR event is hours 16-20.

Hot water consumption profile of June 15 is shown in first subplot of Fig. 6.12. Demand profile without water preheating is shown in second subplot of Fig. 6.12. In June 15, there is very little amount of water heating electricity demand just before 8 pm. To shift this demand away, required increase in temperature set-point is less than 1 °F. It can be observed from the third subplot of Fig. 6.12 that power demand is completely shifted away from the demand response event duration (4 pm to 8 pm) in case of preheating operation. Comparison of cumulative energy demands without and with preheating is shown in fourth subplot Fig. 6.12. Comparison of hot water temperature profiles is shown in fifth subplot of Fig. 6.12 It can be seen from the third subplot of Fig. 6.12 that modified temperature set-point successfully reduce energy demand during demand response event hours from 0.7 kWh to 0 kWh.

Summary of water preheating case studies is provided in Table 6.2. It is observable from the table that water heating power demand can be successfully shifted away from demand response event hours by manipulating temperature set-point. However, required preheating temperature set-point requirement can be excessively high if hot water consumption during demand response event is too high. 140 °F is a safe hot water temperature set-point, recommended by ASHRAE [29]. Therefore, temperature set-point is always kept at or below 140 °F. In June 09 excessive hot water demand occurred. Therefore, only partial amount (60%) of electricity demand can be shifted away from demand response event duration (4 pm to 8 pm) by keeping preheat temperature set-point at 140 °F for that particular day. For all other days, 100% of water heating loads have been successfully shifted away from demand response event hours with the help of water preheating.

Table 6.2: Summary of case studies of water heating load control

day	Total 24 hour's energy demand without preheat (kWh)	Total 24 hour's energy demand with preheat (kWh)	Without preheating: Water heating power demands in various hours of demand response event (kW)				With preheating: Water heating power demands in various hours of demand response event (kW)			
			hour 16-17	hour 17-18	hour 18-19	hour 19-20	hours 16-17	hours 17-18	hours 18-19	hours 19-20
1-Jun	12.5	12.5	0	0	0	0	0	0	0	0
2-Jun	6.2	6.2	0	0	0	0	0	0	0	0
3-Jun	10.5	11.6	0	0	1.6	0.75	0	0	0	0
4-Jun	5.1	5.1	0	0	0	0	0	0	0	0
5-Jun	16.1	16.1	0	0	0	0	0	0	0	0
6-Jun	11.7	11.7	0	0	0	0	0	0	0	0
7-Jun	10.8	10.95	1.3	0.98	0	0	0	0	0	0
8-Jun	5.1	5.8	0	0.23	2.2	0	0	0	0	0
9-Jun	16.8	20.7/ 18.8	4.5	2.7	0	0	3.15/ 2.8	0	0	0
10-Jun	12.9	13.65	0	0.75	1.65	0	0	0	0	0
11-Jun	7	7	0	0	0	0	0	0	0	0
12-Jun	7.4	7.4	0	0	0	0	0	0	0	0
13-Jun	12.3	12.3	0	0	0	0	0	0	0	0
14-Jun	14.8	14.8	0	0	0	0	0	0	0	0
15-Jun	6.5	6.6	0	0	0	0.7	0	0	0	0

6.2 Demand Response Participation of Air-Conditioning Load

PARAMETER NOTATIONS

$C_{thermal}$	Combined thermal capacitance of a house
cop	Coefficient of performance
E_{ac}	Air-conditioning energy demand during demand response event
$G_{leakage}$	Leakage thermal conductivity of house
$H_{air.cond}$	Heat removal rate of air-conditioner
$H_{element}$	Heat release rate of indoor elements of a house
H_{gain}	Net heat gain rate of a house
H_{out2in}	Heat absorption rate of a house from outside
$P_{ventilation}$	HVAC power demand for ventilation/ air circulation
$R_{thermal}$	Combined thermal resistance of a house
T_{avg}	Average outdoor temperature during demand response event
$Time_{dr}$	Demand response event duration
T_{in}	Indoor temperature of house
T_{out}	Outdoor temperature of a house
T_{set}	Regular temperature set-point of air-conditioner
Δ_{ac}	Pre-cooling temperature reduction of air-conditioner

Air-conditioning load of a particular house is highly dependent on ambient temperature profile. Pre-cooling provides heat absorption capability to the thermal masses of a house. After pre-cooling, air temperature rises mainly because of the heat leakage component $G_{leakage}$ and indoor heat emissions $H_{elements}$ [44]. Initial conduction heat through exterior wall is absorbed by thermal mass of the building structure (inner 3 inch layer of the building), as discussed in Chapter 5.

6.2.1 Pre-cooling Temperature Set-point Calculation

From equation (5.5) we get following,

$$\int dT_{in} = \frac{1}{C_{thermal}} * \int (H_{element} + \frac{(T_{out} - T_{in})}{R_{thermal}} - H_{air.cond})\, dt$$

$$or, \int dT_{in} = \frac{1}{C_{thermal}} * [\int (H_{element} + \frac{(T_{out} - T_{in})}{R_{thermal}})\, dt - \int H_{air.cond}\, dt] \ldots\ldots\ldots (6.6)$$

Air-conditioning energy demand E_{ac} is related to $H_{air.cond}$ by following relationship:

$$E_{ac} = \int \frac{H_{air.cond}}{cop}\, dt + \int P_{ventilation}\, dt$$

Energy required for air circulation is $E_{ventilation}$. So,

$$E_{ac} = \int \frac{H_{air.cond}}{cop}\, dt + E_{ventilation}$$

$$or, \int H_{air.cond}\, dt = cop * (E_{ac} - E_{ventilation})$$

Therefore, from equation (6.2), it can be written,

$$\int dT_{in} = \frac{1}{C_{thermal}} * [\int \{H_{element} + \frac{(T_{out} - T_{in})}{R_{thermal}}\}\, dt - cop * (E_{ac} - E_{ventilation})]$$

For demand response event duration, Integral $\int dT_{in}$ represents total indoor temperature change. For pre-cooling purpose, temperature set-point will be reduced to (T_{set} - Δ_{ac}). On the other hand, temperature set-point will be increased to (T_{set} + Δ_{ac}) during demand response event. Therefore, total indoor temperature change during demand response event is 2 Δ_{ac}. So, we can write $\int dT_{in} = 2 * \Delta_{ac}$ for the demand response event duration.

$$2 * \Delta_{ac} = \frac{1}{C_{thermal}} * [\int_{t_{dr.start}}^{t_{dr.end}} \{H_{element} + \frac{(T_{out} - T_{in})}{R_{thermal}}\}\, dt - cop * (E_{ac} - E_{ventilation})]$$

$$2 * \Delta_{ac} = \frac{1}{C_{thermal}} * [\{H_{element} * Time_{dr} + \int_{t_{dr.start}}^{t_{dr.end}} \frac{T_{out}}{R_{thermal}}\, dt - \int_{t_{dr.start}}^{t_{dr.end}} \frac{T_{in}}{R_{thermal}}\, dt - cop * (E_{ac} - E_{ventilation})] \ldots\ldots\ldots\ldots\ldots\ldots\ldots\ldots\ldots\ldots\ldots\ldots\ldots\ldots\ldots\ldots\ldots\ldots (6.7)$$

For outdoor temperature data of short time intervals, we can evaluate $\int T_{out}\, dt$ numerically by considering total area under curve as summation of rectangles of small widths. Therefore,

$$\int T_{out}\, dt \approx \sum_{k=1}^{k=N} T_{out.k}\, \Delta t\,; \quad \Delta t\ is\ small\ (e.g.\ 1\ minute)$$

$$or, \int T_{out}\, dt \approx \sum_{k=1}^{k=N} T_{out.k} \frac{Time_{dr}}{N} \quad ; N\ is\ number\ of\ data\ points$$

$$or, \int T_{out}\, dt \approx \frac{\sum_{k=1}^{k=N} T_{out.k}}{N} * Time_{dr}$$

$$or, \int T_{out}\, dt \approx T_{avg} * Time_{dr}$$

T_{avg} is the average outdoor temperature during demand response event. Similarly, T_{in} varies from (T_{set} - Δ_{ac}) to (T_{set} + Δ_{ac}). T_{set} is the regular temperature set-point of air-conditioner. Thus,

$$\int T_{in}\, dt \approx T_{set} * Time_{dr}$$

Therefore, equation (6.7) can be rewritten as following:

$$2 * \Delta_{ac} = \frac{1}{C_{thermal}} * [\{H_{element} + \frac{(T_{avg} - T_{set})}{R_{thermal}}\} * Time_{dr} - cop * (E_{ac} - E_{ventilation})]$$

$$\Delta_{ac} = \frac{1}{2 * C_{thermal}} * [\{H_{element} + \frac{(T_{avg} - T_{set})}{R_{thermal}}\} * Time_{dr} - cop * (E_{ac} - E_{ventilation})] \ldots. (6.8)$$

Value of pre-cooling temperature set-point reduction (Δ_{ac}) can be calculated using equation (6.8). Temperature set-point modification for pre-cooling is shown in Fig. 6.13.

6.2.2 Case Studies for Air-Conditioning Load Control

Simulation is performed by taking upper integer value of the calculated Δ_{ac}. However, temperature set-point reduction or increase is kept up to 3 °F to satisfy thermal comfort of the household residents. Therefore, if calculated value of $\Delta_{ac} > 3$ °F then only partial demand reduction will be possible by setting adjusted set-point at ($T_{set} - 3$). Simulation is performed using the air-conditioner model developed in Chapter 5. Temperature profiles of various days of June are taken from [21]. Regular temperature set-point of the house is considered 72 °F. Pre-cooling is achieved by reducing set-point to the level ($T_{set} - \Delta_{ac}$). Temperature set-point is raised to the level ($T_{set} + \Delta_{ac}$) during a demand response event. Set-point manipulation is shown in Fig. 6.13, in case of $\Delta_{ac} = 3$ °F.

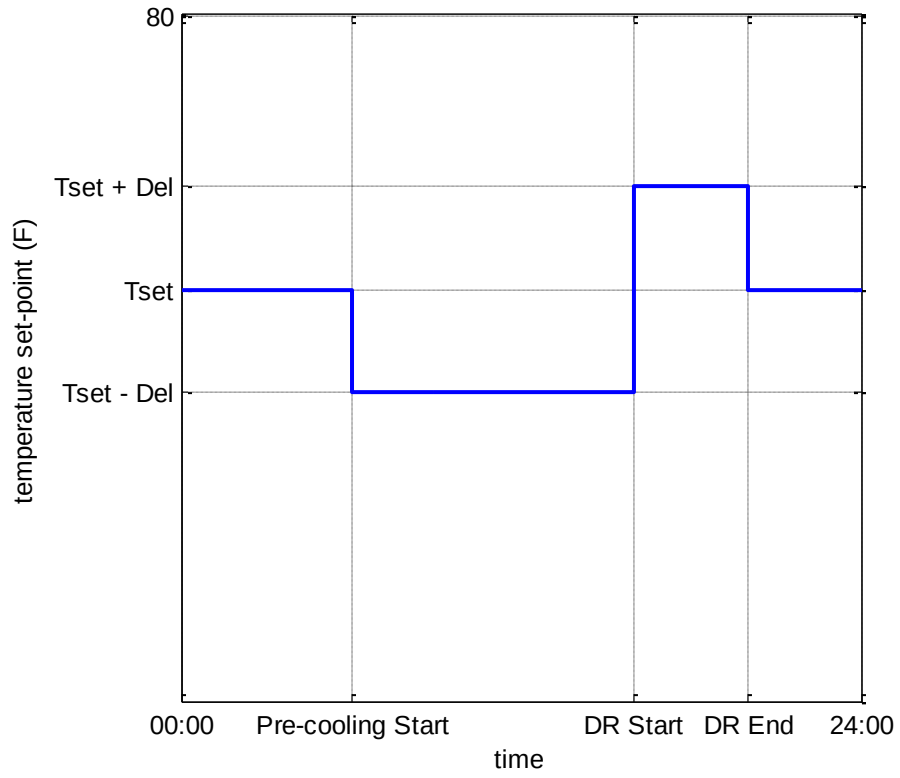

Fig. 6.13: Temperature set-point modification for demand response participation of air-conditioner (pre-cooling).

Simulation results for various days of June 2011 are shown below:

June 01:

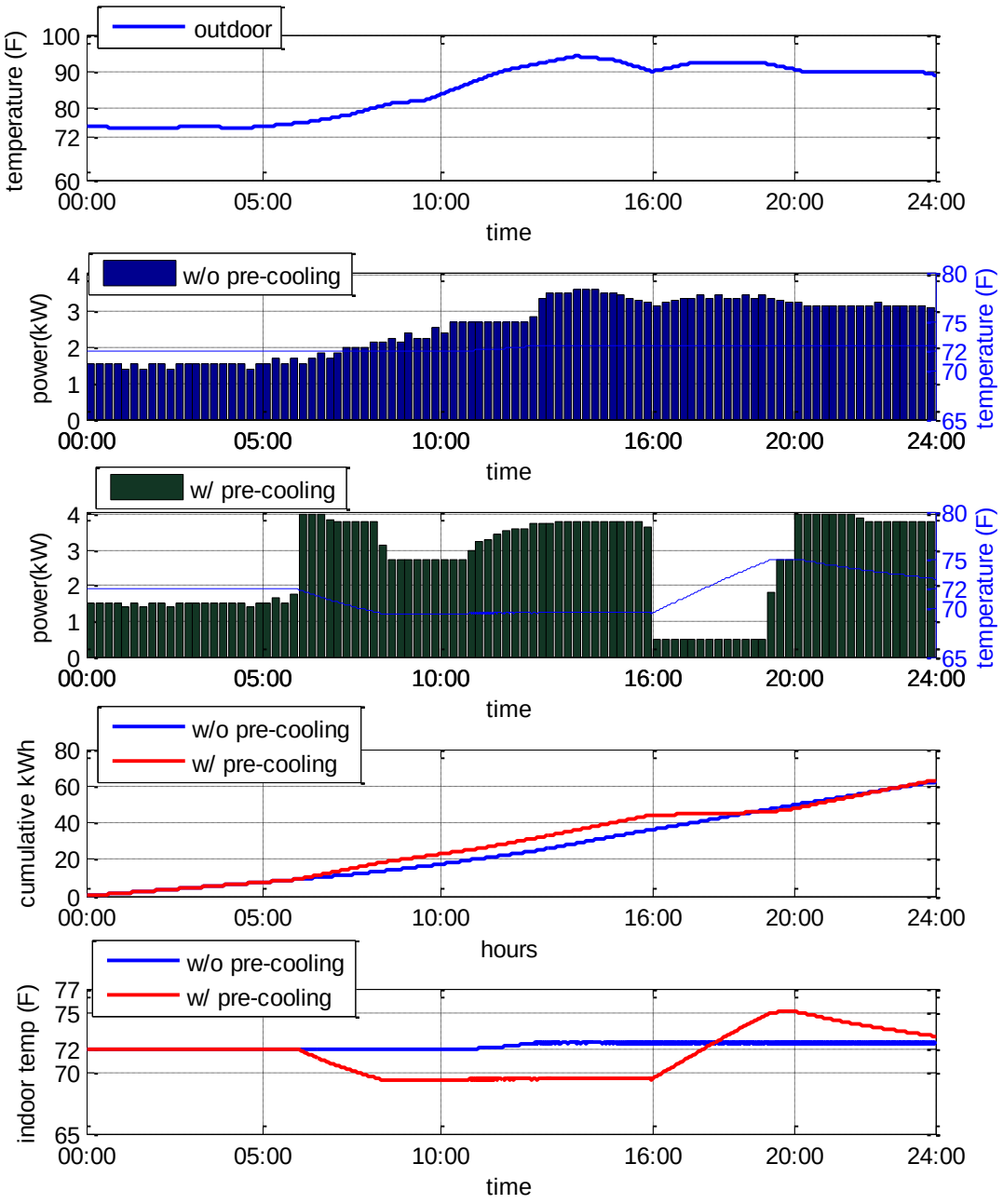

Fig. 6.14: Comparison between profiles with and without pre-cooling for power demand, cumulative energy demand and indoor temperature. June 01. DR event is hours 16-20.

Outdoor temperature profile of June 01 is shown in the first subplot of Fig. 6.14. Temperature rises above 80 °F around 10 am. Air-conditioning power demand profile without pre-cooling is shown in the second subplot of Fig. 6.14. Air-conditioning load is very high during the demand response event hours (4 pm to 8 pm). Calculated value of Δ_{ac} is 3.313 °F. Large percentage of air-conditioning demand can be shifted away from demand response event hours with the help of pre-cooling by Δ_{ac} = 3 °F. In case of pre-cooling operation, demand profile is provided in the third subplot of Fig. 6.14. Comparison between cumulative energy demand profiles is shown in the fourth subplot of Fig. 6.14. It can be seen that cumulative energy demand of 24 hours is slightly higher in case of pre-cooling operation. This is because of the additional thermal loss associate with pre-cooling operation. Comparison between indoor temperature profiles is shown in the fifth subplot of Fig. 6.14. In case of pre-cooling, indoor temperature is reduced before demand response event. Afterwards, indoor temperature is allowed to rise during demand response event (16^{th} to 20^{th} hours). However, temperature variation is limited in the range of (T_{set} ± 3 °F) to satisfy thermal comfort of household residents. With pre-cooling operation, demand response event time energy demand is reduced from 13.5 kWh to 3.4 kWh.

June 02:

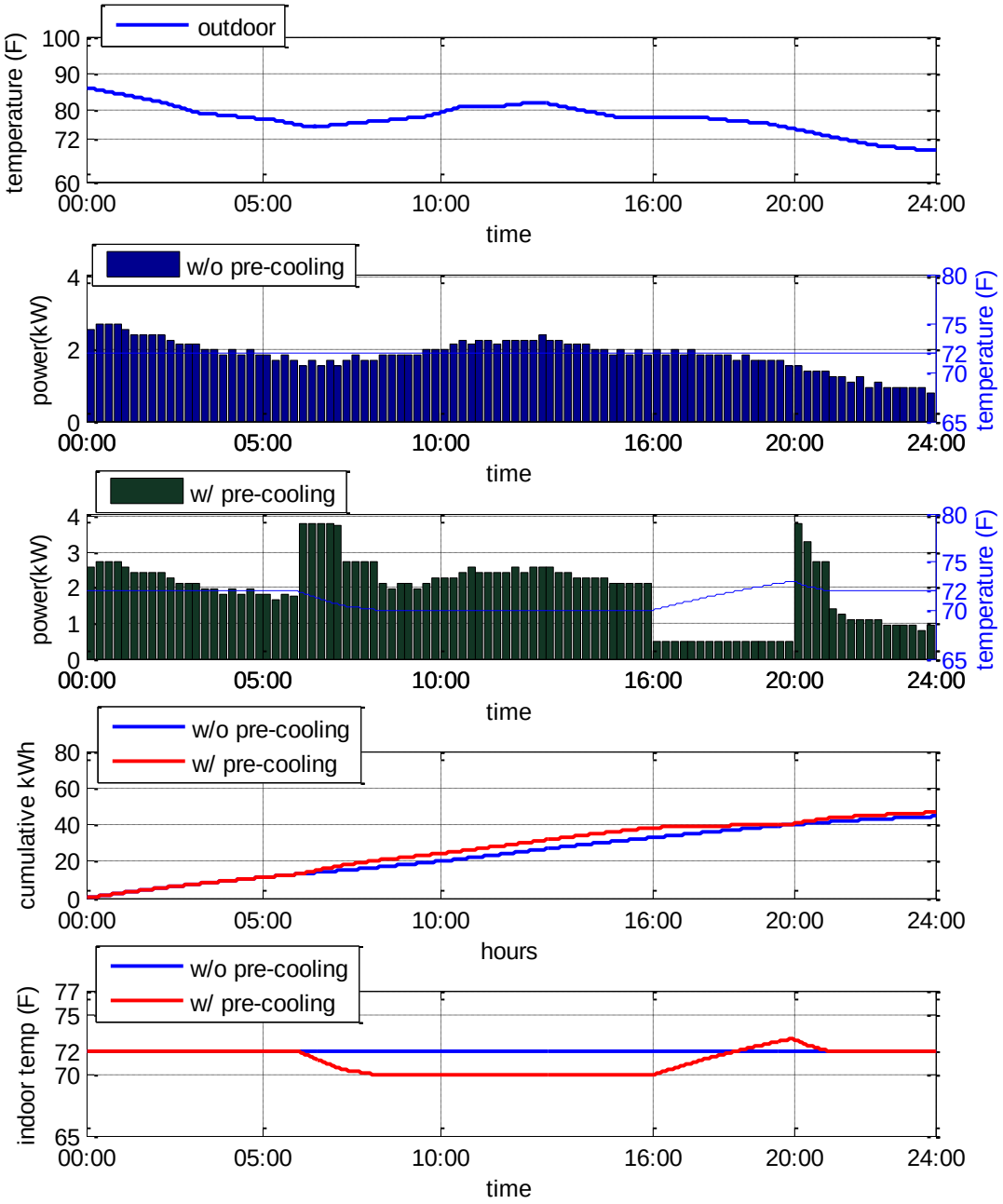

Fig. 6.15: Comparison between profiles with and without pre-cooling for power demand, cumulative energy demand and indoor temperature. June 02. DR event is hours 16-20.

Outdoor temperature profile of June 02 is shown in the first subplot of Fig. 6.15. Air-conditioning power demand profile without pre-cooling is shown in the second subplot of Fig. 6.15. Air-conditioning load is low during the demand response event hours (4 pm to 8 pm). Calculated value of Δ_{ac} is 1.46 °F. Therefore air-conditioning demand can be shifted away from demand response event hours with the help of pre-cooling. In case of pre-cooling operation, demand profile is provided in the third subplot of Fig. 6.15. Comparison between cumulative energy demand profiles is shown in the fourth subplot of Fig. 6.15. It can be seen that cumulative energy demand of 24 hours is slightly higher in case of pre-cooling operation. This is because of the additional thermal loss associate with pre-cooling operation. Comparison between indoor temperature profiles is shown in the fifth subplot of Fig. 6.15. In case of pre-cooling, indoor temperature is reduced before demand response event. Afterwards, indoor temperature is allowed to rise during demand response event (16^{th} to 20^{th} hours). However, temperature variation is limited in the range of (T_{set} ± 3 °F) to satisfy thermal comfort of household residents. In case of pre-cooling, demand response event time energy demand is reduced from 7.2 kWh to the lowest level of 2 kWh for ventillation and latent heat removal purpose.

June 03, 04, 05:

Temperature set-point modification is not required. Outdoor temperature is low.

June 06:

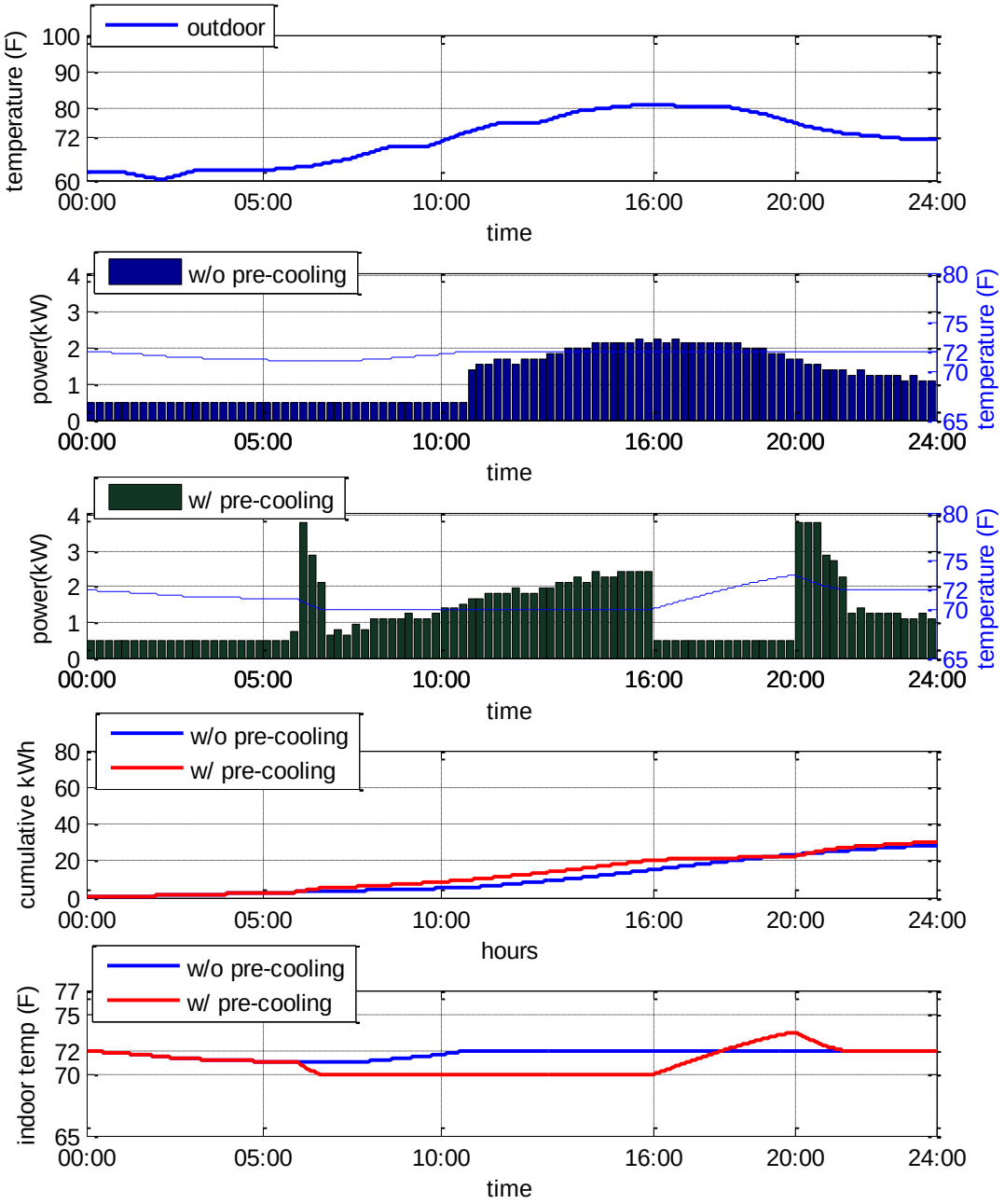

Fig. 6.16: Comparison between profiles with and without pre-cooling for power demand, cumulative energy demand and indoor temperature. June 06. DR event is hours 16-20.

Outdoor temperature profile of June 06 is shown in the first subplot of Fig. 6.16. Air-conditioning power demand profile without pre-cooling is shown in the second subplot of Fig. 6.16. In June 06, air-conditioning load is low during the demand response event hours (4 pm to 8 pm). Calculated value of Δ_{ac} is 1.76 °F. Therefore air-conditioning demand can be shifted away from demand response event hours with the help of pre-cooling. In case of pre-cooling operation, demand profile is provided in the third subplot of Fig. 6.16. Comparison between cumulative energy demand profiles is shown in the fourth subplot of Fig. 6.16. It can be seen that cumulative energy demand of 24 hours is slightly higher in case of pre-cooling operation. This is because of the additional thermal loss associate with pre-cooling operation. Comparison between indoor temperature profiles is shown in the fifth subplot of Fig. 6.16. In case of pre-cooling, indoor temperature is reduced before demand response event. Afterwards, indoor temperature is allowed to rise during demand response event (16^{th} to 20^{th} hours). However, temperature variation is limited in the range of ($T_{set} \pm 3$ °F) to satisfy thermal comfort of household residents. In case of pre-cooling, demand response event time energy demand is reduced from 8.2 kWh to the lowest level of 2 kWh for ventillation and latent heat removal purpose.

June 07:

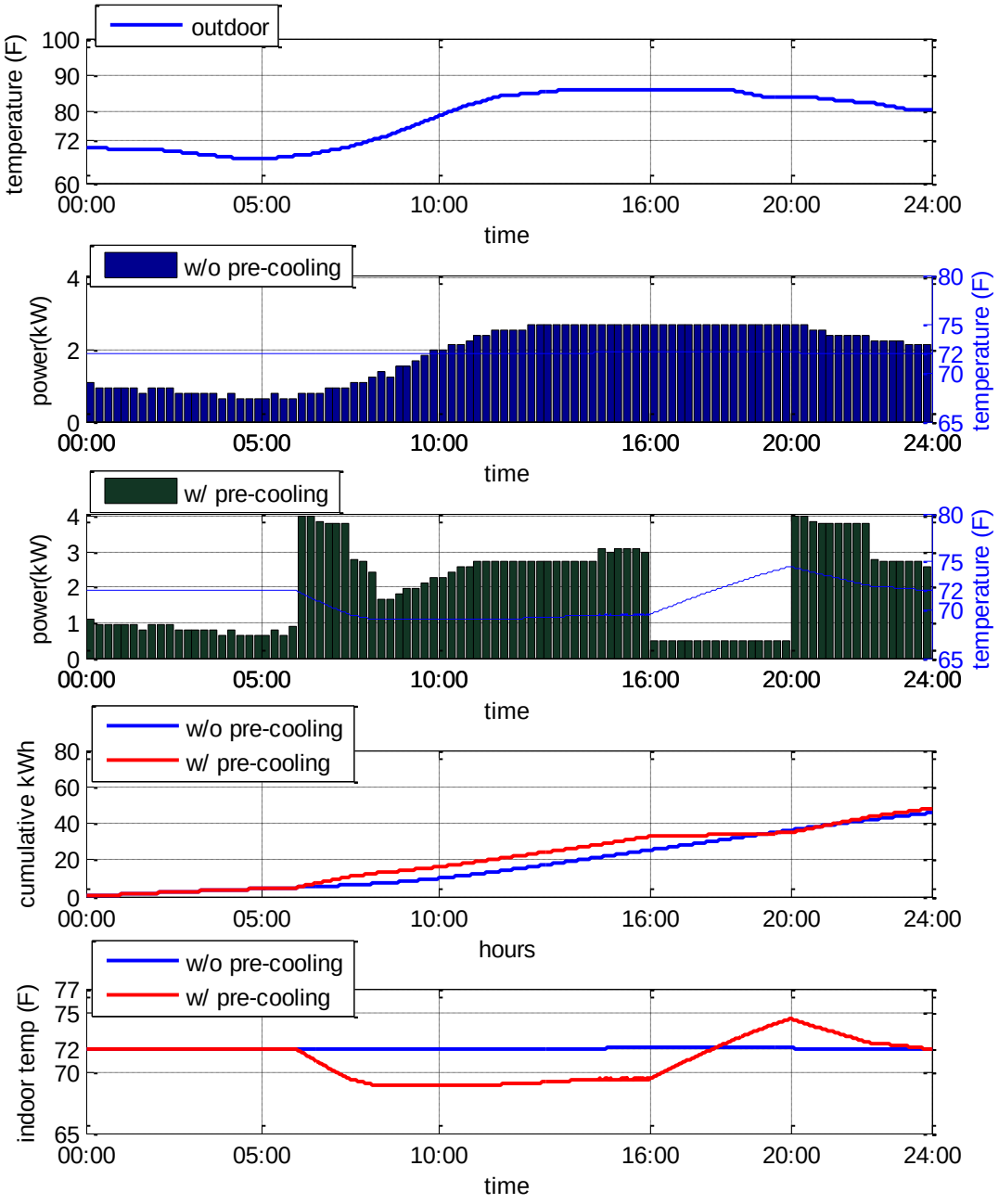

Fig. 6.17: Comparison between profiles with and without pre-cooling for power demand, cumulative energy demand and indoor temperature. June 07. DR event is hours 16-20.

Outdoor temperature profile of June 07 is shown in the first subplot of Fig. 6.17. Temperature rises above 80 °F after 10 am. Air-conditioning power demand profile without pre-cooling is shown in the second subplot of Fig. 6.17. There is moderate amount of air-conditioning load during the demand response event hours (4 pm to 8 pm) of June 07. Calculated value of Δ_{ac} is 2.52 °F. Therefore air-conditioning demand can be shifted away from demand response event hours with the help of pre-cooling. In case of pre-cooling operation, demand profile is provided in the third subplot of Fig. 6.17. Comparison between cumulative energy demand profiles is shown in the fourth subplot of Fig. 6.17. It can be seen that cumulative energy demand of 24 hours is slightly higher in case of pre-cooling operation. This is because of the additional thermal loss associate with pre-cooling operation. Comparison between indoor temperature profiles is shown in the fifth subplot of Fig. 6.17. In case of pre-cooling, indoor temperature is reduced before demand response event. Afterwards, indoor temperature is allowed to rise during demand response event (16^{th} to 20^{th} hours). However, temperature variation is limited in the range of (T_{set} ± 3 °F) to satisfy thermal comfort of household residents. In case of pre-cooling, demand response event time energy demand is reduced from 10.9 kWh to the lowest level of 2 kWh for ventillation and latent heat removal purpose.

June08:

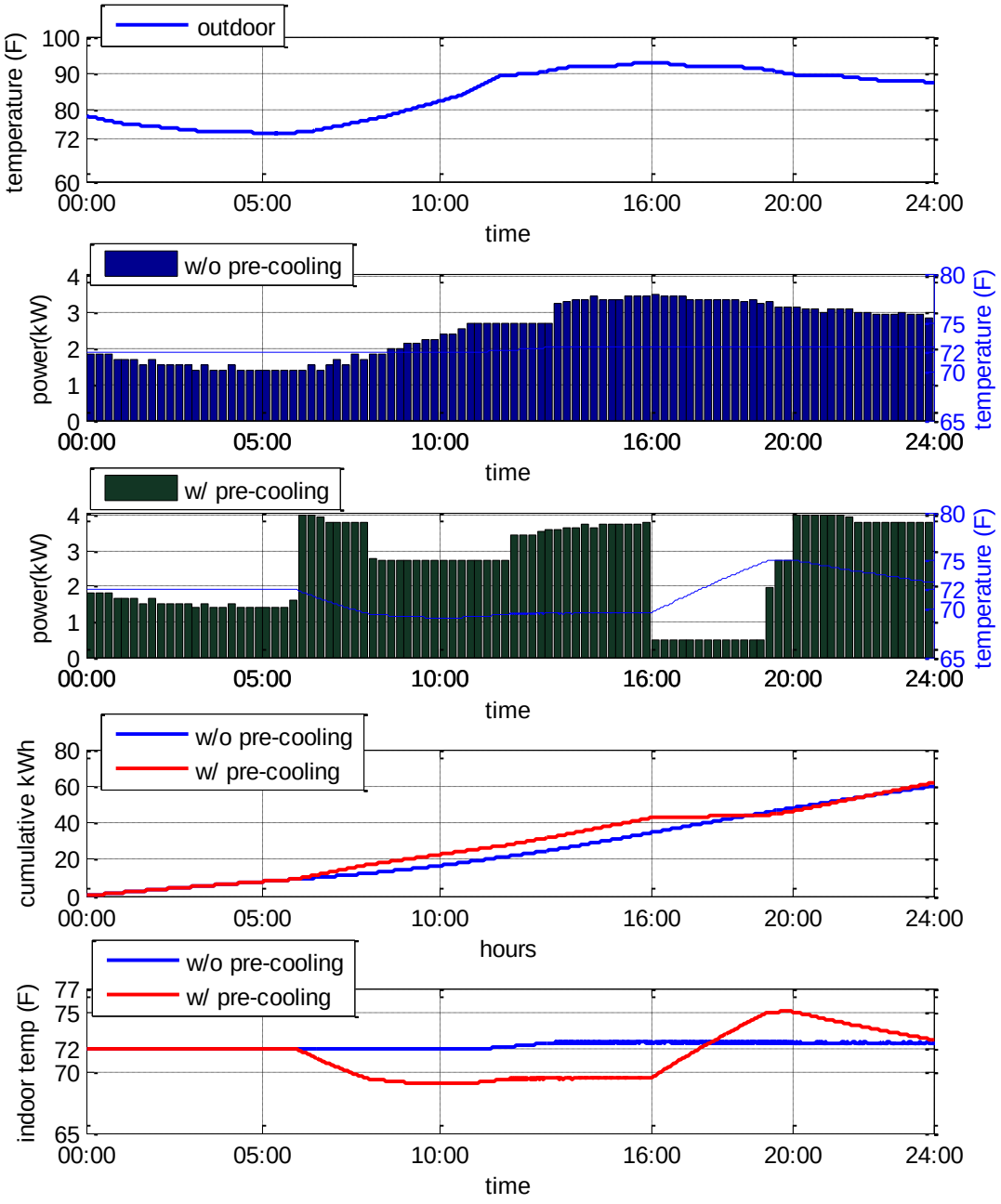

Fig. 6.18: Comparison between profiles with and without pre-cooling for power demand, cumulative energy demand and indoor temperature. June 08. DR event is hours 16-20.

Outdoor temperature profile of June 08 is shown in the first subplot of Fig. 6.18. Temperature rises above 90 °F around 1 pm. Air-conditioning power demand profile without pre-cooling is shown in the second subplot of Fig. 6.18. Air-conditioning load is very high during the demand response event hours (4 pm to 8 pm). Calculated value of Δ_{ac} is 3.3 ° F. Large percentage of air-conditioning demand can be shifted away from demand response event hours with the help of pre-cooling by Δ_{ac} = 3 °F. In case of pre-cooling operation, demand profile is provided in the third subplot of Fig. 6.18. Comparison between cumulative energy demand profiles is shown in the fourth subplot of Fig. 6.18. It can be seen that cumulative energy demand of 24 hours is slightly higher in case of pre-cooling operation. This is because of the additional thermal loss associate with pre-cooling operation. Comparison between indoor temperature profiles is shown in the fifth subplot of Fig. 6.18. In case of pre-cooling, indoor temperature is reduced before demand response event. Afterwards, indoor temperature is allowed to rise during demand response event (16^{th} to 20^{th} hours). However, temperature variation is limited in the range of (T_{set} ± 3 °F) to satisfy thermal comfort of household residents. With pre-cooling operation, demand response event time energy demand is reduced from 13.5 kWh to 3.5 kWh.

June 09:

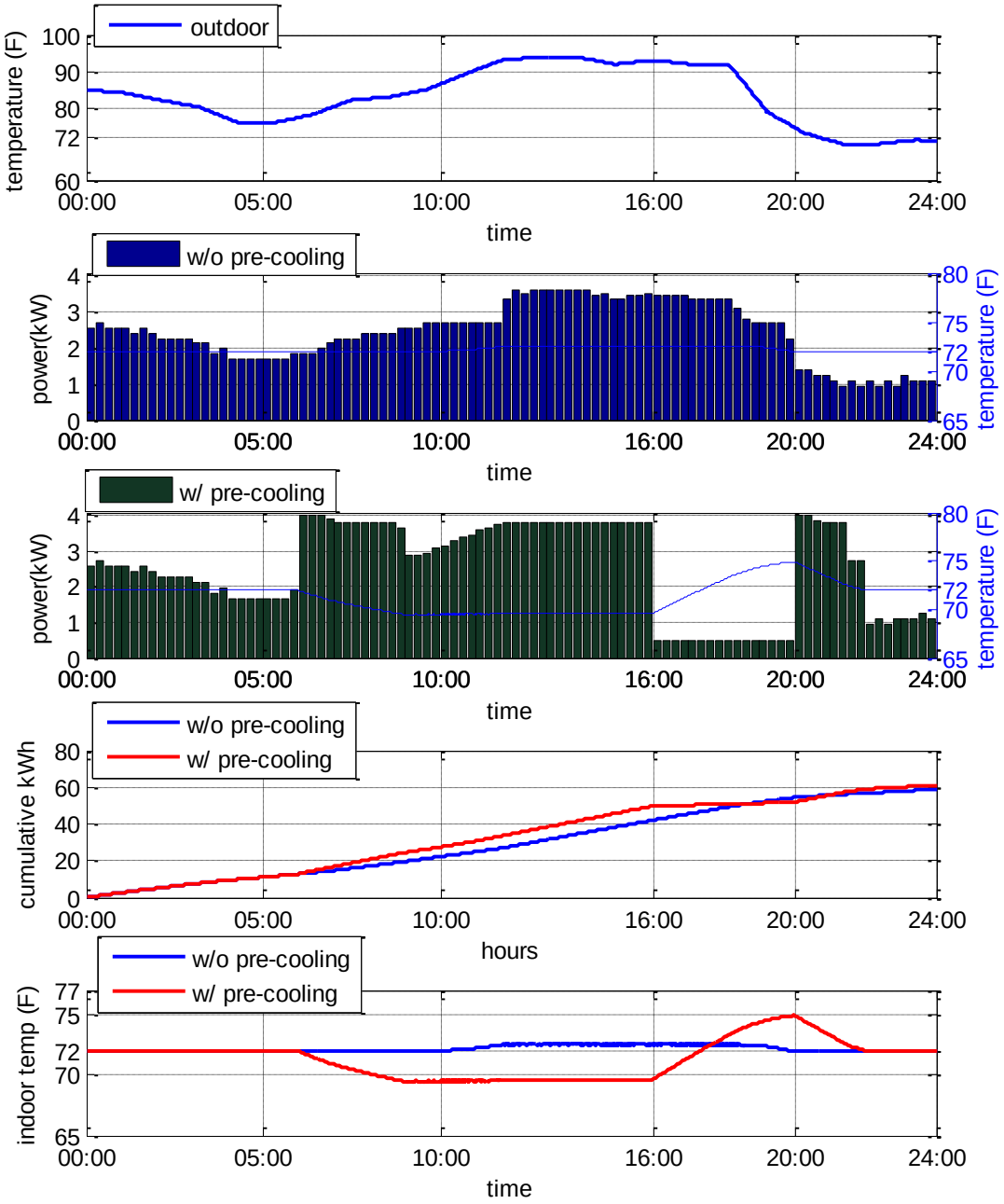

Fig. 6.19: Comparison between profiles with and without pre-cooling for power demand, cumulative energy demand and indoor temperature. June 09. DR event is hours 16-20.

Outdoor temperature profile of June 09 is shown in the first subplot of Fig. 6.19. Temperature rises above 90 °F around 12 pm. However, temperature starts to drop rapidly after 6 pm. Air-conditioning power demand profile without pre-cooling is shown in the second subplot of Fig. 6.19. There is moderate amount of air-conditioning load during the demand response event hours (4 pm to 8 pm). Calculated value of Δ_{ac} is 2.77 °F. Therefore air-conditioning demand can be shifted away from demand response event hours with the help of pre-cooling. In case of pre-cooling operation, demand profile is provided in the third subplot of Fig. 6.19. Comparison between cumulative energy demand profiles is shown in the fourth subplot of Fig. 6.19. It can be seen that cumulative energy demand of 24 hours is slightly higher in case of pre-cooling operation. This is because of the additional thermal loss associate with pre-cooling operation. Comparison between indoor temperature profiles is shown in the fifth subplot of Fig. 6.19. In case of pre-cooling, indoor temperature is reduced before demand response event (16^{th} to 20^{th} hours). Afterwards, indoor temperature is allowed to rise during demand response event. However, temperature variation is limited in the range of (T_{set} ± 3 °F) to satisfy thermal comfort of household residents. With pre-cooling operation, demand response event time energy demand is reduced from 12.5 kWh to 2 kWh.

June 10:

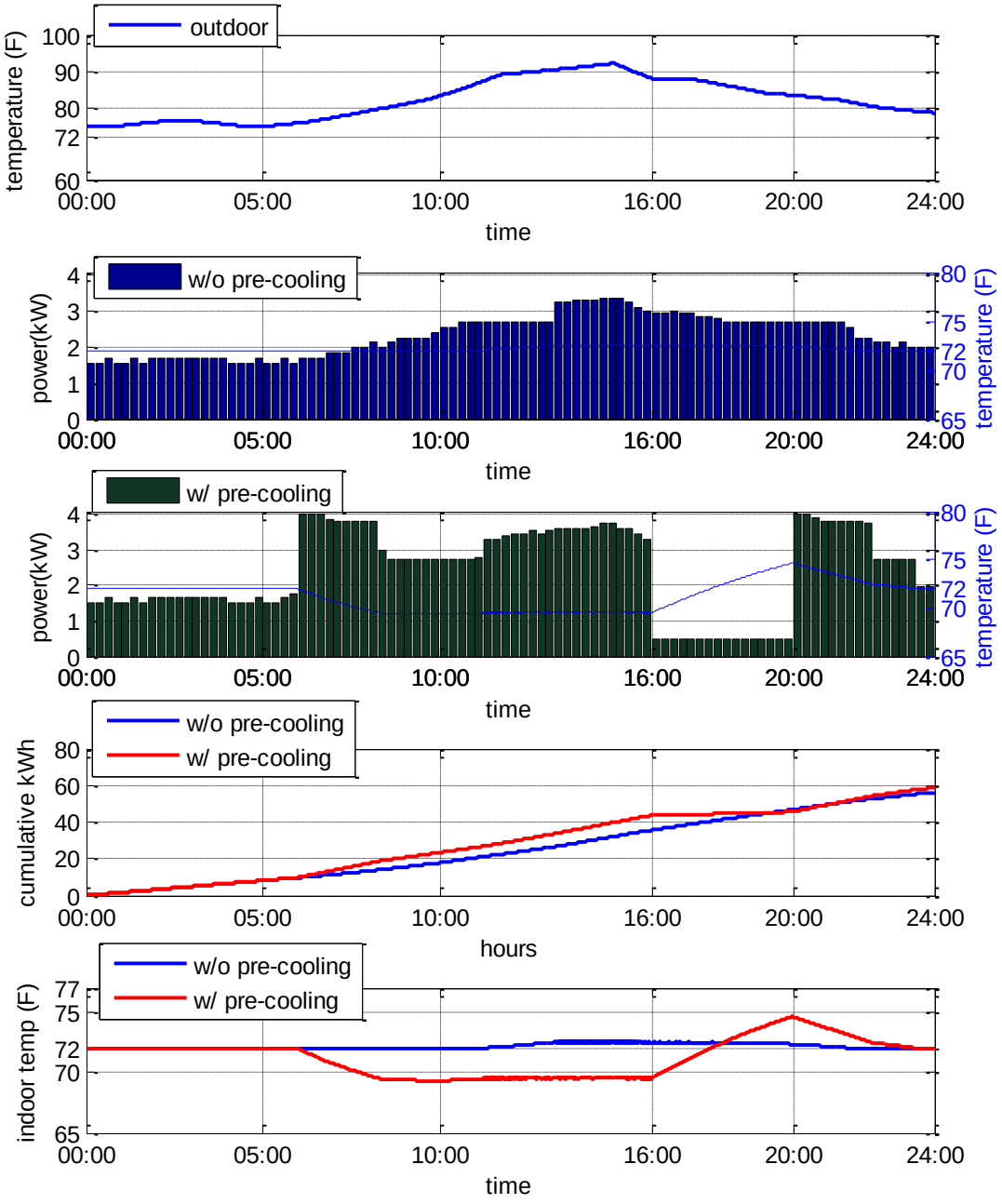

Fig. 6.20: Comparison between profiles with and without pre-cooling for power demand, cumulative energy demand and indoor temperature. June 10. DR event is hours 16-20.

Outdoor temperature profile of June 10 is shown in the first subplot of Fig. 6.20. Temperature remains below 90 °F during demand response event hours (4 pm to 8 pm). Air-conditioning power demand profile without pre-cooling is shown in the second subplot of Fig. 6.20. There is moderate amount of air-conditioning load during the demand response event hours (4 pm to 8 pm). Calculated value of Δ_{ac} is 2.6 ° F. Therefore air-conditioning demand can be shifted away from demand response event hours with the help of pre-cooling. In case of pre-cooling operation, demand profile is provided in the third subplot of Fig. 6.20. Comparison between cumulative energy demand profiles is shown in the fourth subplot of Fig. 6.20. It can be seen that cumulative energy demand of 24 hours is slightly higher in case of pre-cooling operation. This is because of the additional thermal loss associate with pre-cooling operation. Comparison between indoor temperature profiles is shown in the fifth subplot of Fig. 6.20. In case of pre-cooling, indoor temperature is reduced before demand response event (16^{th} to 20^{th} hours). Afterwards, indoor temperature is allowed to rise during demand response event. However, temperature variation is limited in the range of (T_{set} ± 3 °F) to satisfy thermal comfort of household residents. With pre-cooling operation, demand response event time energy demand is reduced from 11.3 kWh to the lowest level of 2 kWh for ventillation and latent heat removal purpose.

June 11:

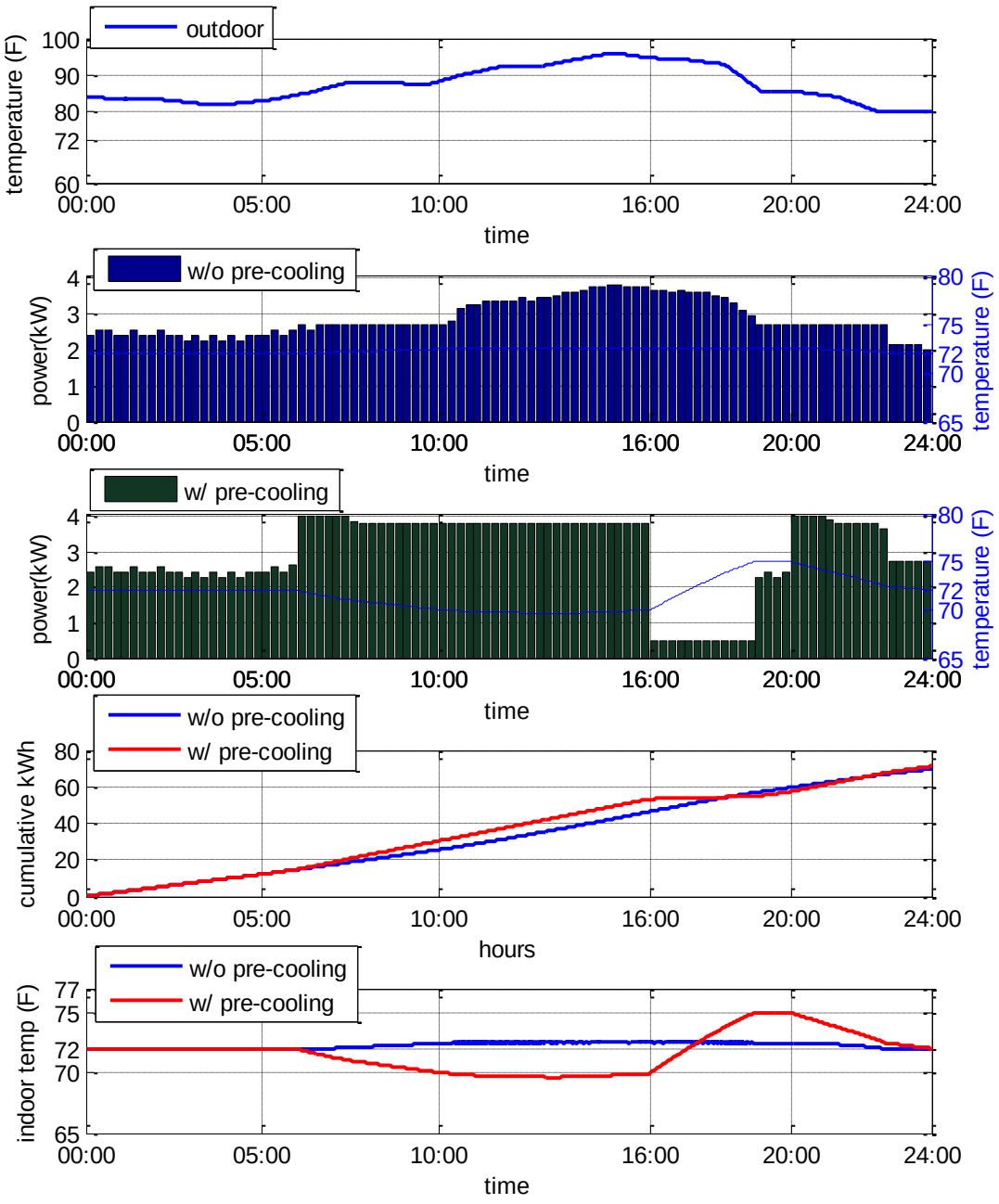

Fig. 6.21: Comparison between profiles with and without pre-cooling for power demand, cumulative energy demand and indoor temperature. June 11. DR event is hours 16-20.

Outdoor temperature profile of June 11 is shown in the first subplot of Fig. 6.21. Temperature rises above 90 °F at around 11 am. Air-conditioning power demand profile without pre-cooling is shown in the second subplot of Fig. 6.21. There is high air-conditioning load during the demand response event hours (4 pm to 8 pm). Calculated value of Δ_{ac} is 3.2 ° F. Therefore, large percentage of air-conditioning demand can be shifted away from demand response event hours with the help of pre-cooling by setting Δ_{ac} = 3 °F. In case of pre-cooling operation, demand profile is provided in the third subplot of Fig. 6.21. Comparison between cumulative energy demand profiles is shown in the fourth subplot of Fig. 6.21. It can be seen that cumulative energy demand of 24 hours is slightly higher in case of pre-cooling operation. This is because of the additional thermal loss associate with pre-cooling operation. Comparison between indoor temperature profiles is shown in the fifth subplot of Fig. 6.21. In case of pre-cooling, indoor temperature is reduced before demand response event (16^{th} to 20^{th} hours). Afterwards, indoor temperature is allowed to rise during demand response event. However, temperature variation is limited in the range of (T_{set} ± 3 °F) to satisfy thermal comfort of household residents. With pre-cooling operation, demand response event time energy demand is reduced from 13.2 kWh to 3.9 kWh.

June 12:

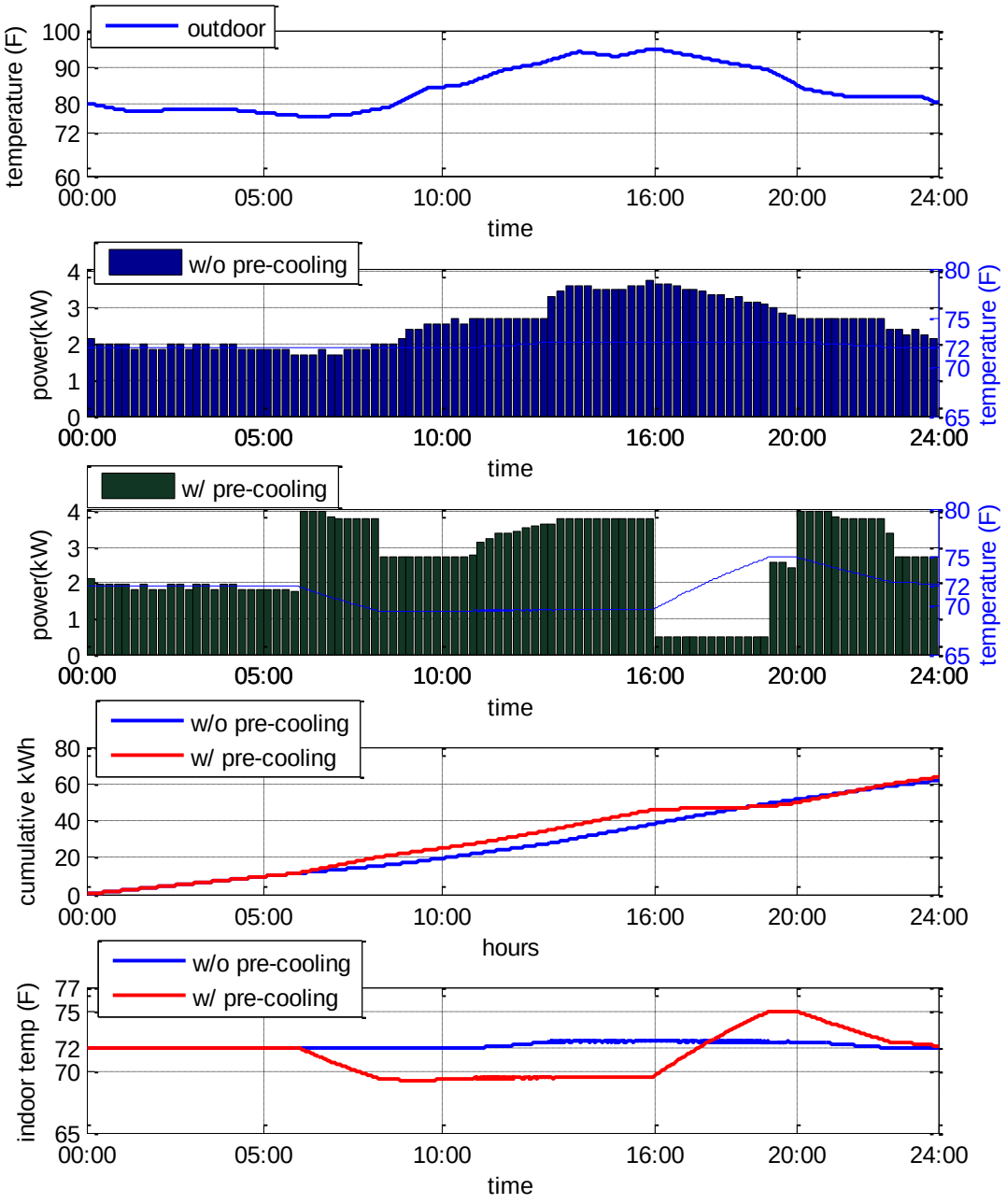

Fig. 6.22: Comparison between profiles with and without pre-cooling for power demand, cumulative energy demand and indoor temperature. June 12. DR event is hours 16-20.

Outdoor temperature profile of June 12 is shown in the first subplot of Fig. 6.22. Temperature rises above 90 °F at around 12 pm. Air-conditioning power demand profile without pre-cooling is shown in the second subplot of Fig. 6.22. There is high air-conditioning load during the demand response event hours (4 pm to 8 pm). Calculated value of Δ_{ac} is 3.244 ° F. Therefore, large percentage of air-conditioning demand can be shifted away from demand response event hours with the help of pre-cooling by setting Δ_{ac} = 3 °F. In case of pre-cooling operation, demand profile is provided in the third subplot of Fig. 6.22. Comparison between cumulative energy demand profiles is shown in the fourth subplot of Fig. 6.22. It can be seen that cumulative energy demand of 24 hours is slightly higher in case of pre-cooling operation. This is because of the additional thermal loss associate with pre-cooling operation. Comparison between indoor temperature profiles is shown in the fifth subplot of Fig. 6.22. In case of pre-cooling, indoor temperature is reduced before demand response event (16^{th} to 20^{th} hours). Afterwards, indoor temperature is allowed to rise during demand response event. However, temperature variation is limited in the range of (T_{set} ± 3 °F) to satisfy thermal comfort of household residents. With pre-cooling operation, demand response event time energy demand is reduced from 13.2 kWh to 3.5 kWh.

June 13:

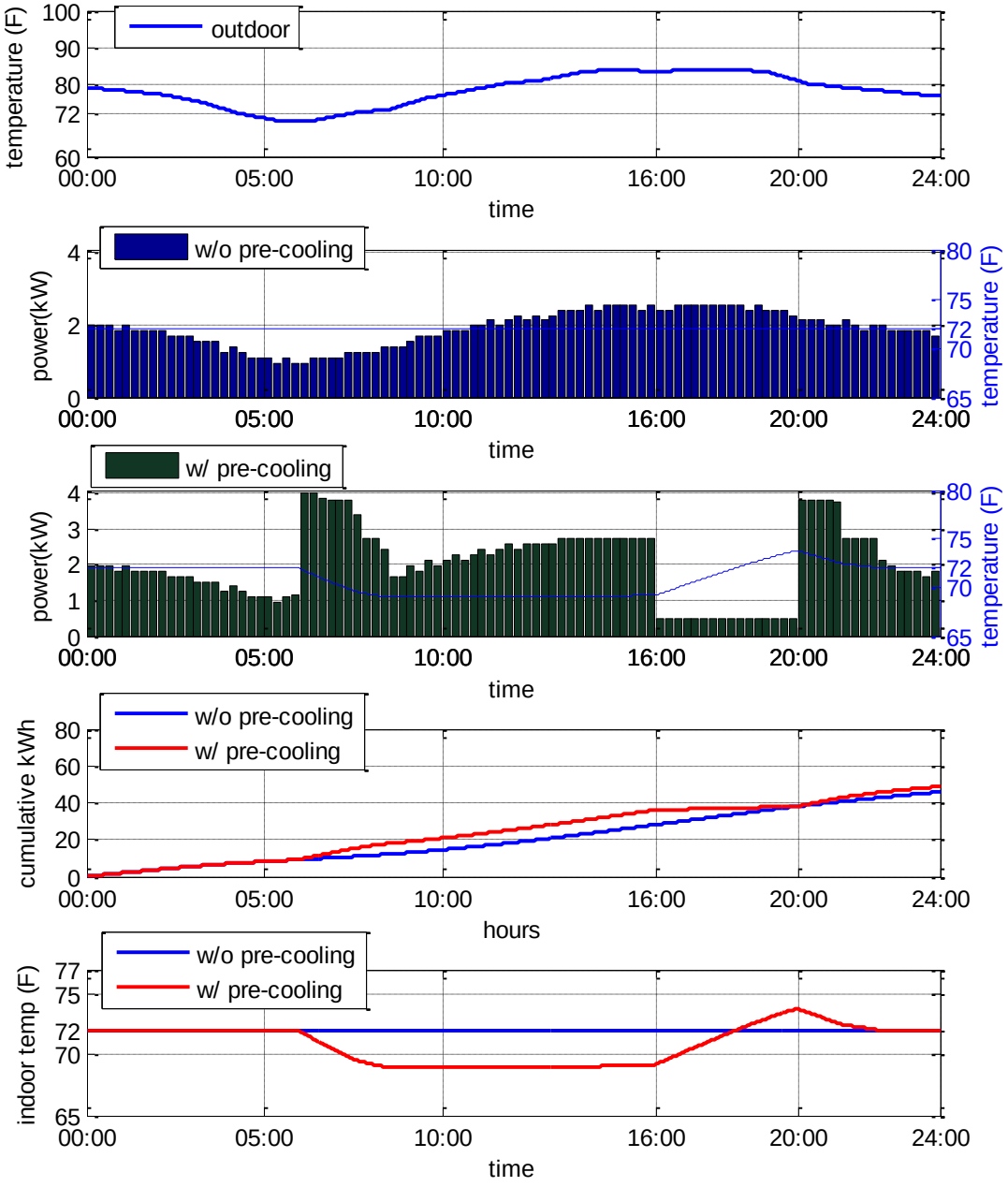

Fig. 6.23: Comparison between profiles with and without pre-cooling for power demand, cumulative energy demand and indoor temperature. June 13. DR event is hours 16-20.

Outdoor temperature profile of June 13 is shown in the first subplot of Fig. 6.23. Temperature remains below 90 °F during demand response event hours (4 pm to 8 pm). Air-conditioning power demand profile without pre-cooling is shown in the second subplot of Fig. 6.23. There is moderate amount of air-conditioning load during the demand response event hours (4 pm to 8 pm) of June 13. Calculated value of Δ_{ac} is 2.67 °F. Therefore air-conditioning demand can be shifted away from demand response event hours with the help of pre-cooling. In case of pre-cooling operation, demand profile is provided in the third subplot of Fig. 6.23. Comparison between cumulative energy demand profiles is shown in the fourth subplot of Fig. 6.23. It can be seen that cumulative energy demand of 24 hours is slightly higher in case of pre-cooling operation. This is because of the additional thermal loss associate with pre-cooling operation. Comparison between indoor temperature profiles is shown in the fifth subplot of Fig. 6.23. In case of pre-cooling, indoor temperature is reduced before demand response event. Afterwards, indoor temperature is allowed to rise during demand response event (16^{th} to 20^{th} hours). However, temperature variation is limited in the range of ($T_{set} \pm 3$ °F) to satisfy thermal comfort of household residents. In case of pre-cooling, demand response event time energy demand is reduced from 10 kWh to the lowest level of 2 kWh for ventillation and latent heat removal purpose.

June 14:

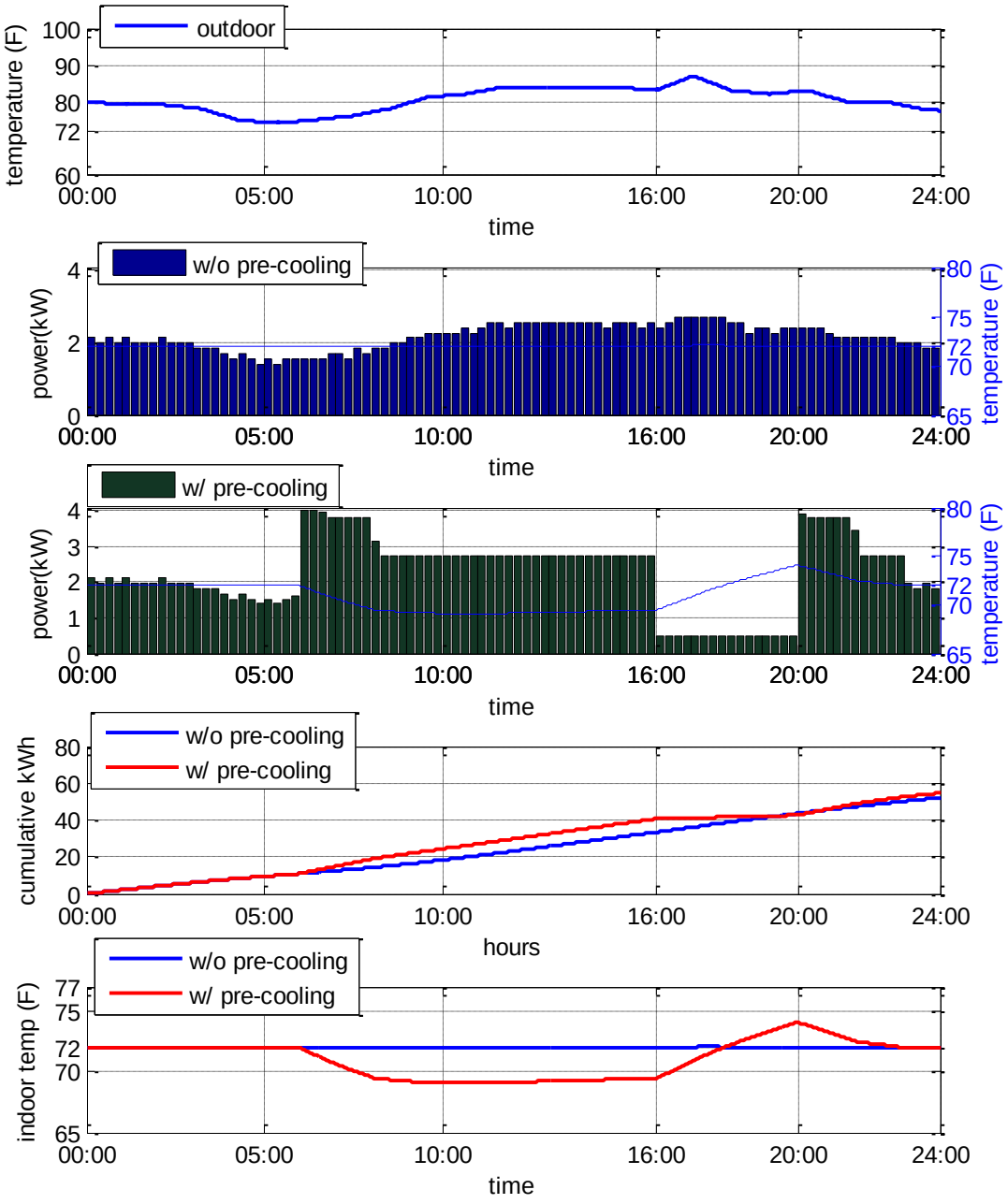

Fig. 6.24: Comparison between profiles with and without pre-cooling for power demand, cumulative energy demand and indoor temperature. June 14. DR event is hours 16-20.

Outdoor temperature profile of June 14 is shown in the first subplot of Fig. 6.24. Temperature remains below 90 °F during demand response event hours (4 pm to 8 pm). Air-conditioning power demand profile without pre-cooling is shown in the second subplot of Fig. 6.24. There is moderate amount of air-conditioning load during the demand response event hours (4 pm to 8 pm) of June 14. Calculated value of Δ_{ac} is 2.32 °F. Therefore air-conditioning demand can be shifted away from demand response event hours with the help of pre-cooling. In case of pre-cooling operation, demand profile is provided in the third subplot of Fig. 6.24. Comparison between cumulative energy demand profiles is shown in the fourth subplot of Fig. 6.24. It can be seen that cumulative energy demand of 24 hours is slightly higher in case of pre-cooling operation. This is because of the additional thermal loss associate with pre-cooling operation. Comparison between indoor temperature profiles is shown in the fifth subplot of Fig. 6.24. In case of pre-cooling, indoor temperature is reduced before demand response event. Afterwards, indoor temperature is allowed to rise during demand response event (16^{th} to 20^{th} hours). However, temperature variation is limited in the range of (T_{set} ± 3 °F) to satisfy thermal comfort of household residents. In case of pre-cooling, demand response event time energy demand is reduced from 10.2 kWh to the lowest level of 2 kWh for ventillation and latent heat removal purpose.

June 15:

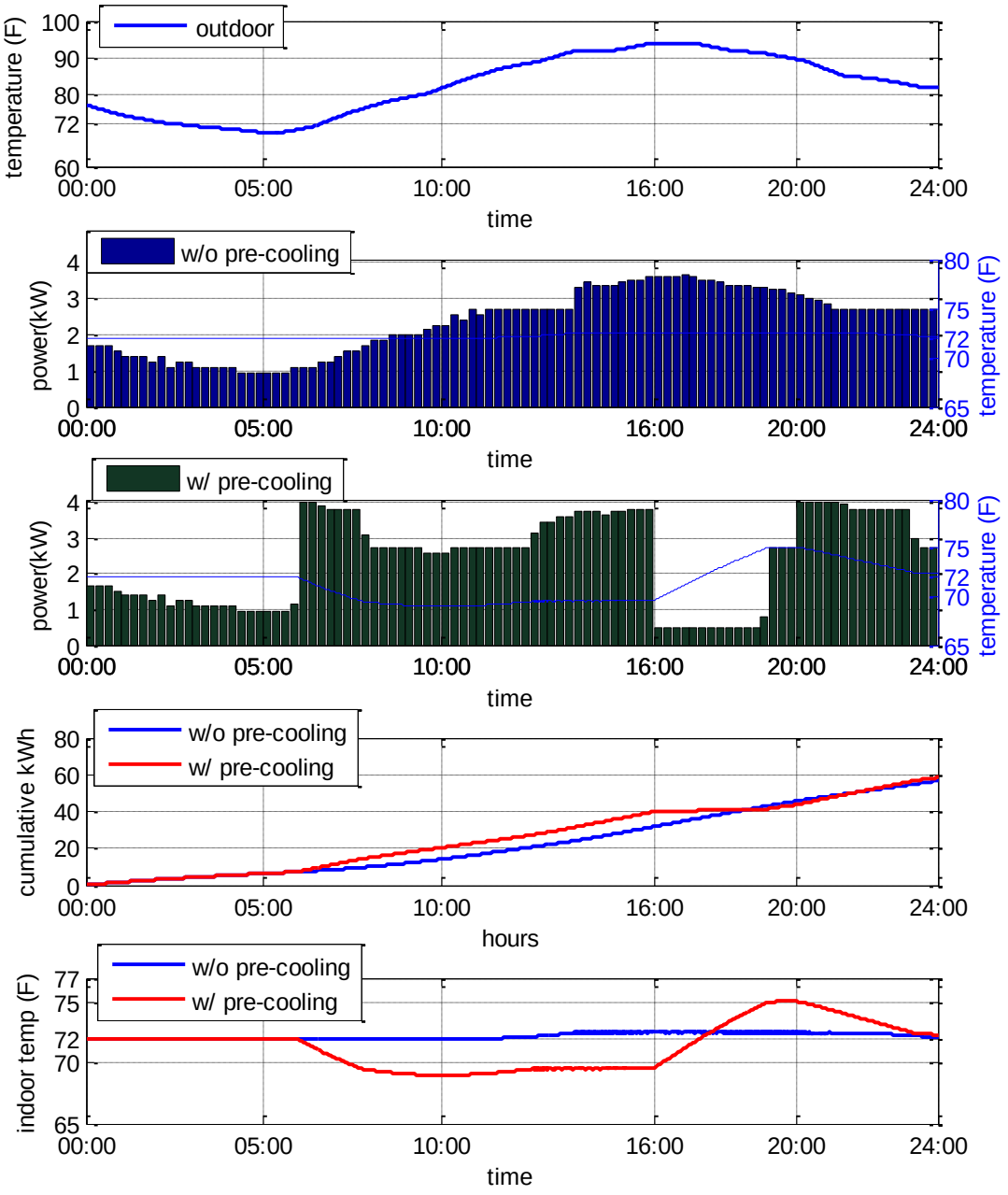

Fig. 6.25: Comparison between profiles with and without pre-cooling for power demand, cumulative energy demand and indoor temperature. June 15. DR event is hours 16-20.

Outdoor temperature profile of June 15 is shown in the first subplot of Fig. 6.25. Temperature rises above 90 °F at around 2 pm. Air-conditioning power demand profile without pre-cooling is shown in the second subplot of Fig. 6.25. There is high air-conditioning load during the demand response event hours (4 pm to 8 pm). Calculated value of Δ_{ac} is 3.4 ° F. Therefore, large percentage of air-conditioning demand can be shifted away from demand response event hours with the help of pre-cooling by setting Δ_{ac} = 3 °F. In case of pre-cooling operation, demand profile is provided in the third subplot of Fig. 6.25. Comparison between cumulative energy demand profiles is shown in the fourth subplot of Fig. 6.25. It can be seen that cumulative energy demand of 24 hours is slightly higher in case of pre-cooling operation. This is because of the additional thermal loss associate with pre-cooling operation. Comparison between indoor temperature profiles is shown in the fifth subplot of Fig. 6.25. In case of pre-cooling, indoor temperature is reduced before demand response event (16^{th} to 20^{th} hours). Afterwards, indoor temperature is allowed to rise during demand response event. However, temperature variation is limited in the range of (T_{set} ± 3 °F) to satisfy thermal comfort of household residents. With pre-cooling operation, demand response event time energy demand is reduced from 13.8 kWh to 3.7 kWh.

Summary of case studies for air-conditioning load control is provided in Table 6.3. It is observable from the table that air-conditioning power demand can be successfully shifted away from demand response event hours by manipulating temperature set-point. However, partial air-conditioning operation is required in case of excessively hot summer days with temperature above 90 °F. To ensure thermal comfort of household residents, temperature set-point is kept within ±3 °F range of preferred temperature set-point of house. In case of pre-cooling, energy demand is slightly higher. Pre-cooling reduces indoor temperature. Thus, temperature difference increases. Thermal loss increases with the increase of temperature difference.

Table 6.3: Summary of case studies for air-conditioning load control

day	Total 24 hour's energy demand without pre-cooling (kWh)	Total 24 hour's energy demand with pre-cooling (kWh)	Without pre-cooling: Air-conditioning power demands at various hours of demand response event (kW)				With pre-cooling: Air-conditioning power demands at various hours of demand response event (kW)			
			hour	hour	hour	hour	hour	hour	hour	hour
			16-17	17-18	18-19	19-20	16-17	17-18	18-19	19-20
1-Jun	62.3	63.2	3.3	3.4	3.4	3.4	0.5	0.5	0.5	1.9
2-Jun	44.5	46.7	1.9	1.9	1.8	1.6	0.5	0.5	0.5	0.5
6-Jun	28.6	30.4	2.2	2.1	2.1	1.8	0.5	0.5	0.5	0.5
7-Jun	45.7	48.2	2.7	2.7	2.7	2.7	0.5	0.5	0.5	0.5
8-Jun	60.0	61.7	3.5	3.4	3.4	3.2	0.5	0.5	0.5	2.0
9-Jun	58.9	61.1	3.5	3.4	3.0	2.6	0.5	0.5	0.5	0.5
10-Jun	56.3	58.7	3.0	2.9	2.7	2.7	0.5	0.5	0.5	0.5
11-Jun	69.6	71.2	3.7	3.6	3.2	2.7	0.5	0.5	0.5	2.4
12-Jun	61.8	63.6	3.6	3.4	3.2	2.9	0.5	0.5	0.5	2.0
13-Jun	45.9	48.8	2.5	2.6	2.5	2.4	0.5	0.5	0.5	0.5
14-Jun	52.0	54.6	2.6	2.7	2.5	2.4	0.5	0.5	0.5	0.5
15-Jun	56.6	58.4	3.6	3.5	3.4	3.2	0.5	0.5	0.5	2.2

Demand reduction for certain duration of time can cause secondary peak just after the end of demand response event. This phenomenon is called rebound effect of demand response. Air-conditioning demand is determined for the up-next hour after demand response event. Additional energy demands in hour 20-21 are calculated from simulation results. For demand response participation of air-conditioning load, temperature set-point is reduced before demand response event. During the event, set-point is increased to an upper level. After demand response event, set-point returns back to the preferred level. In the first case, temperature set-point is decreased abruptly after the end of demand response event. In the second case, set-point is decreased gradually over one hour period. Air-conditioning rebound load amounts for the up-next hour of demand response events are shown in Table 6.4.

Table 6.4: Rebound loads in case of abrupt and gradual changes of temperature set-point

Days	W/O Pre-cooling: Power demand in the hour just after demand response event (kW)	W/ Pre-cooling -gradual set-point change: Power demand in the hour just after demand response event (kW)	W/ Pre-cooling - abrupt set-point change: Power demand in the hour just after demand response event (kW)
1-Jun	3.2	3.8	4.0
2-Jun	1.4	2.1	3.1
6-Jun	1.5	2.8	3.6
7-Jun	2.6	3.2	3.9
8-Jun	3.1	3.7	4.0
9-Jun	1.3	3.5	3.9
10-Jun	2.7	3.4	3.9
11-Jun	2.7	3.7	4.0
12-Jun	2.7	3.7	4.0
13-Jun	2.1	2.6	3.8
14-Jun	2.4	2.9	3.9
15-Jun	3.0	3.7	4.0

Summary of combined load control (water heating and air-conditioning) is provided in Table 6.5. It can be observed from the table that typical value of combined power demand reduction for demand response event hours of a hot summer day is around 2.5 kW. Obtained results are based on the demand response criteria set by ConEdison. These criteria are provided in section 3.2. Outcomes are criteria dependent. If demand response model is considered different then results may vary.

Table 6.5: Summary of case studies for combined water heating and air-conditioning load control

Day	Total 24 hour's energy demand without load control (kWh)	Total 24 hour's energy demand with load control (kWh)	Without load control: Combined (air-conditioning and water heating) power demands at various hours of demand response event (kW)				With load control: Combined (air-conditioning and water heating) power demands at various hours of demand response event (kW)			
			hour 16-17	hour 17-18	hour 18-19	hour 19-20	hour 16-17	hour 17-18	hour 18-19	hour 19-20
1-Jun	74.8	75.7	3.3	3.4	3.4	3.4	0.5	0.5	0.5	1.9
2-Jun	50.7	52.9	1.9	1.9	1.8	1.6	0.5	0.5	0.5	0.5
6-Jun	40.3	42.1	2.2	2.1	2.1	1.8	0.5	0.5	0.5	0.5
7-Jun	56.5	59.2	4.0	3.7	2.7	2.7	0.5	0.5	0.5	0.5
8-Jun	65.1	67.5	3.5	3.6	5.5	3.2	0.5	0.5	0.5	2.0
9-Jun	75.7	81.8	8.0	6.1	3.0	2.6	3.7	0.5	0.5	0.5
10-Jun	69.2	72.3	3.0	3.6	4.4	2.7	0.5	0.5	0.5	0.5
11-Jun	76.6	78.2	3.7	3.6	3.2	2.7	0.5	0.5	0.5	2.4
12-Jun	69.2	71.0	3.6	3.4	3.2	2.9	0.5	0.5	0.5	2.0
13-Jun	58.2	61.1	2.5	2.6	2.5	2.4	0.5	0.5	0.5	0.5
14-Jun	66.8	69.4	2.6	2.7	2.5	2.4	0.5	0.5	0.5	0.5
15-Jun	63.1	65.0	3.6	3.5	3.4	3.9	0.5	0.5	0.5	2.2

CHAPTER 7

Aggregator-Assisted Residential Participation in Demand Response Program

7.1 Aggregate Demand Response of Electrical Water Heating Load

Let us consider 25 houses with electrical water heaters. Aggregate demand response scope is investigated in this section with the help of Monte Carlo simulations. Various simulation parameters (such as: water consumption profile, tank volume, energy factor, ambient temperature, starting time of preheating etc.) are randomized with maximum 10% to 20% variability. Aggregate load profiles are determined without and with preheating. Parameters are randomized and demand response amounts associated with various samples are recorded. High and low demand response amounts are tracked. Simulation is repeated 200 times. Considered variations of parameters are provided below:

- Water flow: Hot water consumption profiles are chosen from the hot water consumption profiles provided by IEA [31].
- Tank volume: Maximum 20% variation of water heater tank volume is considered.
- Energy factor and heating coil efficiency: Maximum 10% variation.
- Regular temperature set-point: Between 120 °F to 130 °F.
- Preheating start time: Between 5 am to 10 am.

Monte Carlo simulations are performed to obtain results under various circumstances. In case of high demand, demand response amount is found 25.6 kWh for the 4 hours of demand response event (shown in Fig. 7.1). 11.4 kW of aggregate peak reduction is achieved. Average profile of all the Monte Carlo simulation outcomes is shown in Fig. 7.2. Average demand response amount is found to be 13.7 kWh for the entire duration (4 hours) of demand response event.

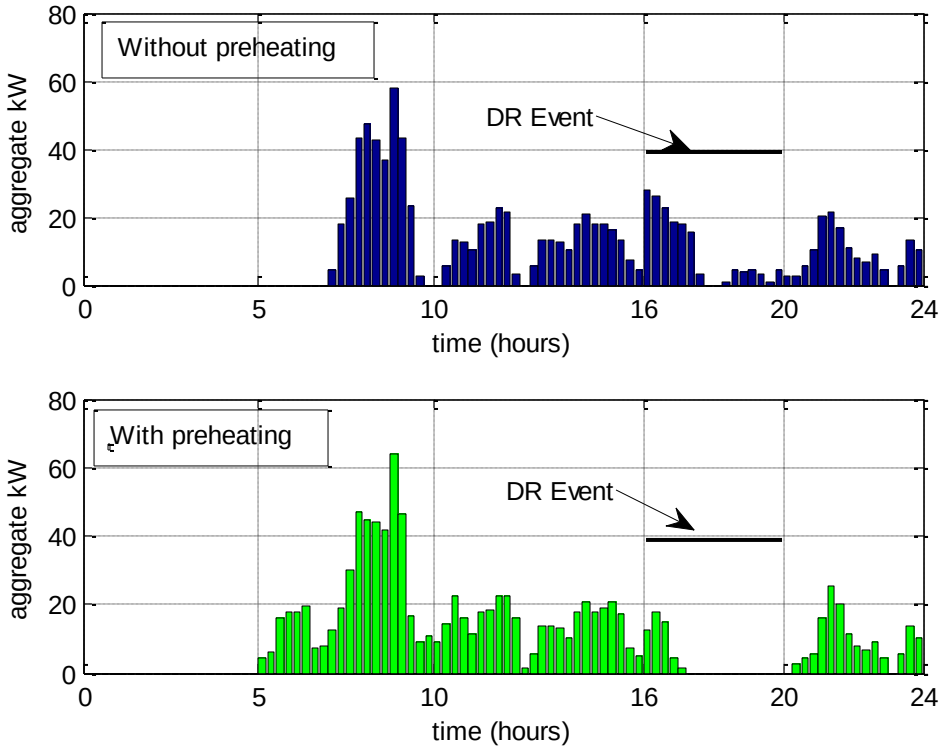

Fig. 7.1: Aggregate water heating demand profiles for Monte Carlo outcome with high demand response amount (i.e. 25.65 kWh in 4 hours for 25 houses).

It can be seen from Fig. 7.1 that there is 11.4 kW of aggregate peak reduction by water heating load control. Total 25.65 kWh of energy reduction is achieved.

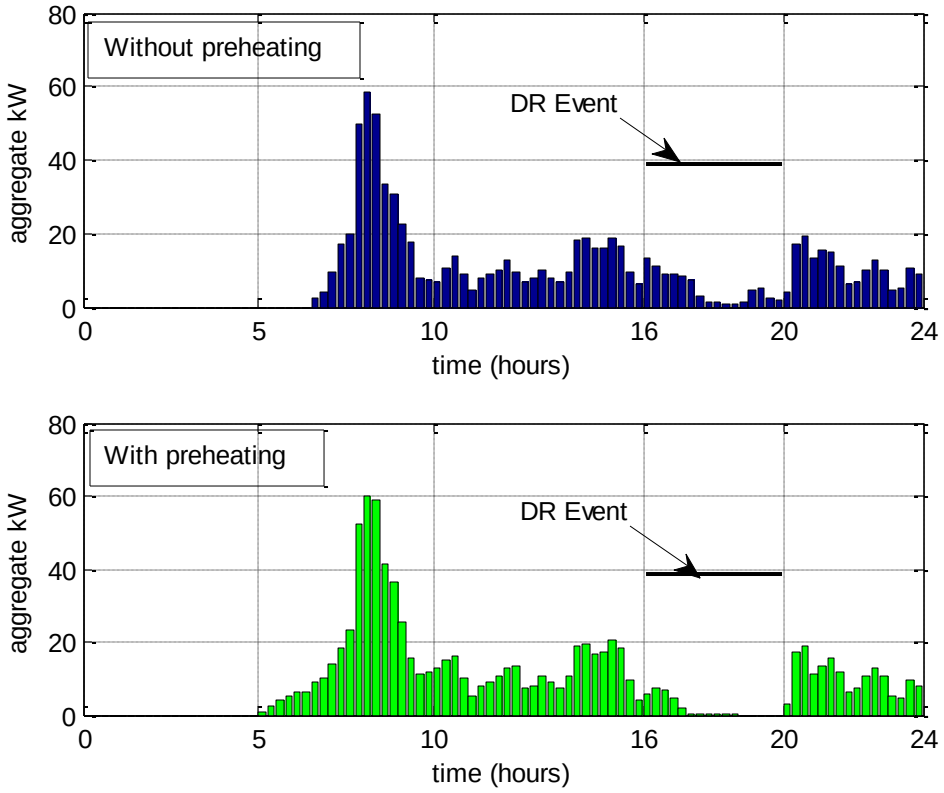

Fig. 7.2: Aggregate electrical water heating demand profiles (average profile of all the Monte Carlo samples), average demand response amount is 13.7 kWh in 4 hours for 25 houses.

Average profile does not demonstrate high demand response potential by water heating load, because water heating energy demands are sparsely distributed over time.

Summary of Monte Carlo simulations for water heating load is provided in Table 7.1. Water heating demand profiles are found to be highly uneven. It is also found that water heater operates sparsely over the typical demand response event duration (4 pm to 8 pm) of summer time. Therefore, demand response potential from electric water heater control is found to be around 11 kW peak reduction. However, this result is based on the hot water consumption profiles provided by IEA [31]. Potential demand response amount can be higher if the typical rate of hot water consumption is higher for the houses under consideration.

Table 7.1: Summary of Monte Carlo simulation for aggregate water heating load of 25 houses

Demand response outcomes from Monte Carlo simulation	Total 24 hour's energy demand without preheating (kWh)	Total 24 hour's energy demand with preheating (kWh)	Without preheating: Aggregate water heating power demands of 25 houses in various hours of demand response event (kW)				With preheating: Aggregate water heating power demands of 25 houses in various hours of demand response event (kW)			
			hour 16-17	hour 17-18	hour 18-19	hour 19-20	hour 16-17	hour 17-18	hour 18-19	hour 19-20
Profile for high DR	235.8	257.9	23.8	9.1	2.3	3.2	12.4	0.3	0.0	0.0
Average Profile	212.7	224.5	10.6	5.1	1.1	3.5	6.1	0.5	0.1	0.0

7.2 Aggregate Demand Response of Air-Conditioning Load

Aggregate demand response scope for air-conditioners of 25 houses is investigated in this section with the help of Monte Carlo simulations. Various simulation parameters (such as: floor space, air-conditioner size, SEER rating, insulation values, temperature set-point etc.) are randomized with maximum 10% to 20% variability. Aggregate load profiles are calculated for both cases of without and with pre-cooling operation. Simulation is repeated 500 times to obtain best and worst case results. Considered variations of parameters are provided below:

- Floor space: Floor space is taken between 2000 ft^2 to 3000 ft^2.
- Areas of wall and window: Maximum 10% variation is considered.
- Insulation levels: Maximum 10% variation.
- SEER rating: Maximum 10% variation.
- Regular temperature set-point: Between 68 °F to 72 °F.
- Outdoor temperature profile: June 08, 2011, NYC [21].
- Pre-cooling start time: Between 6 am to 10 am.

Monte Carlo simulations are performed to obtain best case and worst case results. High demand response amount is found 221 kWh for the 4 hours of demand response event (shown in Fig. 7.3). On the other hand, low demand response amount is found 207 kWh for four hours (shown in Fig. 7.4). Average profile of all the Monte Carlo simulation outcomes is shown in Fig. 7.5. Average demand response amount is found to be 214 kWh for the entire duration (4 hours) of demand response event. It can be observed, that there is about 20 kW of rebound load in the hour just after demand response event. Therefore, air-conditioning control for demand response can cause around 25% of rebound load.

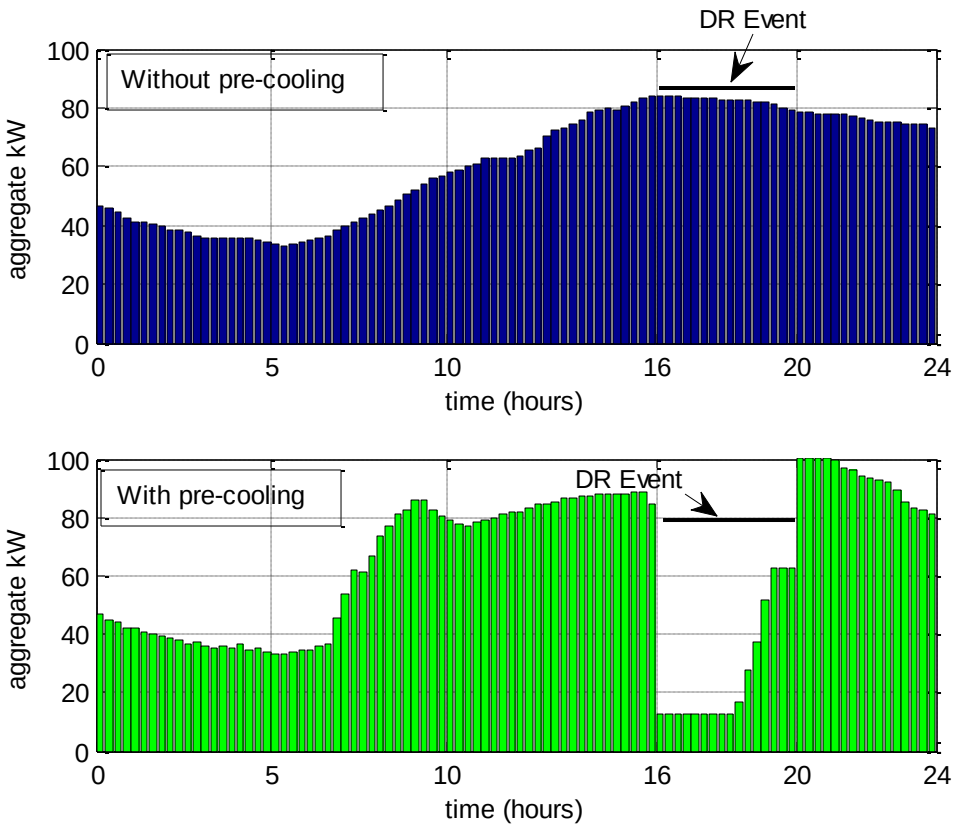

Fig. 7.3: Aggregate air-conditioning demand profiles for Monte Carlo outcome with high demand response amount (i.e. 221 kWh in 4 hours for 25 houses).

It can be seen from Fig. 7.3 that air-conditioning load of demand response event duration is shifted by pre-cooling operation. However, demand increases in the last hour of demand response event to keep indoor temperature within 3 °F range of preferred temperature set-point. This increased demand is required to be uniformly distributed over the entire duration of demand response event to keep aggregate power demand low throughout the event duration. Air-conditioning demand scheduling is discussed in section 7.3.

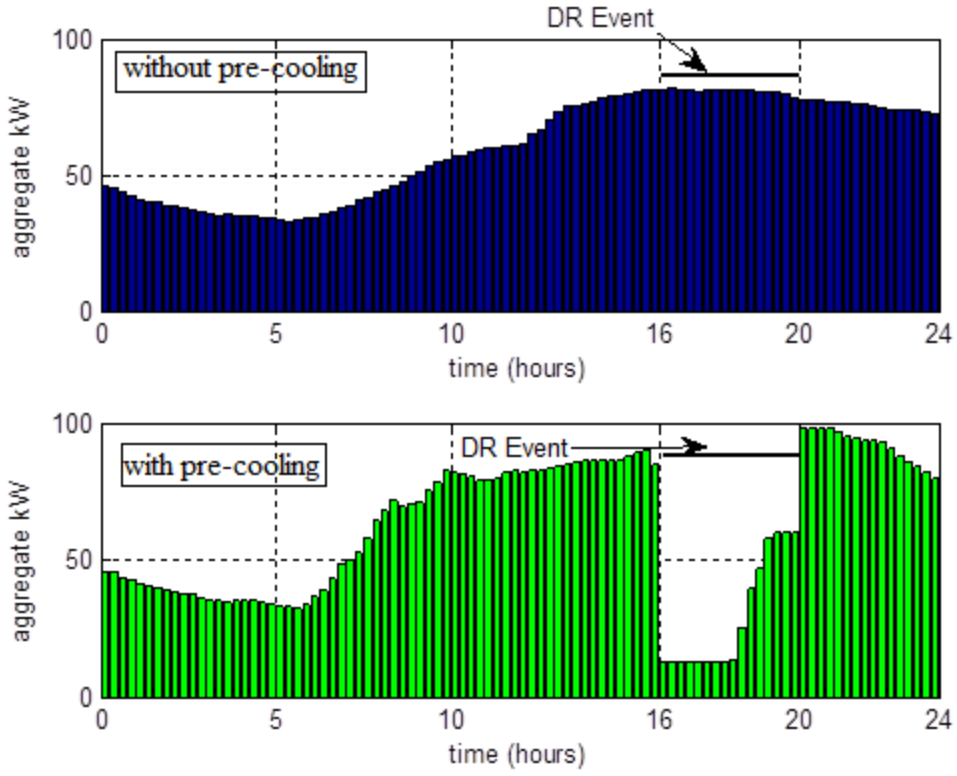

Fig. 7.4: Aggregate air-conditioning demand profile for Monte Carlo outcome with low demand response amount (i.e. 207 kWh in 4 hours for 25 houses).

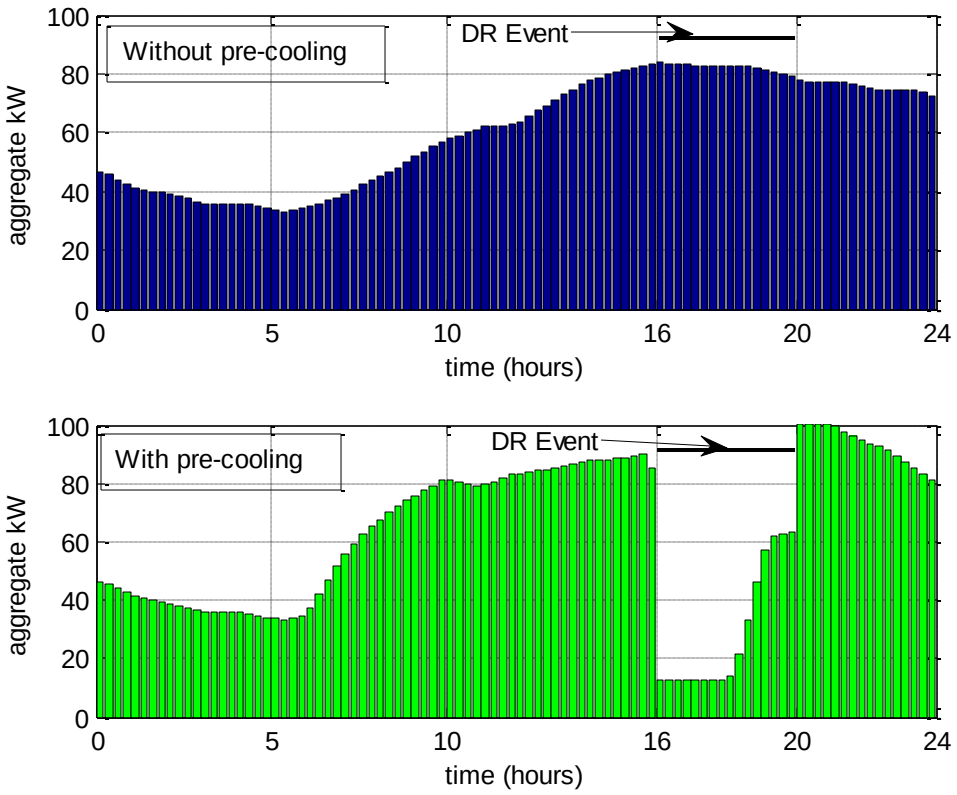

Fig. 7.5: Aggregate air-conditioning demand profile (average profile of all Monte Carlo outcomes), Average demand response amount is 214 kWh in 4 hours for 25 houses.

Summary of Monte Carlo simulation for air-conditioning load is provided in Table 7.2. It can be observed that demand increases in the 4th hour of demand response event. Air-conditioners' operations of various houses should be scheduled to avoid excessive power demand in a particular demand response event hour. Around 65% of air-conditioning demand reduction has been possible with the help of pre-cooling. Pre-cooling amount has been constrained to maximum reduction limit of 3 °F to satisfy thermal comfort of household residents.

Table 7.2: Summary of Monte Carlo simulation for aggregate air-conditioning load of 25 houses

Demand response outcomes from Monte Carlo simulation	Total 24 hour's energy demand without pre-cooling (kWh)	Total 24 hour's energy demand with pre-cooling (kWh)	Without pre-cooling: Aggregate air-conditioning power demands of 25 houses in various hours of demand response event (kW)				With pre-cooling: Aggregate air-conditioning power demands of 25 houses in various hours of demand response event (kW)			
			Hour 16-17	Hour 17-18	Hour 18-19	Hour 19-20	Hour 16-17	Hour 17-18	Hour 18-19	Hour 19-20
Profile for high DR	1469.0	1473.0	83.7	83.0	82.6	80.6	12.5	12.5	23.6	59.9
Profile for low DR	1454.0	1465.0	81.4	81.2	81.2	79.8	12.5	12.5	31.4	59.6
Average Profile	1463	1465.5	83.1	82.5	82.1	80.3	12.5	12.5	28.6	60.3

Summary of Monte Carlo simulation for combined load (air-conditioning and water heating) is provided in Table 7.3. Around 65% of aggregate load reduction has been possible by water heater and air-conditioner control (preheating and pre-cooling respectively). This is a significant amount of residential load reduction potential after satisfying residents' comfort.

Table 7.3: Summary of Monte Carlo simulation for combined (air-conditioning and water heating) load of 25 houses.

Demand response outcomes from Monte Carlo simulation	Total 24 hour's energy demand without load control (kWh)	Total 24 hour's energy demand with load control (kWh)	Without load control: Aggregate combined (air-conditioning and water heating) power demands of 25 houses in various hours of demand response event (kW)				With load control: Aggregate combined (air-conditioning and water heating) power demands of 25 houses in various hours of demand response event (kW)			
			Hour 16-17	Hour 17-18	Hour 18-19	Hour 19-20	Hour 16-17	Hour 17-18	Hour 18-19	Hour 19-20
Profile for high DR	1704.8	1730.9	107.5	92.1	84.9	83.8	24.9	12.8	23.6	59.9
Average Profile	1675.7	1690.0	93.7	87.6	83.2	83.8	18.6	13.0	28.7	60.3

7.3 Demand Scheduling of Aggregate Air-Conditioning Load

PARAMETER NOTATIONS

n_{ac}	Number of air-conditioners in "on"-state during a particular time block
$n_{ac.max}$	Maximum allowable n_{ac} value during demand response event
N_{block}	Total number of time blocks during demand response event
n_{on}	Number of time blocks one air-conditioner remains on during demand response
N_{on}	Summation of n_{on}-values of all the air-conditioners under consideration
$Time_{dr}$	Demand response event duration
t_{block}	Duration of one time block
t_{off}	Air-conditioner turn-off duration during demand response event
t_{on}	Air-conditioner turn-on duration during demand response event
Δ_{ac}	Pre-cooling temperature set-point reduction amount for air-conditioner
Δ_{max}	Maximum allowable reduction in temperature set-point for pre-cooling

In section 6.2.1 of Chapter 6, we have seen that expected temperature rise during demand response event is $2^* \Delta_{ac}$, if air-conditioner is turned off completely (except ventilation). Value Δ_{ac} can be calculated using equation (6.8). It is also observed from the case studies that indoor temperature typically rises with gradually decaying slope. Heat gain of a house depends on the difference of indoor and outdoor temperature. With the increase of indoor temperature, heat gain rate slows down. Thus, slope of the curve reduces over time. A typical indoor temperature profile during a demand response event is provided in Fig. 7.6.

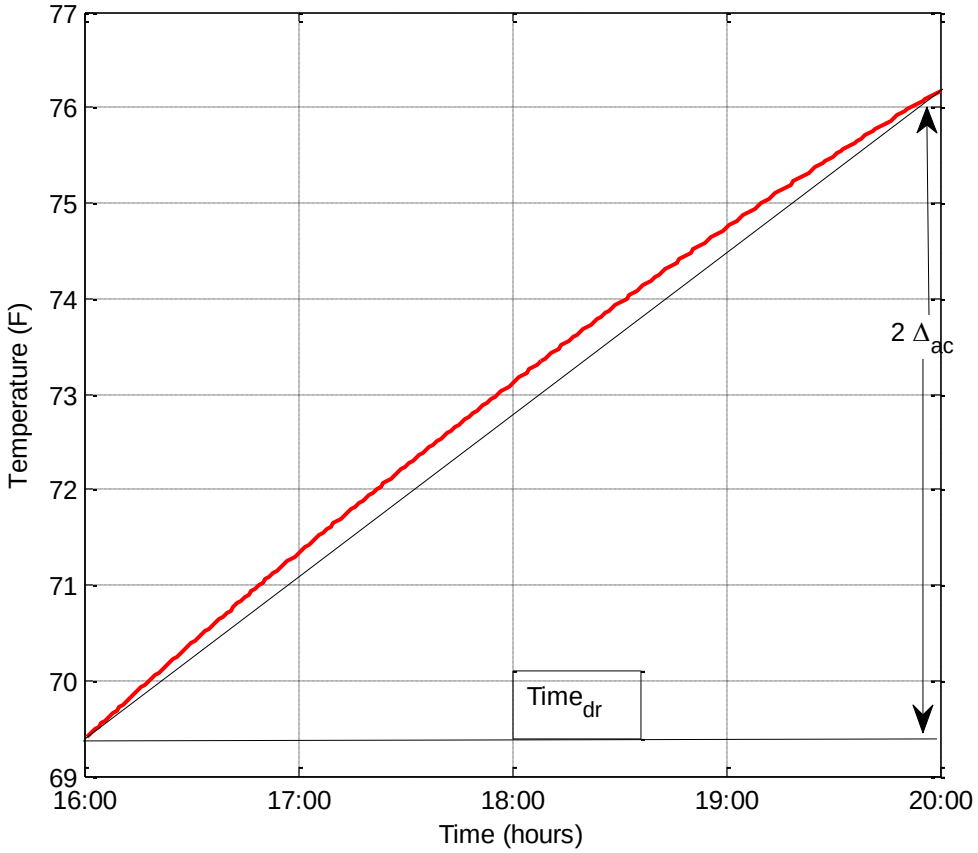

Fig. 7.6: Typical indoor temperature profile during demand response event

It can be seen from Fig. 7.6, that curvature of the temperature profile is low during the short duration of demand response event. Thus, this profile can be approximated by a straight line. In that case,

$$Slope\ of\ the\ line, m\ = \frac{2 * \Delta_{ac}}{Time_{dr}}$$

If maximum allowable indoor temperature change is 2 Δ_{max} °F (T_{set} - Δ_{max} to T_{set} + Δ_{max}) then maximum allowable air-conditioner turn-off duration can be calculated from the equation of line,

$$y = mx$$

$$or, \qquad (2 * \Delta_{max}) = \left(\frac{2 * \Delta_{ac}}{Time_{dr}}\right) * t_{off}$$

$$t_{off} = \Delta_{max} * \frac{Time_{dr}}{\Delta_{ac}} \ldots\ldots\ldots\ldots (7.1)$$

However, it can be seen from Fig. 7.6 that actual indoor temperature is slightly higher than the temperature calculation from linear model. In other words, indoor temperature reaches a certain level few minutes earlier than the time calculated from linear model. Therefore, air-conditioner turn-off duration will be few minutes less than the calculated duration. Equation (7.1) can be modified as,

$$t_{off} = \Delta_{max} * \frac{Time_{dr}}{\Delta_{ac}} - \delta t; \quad \ldots\ldots\ldots\ldots (7.2)$$

To obtain uniformity of power demand, turn-off/ turn-on durations of air-conditioners can be broken into small time blocks (e.g. t_{block} =15 minutes) and distributed uniformly over the entire demand response event duration.

Methodology:

1. Determine values of Δ_{ac} for every house.
2. Determine turn-off durations.
3. Determine turn-on durations
$$t_{on} = Time_{dr} - t_{off}$$
4. Determine the required number of time blocks one air-conditioner needs to remain on. Each time air conditioner remains 'on' for the duration t_{block}.
$$n_{on} = upper\ integer\ (t_{on} * \frac{60}{t_{block}}).$$
5. Determine total number of on-states of air-conditioners of all the houses
$$N_{on} = \sum n_{on,i}$$
6. Total number of time blocks during demand response event,
$$N_{block} = \frac{Time_{dr}}{t_{block}}$$

Determine maximum number of air-conditioners to be operating in each time block during demand response event.

$$n_{ac.max} = upper\ integer(\frac{N_{on}}{N_{block}})$$

7. Schedule all the air-conditioners by satisfying following condition for each time block:

$$number\ of\ operating\ air.conditioners\ (n_{ac}) \leq\ n_{ac.max}$$

Simulation Results:

Let's consider 25 houses with different thermal characteristics. Time block duration is taken, t_{block} = 15 minutes. Value of time offset δt is taken 10 minutes. Calculated values of Δ_{ac} and n_{on} are shown in Fig. 7.7.

- Total number on-states of air-conditioners of 25 houses is, N_{on} = 93, each on-state is for a duration of 15 minutes.
- 4 hours demand response event duration is divided into 16 time blocks (each 15 minutes). Therefore, maximum number of air-conditioners operating at one time block is, $n_{ac.max}$ = upper_integer(93/16) = 6.
- Air-conditioners of 25 houses are scheduled to keep the number of operating air-conditioner at each time block, $n_{ac} \leq 6$. Total numbers of operating (in on-state) air-conditioners during various time blocks are shown in Fig. 7.8. Schedule details are shown in Fig. 7.9. Aggregate demand profiles of 25 air-conditioners are shown in Fig. 7.10 (with and without demand scheduling).

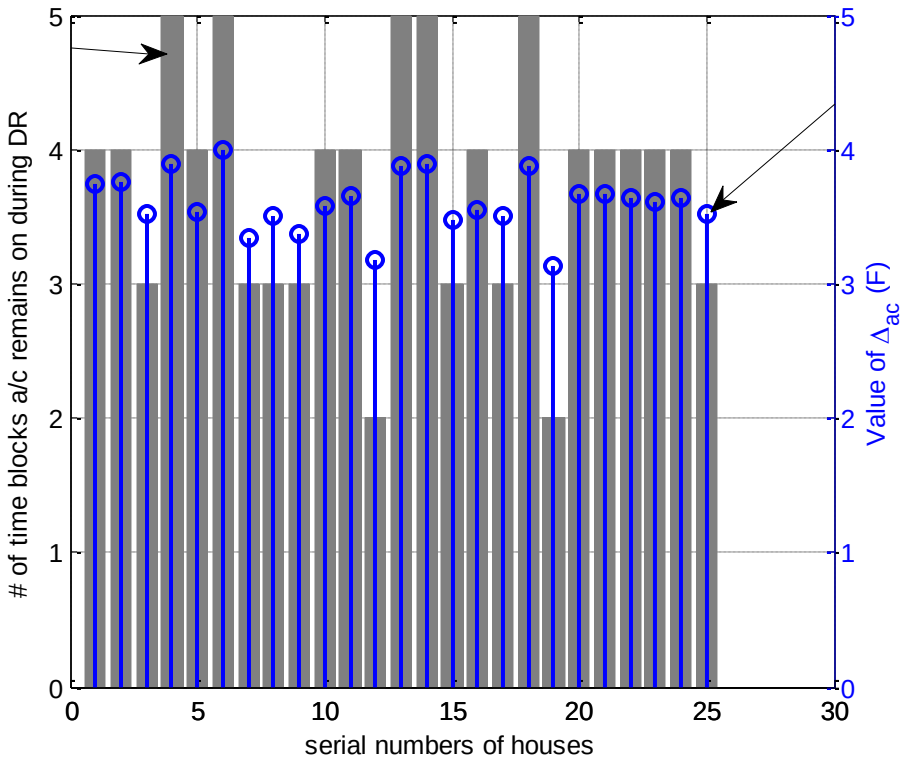

Fig. 7.7: Calculated values of Δ_{ac} and n_{on} for 25 houses.

It can be seen from Fig. 7.7 that calculated values of Δ_{ac} are between 3 to 4 °F. Maximum allowable temperature change is considered ±3 °F, to satisfy thermal comfort of household residents. Therefore, air-conditioners are required to be turned on for certain duration of time.

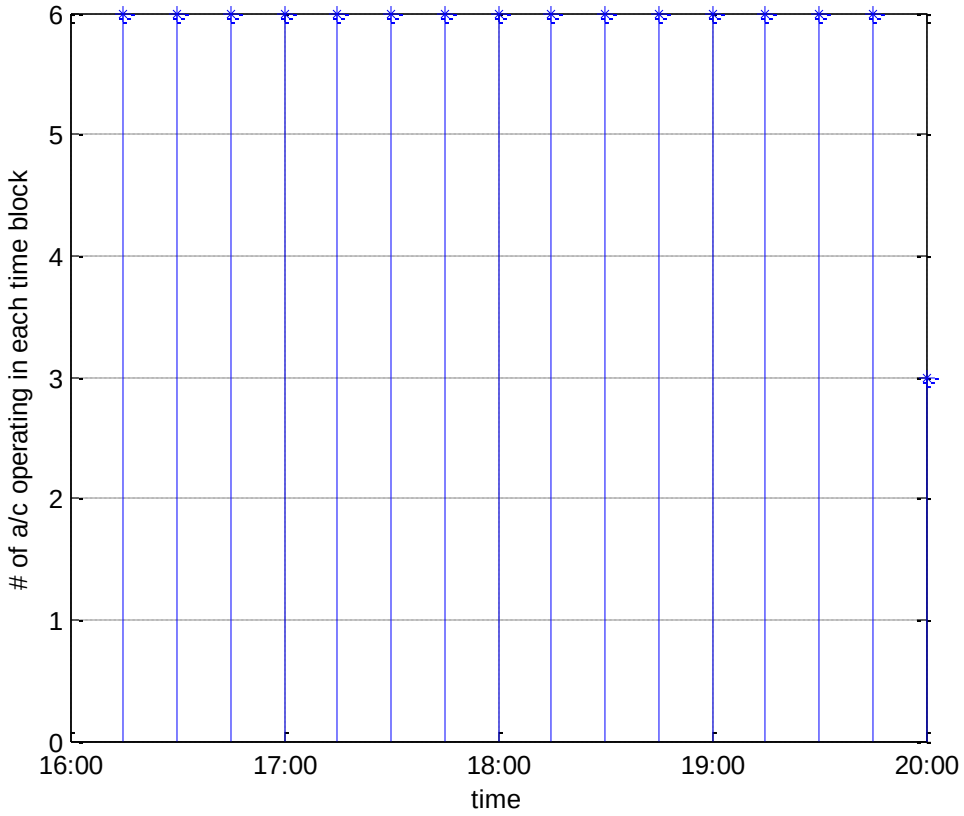

Fig. 7.8: Numbers of operating air-conditioners at various time blocks

It can be seen from Fig. 7.8 that air-conditioners are scheduled almost uniformly over the entire demand response event duration. Number of operating air-conditioners in each time block is 6, except the last time block. This methodology distributes air-conditioning load over the entire duration of demand response event.

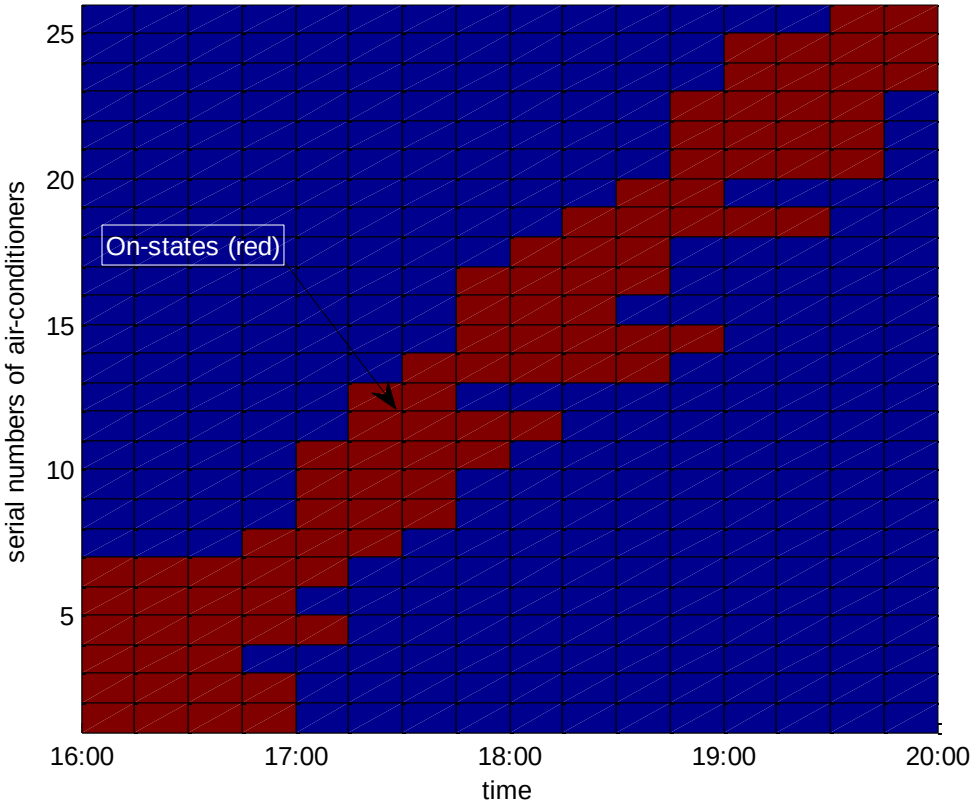

Fig. 7.9: Demand response event time operating schedule of air-conditioners of 25 houses (blue color indicates off-states and red indicates on-states)

Operational schedule of various air-conditioners is shown in Fig. 7.9. It is observable that number of red blocks in each column is 6, except the last column. Turn-on/off times of air-conditioners are distributed to keep peak demand low.

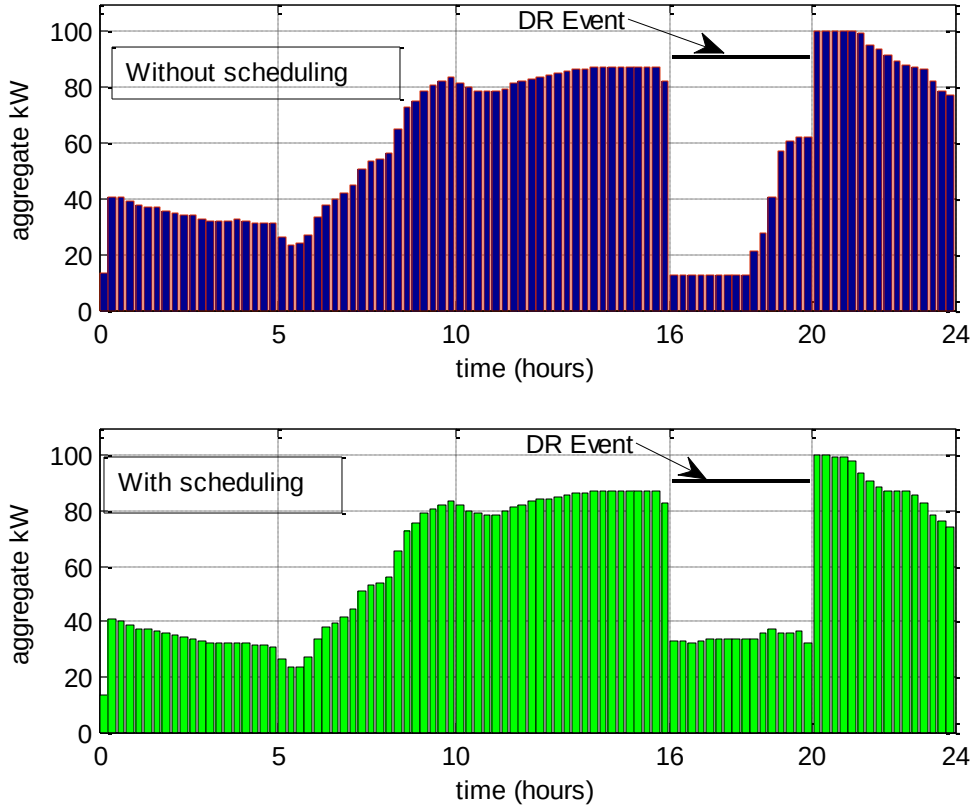

Fig. 7.10: Aggregate air-conditioning demand profile of 25 houses, after pre-cooling and demand scheduling.

Demand profiles without and with scheduling are shown in Fig. 7.10. It can be seen that 25 kW of peak reduction has been possible by scheduling operating times of air-conditioners of 25 houses. With the help of pre-cooling and demand scheduling, total peak reduction is 45 kW with respect to the baseline air-conditioning load.

Comparison of demands with and without scheduling is shown in Table 7.4. High power demand of hour 19-20 is distributed among 3 previous hours. This scheduling methodology distributes air-conditioning power demand over the entire duration of demand response event. This methodology successfully reduces peak power in the expense of increased total energy demand. However, that consequence provides an added benefit by reducing rebound load after demand response event (can be seen from Fig. 7.10).

Table 7.4: Comparison of load profiles with and without demand scheduling

	Power demands of 25 houses in various hours of demand response event (kW)			
	Hour 16-17	Hour 17-18	Hour 18-19	Hour 19-20
Profile without demand scheduling	12.5	12.5	25.6	60.7
Profile with demand scheduling	32.8	33.5	35.1	34.9

CHAPTER 8

Summary, Conclusion and Future Work

8.1 Summary

In this research work, a thorough investigation of residential demand response potential is provided. The incentive-based demand response model is considered and the scope of aggregate demand response participation of several houses is analyzed. Demand response potential for electrical water heater and air-conditioner are evaluated based on their demand profiles. Hot water preheating and air-conditioning pre-cooling techniques are investigated with the help of the developed mathematical models to determine demand response potential of those loads. Additional energy loss possibility associated with water preheating is also investigated using the developed energy loss model. Preheating temperature set-point is mathematically determined to obtain maximum demand reduction by keeping thermal loss to a minimal level. Case studies are performed for 15 summer days to investigate the demand response potential of water preheating. Similarly, demand response potential associated with pre-cooling operation of air-conditioning is also investigated using the developed mathematical model. The required temperature set-point modification is determined mathematically and validated with the help of known outdoor temperature profiles. Case studies are performed for 15 summer days to demonstrate effectiveness of this procedure. On the other hand, total load and demand response potential of a single house is usually too small to participate in an incentive-based demand response program. Thus, the scopes of combining several houses together under a single platform are also investigated in this work. Monte Carlo procedure-based simulations are performed to get an insight into the best and the worst case demand response outcomes of a cluster of houses. In case of electrical water heater control, aggregate demand response potential of 25 houses is determined. Similarly, in case of air-conditioning control (pre-cooling), approximate values of maximum, minimum and mean demand reduction amounts are determined for a cluster of 25 houses. Expected increase of indoor temperature of a house is calculated by using the derived

equation. Afterwards, air-conditioning demand scheduling algorithm is developed to keep aggregate air-conditioning power demand to minimal level during a demand response event. Simulation results are provided to demonstrate the effectiveness of the proposed algorithm. Research findings include:

- With the help of preheating, it is usually possible to shift 100% of water heating load away from a demand response event. However, in some rare instances (1 out of 15 days), required preheat temperature can be excessively high. In such a case, partial amount of demand reduction is possible by water preheating.
- 33% of the case-study days required hot water temperature increase of 4 to 6 °F from the original set-point level. 60% of the days did not require any preheating and did not possess any demand response potential by water heater control.
- Water preheating operations usually increased overall energy demand of water heater by about 1 kWh in a day of demand response event. This increase in thermal loss should be compensated by energy reduction incentive for demand response participation.
- For a cluster of 25 small houses, aggregate potential demand reduction amount by water heater control is found to be around 26 kWh during 4 hours of a demand response event. From the outcomes of Monte Carlo simulations, the aggregate peak reduction by water preheating is found to be around 11 kW. However, this result is based on hot water consumption profiles provided by IEA [31]. Demand response potential can increase in case of higher rate of hot water consumption per house.
- The required temperature set-point modification for a pre-cooling purpose (air-conditioner control) is found to be typically more than 3 °F for a hot summer day of a demand response event. However, the maximum allowable indoor temperature set-point modification is considered ±3 °F to satisfy the thermal comfort of household residents. Therefore, typically, only a partial amount of air-conditioning demand reduction is possible without comfort violation. Simulation results indicate that around 65% of air-conditioning load reduction is possible with pre-cooling operation in hot summer days.
- Power demand by air-conditioners can increase around 25% above the usual level in the hour following a demand response event. The study shows high rebound load can occur because of the abrupt change in temperature set-point. However, this effect can be

minimized by reducing the temperature set-point gradually after demand response event hours.

- In case of ± 3°F maximum allowable change in indoor temperature set-point, aggregate power demand by air-conditioners can rise to 75% level of usual demand in the 4^{th} hour of demand response event. Therefore, proper scheduling of air-conditioner operation is required to keep the aggregate power demand low. With the help of demand scheduling, power demand can be kept at around 35% level of its original aggregate demand.
- In case of the combined control of water heating and air-conditioning loads of a cluster of houses, it is possible to obtain around 65% of load reduction without impacting the comfort level of household residents. In case of 25 houses, the combined peak demand reduction amount is found to be around 56 kW by controlling electrical water heaters and air-conditioners.

8.2 Conclusion

Challenges associated with residential demand response are mainly following: small load size per house, highly stochastic nature of residential load, individual monitoring and control overhead, lack of proper smart-grid infrastructure, concern regarding comfort violation etc. Despite these challenges, there is enormous demand response potential for residential loads if several houses can be aggregated together. Two key issues must be satisfied to popularize residential demand response participation. First is to satisfy residents' comfort for the entire demand response event duration and the second is to keep the residents free from the concern of incentive penalty in case of any demand response threshold violation. Therefore, this research work highly focused on those two aspects. Comfort level is satisfied by providing adequate hot water reserve (to meet hot water demand) during any demand response event. Similarly, thermal comfort level of a house is maintained by intelligent pre-cooling and control of air-conditioning load. The aggregator company based demand response model is considered to relieve residents from the burden of load management.

In this research work, the water preheating methodology is developed to provide adequate hot water reserve for the demand response event hours. Similarly, the pre-cooling methodology is developed for demand response participation of air-conditioning load after satisfying thermal comfort of household residents. The demand scheduling algorithm is developed for aggregate air-conditioning load control of a cluster of houses to keep combined power demand below a threshold level. Monte Carlo method is adopted to get an insight into possible upper and lower bounds of demand response outcomes from a cluster of houses. Results obtained in this thesis indicate that around 65% of demand reduction is possible with aggregated control of electric water heating and air-conditioning loads.

Modeling and mathematical descriptions provided in this thesis is expected to serve as the first stepping stone that will allow researchers in the academia and electric utilities to comprehensively analyze demand response potential of residential customers. Research findings as presented in this thesis can also provide aggregator companies an added insight into expected benefits and constrains of residential load control, in particular, of electric water heater and air-conditioning loads. The preheating/ pre-cooling and demand scheduling methodologies

introduced in this thesis are also expected to contribute to future electric power system planning and operation with demand response as a design criterion.

8.3 Future Work

Demand response literature has discussed elaborately about price signal based approach, energy market, electric vehicle integration, real time energy bidding of supplier and consumer etc., which is easily noticeable from the literature review of Chapter 2. However, residential participation in an incentive-based demand response program has rarely come into light. This thesis provides a baseline analysis of the scopes and associated challenges for residential demand response participation. There are several research spaces which can be pointed out as potential future work scope.

Demand scheduling of air-conditioning load: Further research work can be conducted on air-conditioning demand scheduling. There can be scope of improvement on the mathematical description provided in section 7.3. Research work can also be conducted to minimize rebound effect resulting from residential load control.

Probabilistic approach towards thermal behavior of a house: Thermal behavior of a house depends on the size, construction, insulation, occupancy level etc. Research work can be conducted to estimate thermal behavior of any house by analyzing heat gain and heat loss patterns at various situations. It can also be possible to relate thermal behavior of a house with outdoor temperature to find out the air-conditioner turn-on probability after a particular interval from pre-cooling. In that case, a probability based demand state estimation approach can be taken to analyze potential air-conditioning demand during various time blocks of a demand response event. In this thesis, thermal behaviors of houses are considered as deterministic parameters. Afterwards, Monte Carlo procedure is adopted to investigate the best and the worst case outcomes. In future, thermal behavior of houses can possibly be defined probabilistically with certain distributions.

Residential demand forecast: Demand response event is declared 23 hours in advance. Proper action strategies are required to achieve a demand response goal. However, demand response goal has to be set based on potential demand profile of the day ahead. Residential demand forecast can thus be a future work scope required for demand response implementation.

References

[1] FERC, “Report on demand response and advanced metering,” [Online]. Available: http://www.ferc.gov/industries/electric/indus-act/demand-response/dem-res-adv-metering.asp. (Retrieved in Feb 2012).

[2] J. Berardino and C. Nwankpa , "Dynamic Load Modeling of an HVAC Chiller for Demand Response Applications," Smart Grid Communications (SmartGridComm), 2010 First IEEE International Conference, vol., no., pp.108-113, 4-6 Oct. 2010.

[3] J.C. Fuller, K.P. Schneider, and D. Chassin, "Analysis of Residential Demand Response and double-auction markets," Power and Energy Society General Meeting, 2011 IEEE , vol., no., pp.1-7, 24-29 July 2011.

[4] K.P. Schneider, J.C. Fuller, and D. Chassin, "Analysis of distribution level residential demand response," Power Systems Conference and Exposition (PSCE), 2011 IEEE/PES, vol., no., pp.1-6, 20-23 March 2011.

[5] D. O'Neill, M. Levorato, A. Goldsmith, and U. Mitra, "Residential Demand Response Using Reinforcement Learning," Smart Grid Communications (SmartGridComm), 2010 First IEEE International Conference, vol., no., pp.409-414, 4-6 Oct. 2010.

[6] A. Cuevas, C. Lastres, J. Caffarel, R. Martínez, and A. Santamaría, "Next generation of Energy Residential Gateways for Demand Response and Dynamic Pricing," Consumer Electronics (ICCE), 2011 IEEE International Conference, vol., no., pp.543-544, 9-12 Jan. 2011.

[7] Ying Li and Mark Trayer, "Automated residential demand response: Algorithmic implications of pricing models," Consumer Electronics (ICCE), 2012 IEEE International Conference, vol., no., pp.626-629, 13-16 Jan. 2012.

[8] G.C. Heffner, C.A. Goldman, M.M. Moezzi, "Innovative approaches to verifying demand response of water heater load control," Power Delivery, IEEE Transactions, vol.21, no.1, pp. 388- 397, Jan. 2006.

[9] S. Tiptipakorn, and Wei-Jen Lee, "A Residential Consumer-Centered Load Control Strategy in Real-Time Electricity Pricing Environment," Power Symposium, 2007. NAPS '07. 39th North American, vol., no., pp.505-510, Sept. 30 2007-Oct. 2 2007.

[10] Yanyan Li, M.M. Olama, J.J. Nutaro, "Frequency waves, Grid Friendly Appliances and geographic limits in a smart grid," Innovative Technologies for an Efficient and Reliable Electricity Supply (CITRES), 2010 IEEE Conference, vol., no., pp.220-224, 27-29 Sept. 2010.

[11] C. Roe, S. Meliopoulos, R. Entriken, S. Chhaya, "Simulated demand response of a residential energy management system," Energytech, 2011 IEEE, vol., no., pp.1-6, 25-26 May 2011.

[12] Simone Pagliuca, Ioannis Lampropoulos, Matteo Bonicolini, Barry Rawn, Madeleine Gibescu, and Wil L. Kling, "Capacity Assessment of Residential Demand Response Mechanisms," Universities' Power Engineering Conference (UPEC), Proceedings of 2011 46th International, vol., no., pp.1-6, 5-8 Sept. 2011.

[13] F. Kupzog, C. Roesener, "A closer Look on Load Management," Industrial Informatics, 2007 5th IEEE International Conference, vol.2, no., pp.1151-1156, 23-27 June 2007.

[14] J. Kondoh, Ning Lu; D.J. Hammerstrom, "An Evaluation of the Water Heater Load Potential for Providing Regulation Service," Power Systems, IEEE Transactions, vol.26, no.3, pp.1309-1316, Aug. 2011.

[15] K. Pollhammer, F. Kupzog, T. Gamauf, M. Kremen, "Modeling of demand side shifting potentials for smart power grids," AFRICON, 2011, vol., no., pp.1-5, 13-15 Sept. 2011.

[16] Y. Ito, Y. Murakami, K. Yonezawa, N. Nishimura, Y. Takagi, H. Morimoto, S. Sugawara, and N. Donen, "Next generation HVAC system," SICE Annual Conference, 2008, vol., no., pp.2223-2228, 20-22 Aug. 2008.

[17] J.C. Fuller, K.P. Schneider, D. Chassin, "Analysis of Residential Demand Response and double-auction markets," Power and Energy Society General Meeting, 2011 IEEE , vol., no., pp.1-7, 24-29 July 2011.

[18] P. Ahčin, M. Šikić, "Simulating demand response and energy storage in energy distribution systems," Power System Technology (POWERCON), 2010 International Conference, vol., no., pp.1-7, 24-28 Oct. 2010.

[19] D.P. Chassin, P. Du, J.C. Fuller, "The potential and limits of residential demand response control strategies," Power and Energy Society General Meeting, 2011 IEEE , vol., no., pp.1-6, 24-29 July 2011.

[20] Load archive of FERC NYISO. [Online]. Available: http://www.ferc.gov/market-oversight/mkt-electric/new-york/nyiso-archives.asp. (Retrieved in Feb 2012).

[21] Temperature profiles of Central Park, NYC. [Online] http://www.wunderground.com/history/airport/KNYC/2011/6/9/MonthlyHistory.html?req_city=NA&req_state=NA&req_statename=NA. (Retrieved in Feb 2012).

[22] "California DREAMing: the Design of Residential Demand Responsive Technology with People in Mind," PhD dissertation by Therese Evelyn Peffer, University of California, Berkeley. [Online]. http://escholarship.org/uc/item/8rk0g6mh#page-26. (Retrieved in Mar 2012).

[23] TOU pricing by Portland General Electric. [Online] http://www.portlandgeneral.com/residential/your_account/billing_payment/time_of_use/pricing.aspx. (Retrieved in Dec 2011).

[24] Energy Insight, "Time of use and critical peak pricing." [Online] http://www.aeic.org/load_research/docs/12_Time-of-Use_and_Critical_Peak_Pricing.pdf (Retrieved in Dec 2011).

[25] ConEdison, Inc. Distribution Load Relief (DLF) program. [Online] http://www.coned.com/energyefficiency/dist_load_relief.asp. (Retrieved in Jan 2012).

[26] Hot water heat, the big picture, "Hot water tank heat loss". [Online]. http://www.leaningpinesoftware.com/hot_water_heater_tank_insul.shtml. (Retrieved in Feb 2012).

[27] Engineers Edge, “Conduction, cylindrical coordinates and heat transfer.” [Online] http://www.engineersedge.com/heat_transfer/conduction_cylidrical_coor.htm (Retrieved in Feb 2012).

[28] GE Appliances, typical temperature set point of water heater. [Online] http://www.geappliances.com/heat-pump-hot-water-heater/water-heater-faq.htm#tempsetpoint. (Retrieved in Jan 2012).

[29] 1991 ASHRAE Handbook: Heating, Ventilating, and Air-Conditioning Applications.

[30] T. Arimes Ed., "HVAC and chemical resistance handbook for the engineer and architect", BCT Inc., pp. 17-26, 1994.

[31] IEA Energy Conservation in Buildings and Community Systems. [Online]. http://www.ecbcs.org/annexes/annex42.htm. (Retrieved in Feb 2012).

[32] Truong Nghiem, “Modeling and Advanced Control of HVAC System.” [Online]. Available: http://www.seas.upenn.edu/~cis800/lectures/hvac_mdl_mpc.pdf. (Retrieved Feb 2012).

[33] Oak Ridge National Laboratory. (2008). Insulation Fact Sheer. [Online]. Available: http://www.ornl.gov/sci/roofs+walls/insulation/ins_05.html. (Retrieved in Feb 2012).

[34] Combined simulation of airflow, radiation and moisture transport for heat release from a human body. By, Shuzo Murakamia, Shinsuke Katoa, Jie Zengb. [Online] http://www.sciencedirect.com/science/article/pii/S0360132399000335. (Retrieved in Mar 2012).

[35] Body surface area calculator. [Online]. http://www.medcalc.com/body.html.

[36] SEER rating of HVAC units, Environmental and Energy Study Institute. [Online]. http://www.eesi.org/fact-sheet-air-conditioner-efficiency-standards-seer. (Retrieved in Feb 2012).

[37] iQ drive HVAC, Frigidaire. [Online]. Available: http://www.frigidaire.net/Frigidaire-iQ-Drive-174-Air-Conditioner-p/fs4bi.htm. (Retrieved in Feb 2012).

[38] Environmental design guide, "Thermal mass and insulation for temperate climate." [Online]. Available: http://environmentdesignguide.com.au//media/EDG_65_AH.pdf. (Retrieved: March 2012).

[39] Load calculation, HVAC for beginners. [Online]. http://www.hvac-for-beginners.com/load-calculation.html. (Retrieved in Feb 2012).

[40] Frigidaire air conditioner with 3 levels of compressor speed. [Online]. http://www.frigidaire.com/products/commercial/ductless-split/frs22pys2 (Retrieved in March 2012).

[41] N. Wang, J. Zhang, X. Xia, "Energy consumption of air conditioners at different temperature set points," AFRICON, 2011, vol., no., pp.1-6, 13-15 Sept. 2011.

[42] Wolfram-MathWorld; Kronecker delta function. [Online] http://mathworld.wolfram.com/KroneckerDelta.html. (Retrieved in April 2012).

[43] Ecobee smart thermostat with ZigBee communication capability. [Online]. Available: http://www.ecobee.com/solutions/home/smart/. (Retrieved in March 2012).

[44] Nathan Mendes, Gustavo H.C. Oliveira and Humberto X. de Araújo, "Building thermal performance analysis by using Matlab/ Simulink." [online]. (Retrieved: March 2012). http://www.ibpsa.org/proceedings/BS2001/BS01_0473_480.pdf

[45] GreenTech Media, "Residential Demand Response: Mirage or Reality?" [Online]. Available: http://www.greentechmedia.com/articles/read/residential-demand-response-mirage-or-reality/. (Retrieved in Mar 2012).